

DETERMINATIONS OF THE CRYSTAL STRUCTURES OF
BIS-INDENYL RUTHENIUM AND OF
TWO SO-CALLED γ -BRASS TYPE COMPOUNDS

- I. BIS-INDENYL RUTHENIUM
- II. " $\text{Ni}_5\text{Cd}_{21}$ "
- III. " $\text{Ni}_5\text{Zn}_{21}$ "

Thesis by

Ned Conder Webb

In Partial Fulfillment of the Requirements
for the Degree of
Doctor of Philosophy

California Institute of Technology
Pasadena, California

1963

ACKNOWLEDGEMENTS

I thank Dr. Richard E. Marsh for his help and guidance throughout my graduate career. I thank Dr. Sten Samson for his help and guidance on the alloy studies reported in Parts II and III. During the past four years both of these gentlemen have contributed generously of their time to educate me.

I express my gratitude to the United States Rubber Company, the National Science Foundation, and the California Institute of Technology for financial assistance.

I am thankful for the privilege of working under Professor Jurg Waser as a teaching assistant.

At various times I have used computer programs made available to me by several authors; for different programs I am grateful to Dr. Albert Hybl, Mr. Noel D. Jones, Mr. David J. Duchamp, and Mr. David L. Barker.

I am very grateful to many friends and associates who have taken time to answer questions and to give their assistance on many problems; to Mr. Noel D. Jones, Dr. Albert Hybl, and Dr. B. D. Sharma I am especially grateful. I thank Mr. David J. Duchamp and Mr. Harris J. Silverstone for proofreading.

ABSTRACT

I. The crystal and molecular structure of bis-indenylruthenium was determined by X-ray crystallographic methods. Crystals of bis-indenylruthenium are monoclinic with four molecules per unit cell in space group $P2_{1/a}$. The indenyl groups are in the eclipsed configuration, and the ruthenium atom is midway between the two five-membered rings. Within experimental error, the molecule has mm symmetry, and the planar indenyl groups are parallel. The average Ru-C bond distance is 2.193 \AA , but the ruthenium atom is slightly displaced toward the carbon atoms in position 2.

II and III. The procedures as well as the results of the investigation of the crystal structures of " $\text{Ni}_5\text{Cd}_{21}$ " and " $\text{Ni}_5\text{Zn}_{21}$ " are described. These compounds have been believed to have crystal structures very closely related to that of γ brass. This investigation has shown that the actual atomic arrangements in these compounds are considerably more complicated than was generally assumed. The structures were found to differ drastically from that of γ brass.

TABLE OF CONTENTS

PART		PAGE
I	BIS-INDENYL RUTHENIUM	0
	Introduction	1
	Experimental	2
	i) Finding crystals and collecting intensity data	2
	ii) Lattice constants and density	6
	Determination and refinement of the structure	9
	i) Derivation of the trial structure	9
	ii) Refinement	9
	iii) Behavior of unobserved reflections	18
	iv) Possible sources of error	30
	a) Absorption and extinction	30
	b) Scattering curve of ruthenium	30
	Discussion of results	31
	i) Molecular structure	31
	a) Bond distances and angles	31
	b) General features	37
	c) Prediction of bond distances	38
	d) Temperature factors	50
	ii) Packing of the molecules in the unit cell	50
	iii) Accuracy of the molecular geometry	55
	Disordered bis-indenylruthenium	58
II	"Ni ₅ Cd ₂₁ "	62
	Introduction	63
	Experimental	65
	i) Preparation of single crystals	65
	ii) Intensity data	66
	The derivation of the structure	67
	i) General considerations	67
	ii) Samson's method to derive trial structures of complex cubic intermetallic compounds	68
	iii) Definitions	78
	a) Centers	78
	b) Polyhedra, positions, and complexes	78

TABLE OF CONTENTS (continued)

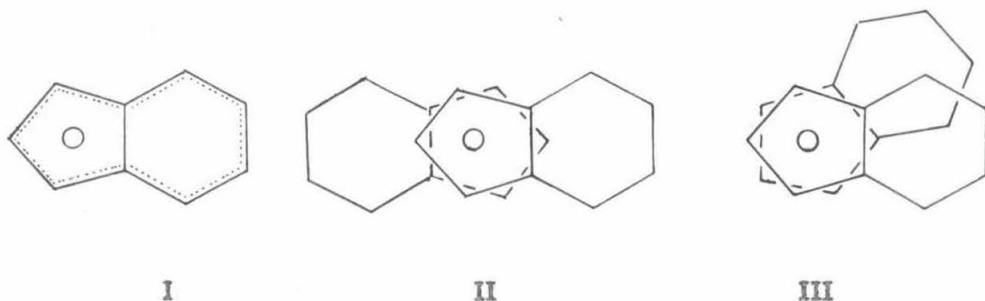
PART	PAGE
iv) Least-squares calculations	80
v) The γ -brass type trial structure	80
vi) Other trial structures	81
vii) A working model	83
viii) Ordered structures	92
Discussion of the structure	101
Future experimental work	105
Future least-squares refinements	109
Summary	113
III "Ni ₅ Zn ₂₁ "	116
Introduction	117
Experimental work	119
The trial structure	119
i) Space group	119
ii) The derivation of the structure	120
Discussion of the structure	121
The diffuse reflections	127
Structure-factor calculations for the disordered structure	128
References	131
PROPOSITIONS	135

PART I

BIS-INDENYL RUTHENIUM

INTRODUCTION

Professor J. H. Richards and his research group have conducted a series of investigations on the chemistry of sandwich compounds (1-5), and, in one of these, Hall (5) prepared and isolated bis-indenylruthenium, $\text{Ru}(\text{C}_9\text{H}_7)_2$. There was speculation as to whether the six-membered rings are cis (I), trans (II), or gauche (III) in the preferred orientation; Trotter (6) had found the six-membered



rings in bis-indenyliron to be gauche. To discover the general features of the molecular geometry and to accurately define the geometry of the carbon framework were the primary objectives in investigating the crystal structure of bis-indenylruthenium. We were especially interested in the bond distances in the six-membered ring because Trotter had reported that the C_5-C_6 bonds in bis-indenyliron are essentially double bonds.

Experimental

i) Finding crystals and collecting intensity data.

A sample of bis-indenylruthenium was supplied by Mr. David Hall of this Institute, and the investigation was started with a crystal selected directly from the sample bottle while a portion was being recrystallized from n-hexane. A study of Weissenberg photographs taken about the c axis indicated the space group to be $P2_1/a$; from rotation and Weissenberg photographs the approximate lattice constants were determined to be $a = 11.1 \text{ \AA}$, $b = 9.3 \text{ \AA}$, $c = 6.2 \text{ \AA}$, and $\beta \approx 90^\circ$. The photographs had a rather disconcerting feature, some of the spots being accompanied by diffuse satellite spots. To us, this indicated disorder in the crystal, but we will discuss this later.

The recrystallization from n-hexane yielded crystals of the same space group as before, but with a unit cell twice as large; the lattice constants were approximately $a = 14.5 \text{ \AA}$, $b = 14.0 \text{ \AA}$, $c = 6.2 \text{ \AA}$, and $\beta = 94.3^\circ$. The crystals were long and rod-like with a truncated-rectangular cross section. One large crystal was selected and cut into pieces varying in length from about 0.1 mm to about 4 mm. Two pieces were then used in collecting all of the X-ray data used in this investigation. One piece was mounted with the needle axis, arbitrarily designated c, parallel to the rotation axis. The second fragment was mounted with the b axis parallel to the rotation axis. The dimensions

of both crystals were approximately 0.1 mm along a by 0.07 mm along b. The third dimension of the crystal mounted for oscillation around b was approximately 0.14 mm, and the length along c for the other crystal was 3 or 4 mm. For collecting intensities from this long crystal, only the tip was placed in the X-ray beam.

Multiple-film equi-inclination Weissenberg photographs were taken with $\text{CuK}\alpha$ radiation for layer lines 0 through 7 about c and for layer lines 0 through 12 about b. The intensities were estimated visually by comparison with intensity strips prepared from the same two crystals. Empirical film factors were obtained for each pair of adjacent films in all sets and were corrected to normal incidence of the X-ray beam. The weighted average of these factors gave a film factor for normal incidence of 3.75 (Eastman Kodak Medical X-ray Film, No Screen). This factor, appropriately modified for the angle of incidence of any layer line set, was then used to relate the intensities on all films within the set to the first film of the set.

The intensities were corrected for Lorentz and polarization effects and compared with values obtained about the other axis to obtain correlation factors for the various exposures. Finally, F^2 values were obtained on an arbitrary scale by taking subjectively-weighted averages of the values observed about the two axes. Altogether, about 2710 reflections were covered, of which about 670 were too weak to be observed. The observed extinctions, $h0l$ when h is odd

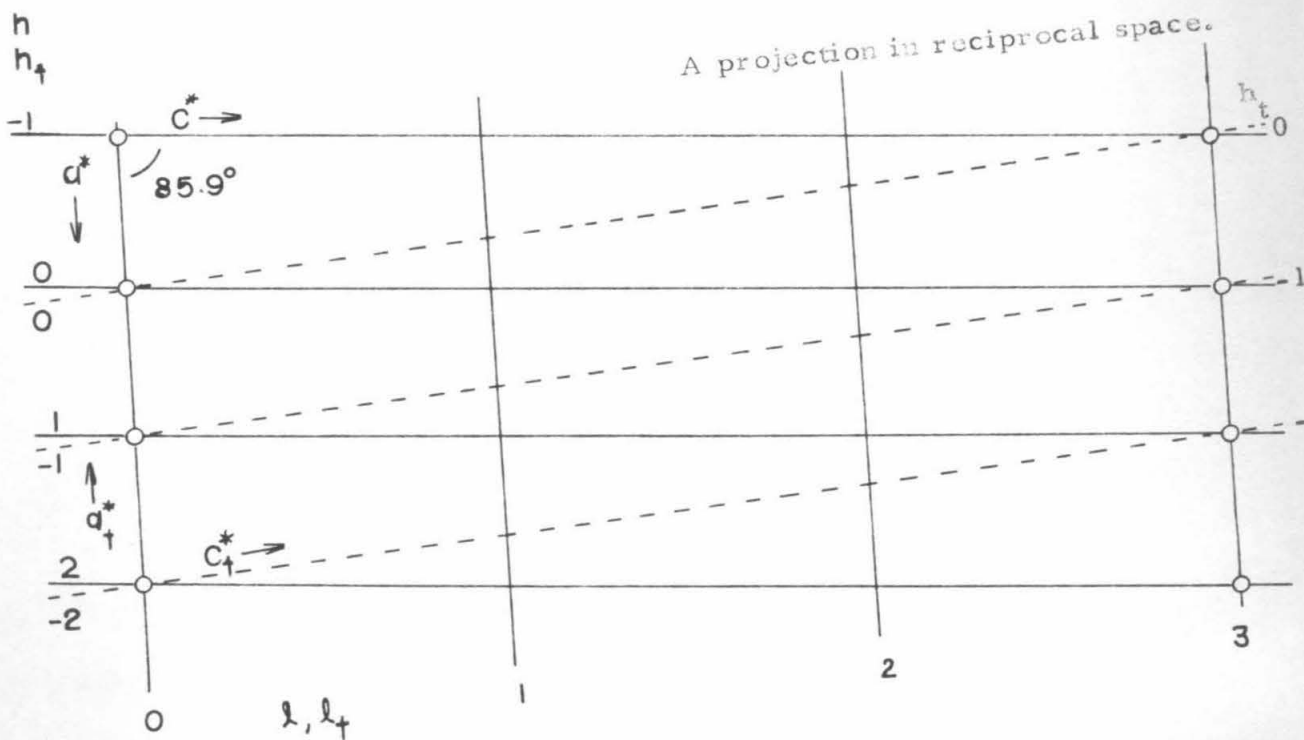
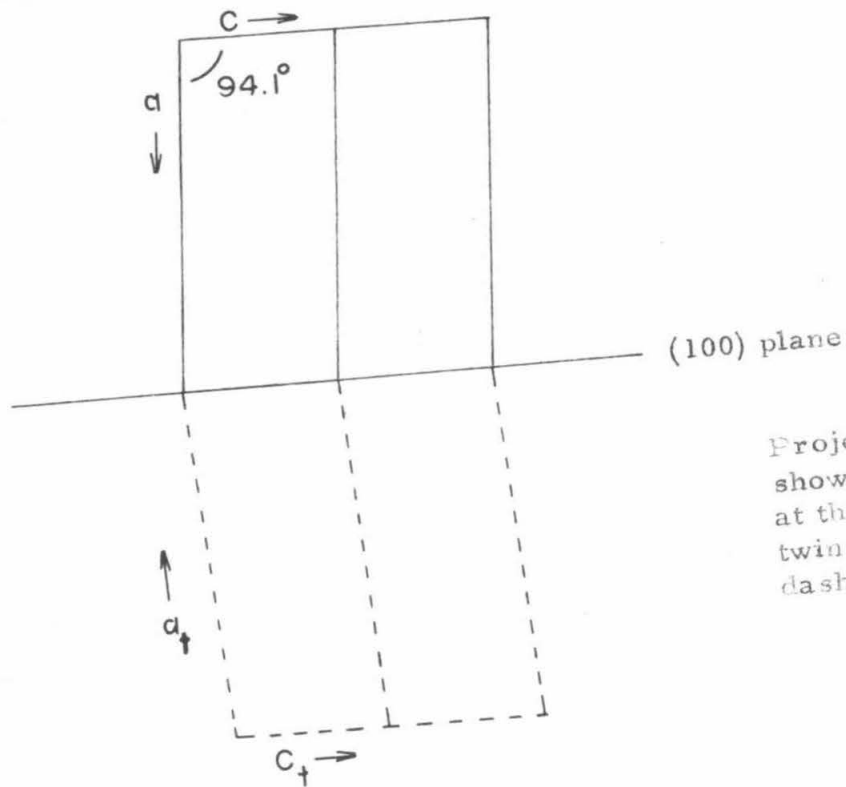
and $0k0$ when k is odd, indicate the space group $P2_1/a$.

The crystal used in collecting the data about the c axis was slightly twinned, giving rise to a large number of weak satellite reflections. On the first and second layers the satellite reflections appeared at positions corresponding to indices $h+\frac{1}{2}, k, l$ and $h+\frac{3}{2}, k, 2$, and, consequently, did not affect the intensities of the primary reflections; on the third layer, however, the satellite reflections were exactly superimposed on the primary reflections. A study of these weak reflections showed that the twinning occurs in the (100) plane, as illustrated in figure 1, and that the reciprocal lattice points of the two lattices coincide every third layer in l . This coincidence does not affect intensities on the zero layer since $hk0$ and $\bar{h}k0$ are space-group equivalent; however, the observed intensities (I_o) on the third layer were not the desired primary intensities (I_p). An examination of the $h03$ reflections, which must have zero intensity for the primary reflections when h is odd because of space-group extinction, indicated the twin to be approximately one-twentieth as large as the primary crystal, and the following equations were used to deduce the values of I_p for the $hk3$ data:

$$I_o(hk3) = I_p(hk3) + .05 I_p(\overline{h+1}k3)$$

$$I_o(\overline{h+1}k3) = I_p(\overline{h+1}k3) + .05 I_p(hk3)$$

Figure 1. Illustration of twinning.



ii) Lattice constants and density.

A Straumanis-type Weissenberg camera, which has a radius of $180/\pi$ mm and a film travel of approximately 23 mm per 180° of rotation, was used to collect data ($\lambda = 1.54051 \text{ \AA}$) for a precise determination of the lattice constants. Two different photographs were taken about the b axis to yield measurement of the diffraction angle of $h0l$ reflections, from one, and of $\bar{h}0l$ reflections from the other, and one photograph was taken about the c axis for $hk0$ reflections. The radiation was $\text{Cu K}\alpha_1$. The lattice parameters were determined by a least-squares fit to

$$a^2 h^2 + b^2 k^2 + c^2 l^2 + 0hl + E\varepsilon = 4/\lambda^2 \sin^2 \theta ,$$

which can be written

$$\frac{h^2}{a^2 \sin^2 \beta} + \frac{k^2}{b^2} + \frac{l^2}{c^2 \sin^2 \beta} - \frac{2hl \cos \beta}{ac \sin^2 \beta} + E \sin^2 2\theta \left(\frac{1}{\theta} + \frac{1}{\sin \theta} \right) = \frac{4}{\lambda^2} \sin^2 \theta ,$$

where the absorption correction ε is taken from Nelson and Riley (7).

We assumed that any error due to eccentricity was negligible. The observational equations were weighted with $w = 1/\sin^2 \theta$, and no reflections at less than 30° in θ were included, in accord with the suggestion of Nelson and Riley.

The results of this least-squares determination of the lattice constants are summarized in table 1; the estimated standard deviations are those given by the least-squares treatment. The averages were obtained by weighting the individual results inversely as the square of the standard deviations.

Table 1. Lattice constants.

Data	h0l	$\bar{h}0l$	hk0	Average
N*	12	12	8	
a	14.5196	14.5147	14.5094	14.514 Å
σ_a	.0012	.0005	.0009	.005 Å
b	-	-	14.0522	14.052 Å
σ_b	-	-	.0001	.005 Å
c	6.2293	6.2256	-	6.229 Å
σ_c	.0003	.0008	-	.004 Å
β	94.113	94.098	-	94.10 Å
σ_β	.203	.078	-	.2°
$E (x 10^5)$	13.9	13.0	-0.4	
$\sigma_E (x 10^5)$	4.0	3.1	2.0	

* N is the number of reflections in the least-squares determination.

The standard deviations given for the average values are subjective estimates.

The twin condition, mentioned above, demands that a^2/D equal the integer 3 because the $\overline{h+1}k3$ reflection from the twin and the $hk3$ reflection from the parent appear to be exactly superimposed.

From the lattice parameters in table 1 we calculate

$$\frac{a^2}{D} = \frac{-a^2}{2a^2 c \cos \beta} = \frac{-a^2}{2c^2 \cos \beta} = \frac{-c}{2a \cos \beta} = 3.001,$$

which is, within experimental error, equal to the integer 3.

The density of the crystal which was mounted about the c axis was measured by the flotation method. The crystal was broken off the mounting well above the adhesive and placed in a zinc chloride solution whose density was greater than that of the crystal. The solution was gradually diluted until the crystal remained suspended after stirring; twelve hours later the crystal was suspended about halfway between the surface and the bottom of the beaker (125 ml, 3/4 full).

The volume of a 2 ml pycnometer was calibrated by filling with distilled water and weighing; the pycnometer was rinsed twice with the zinc chloride solution in which the crystal was suspended, filled with that same solution, and then weighed. The density thus obtained is 1.723 g/cc; the density based on the unit cell dimensions and four molecules per unit cell is 1.737 g/cc. The difference may be due to small air pockets on the surface of the crystal. Before the density was measured, the crystal was examined under the microscope, and its faces appeared to be slightly etched.

Determination and Refinement of the Structure

i) Derivation of the trial structure.

The positions of the ruthenium atoms in the unit cell were readily determined from (001) and (010) Patterson projections. The observed $hk0$ and $h0l$ structure factors were then given the signs of the corresponding ruthenium contributions and used in the preparation of electron density projections onto (001) and (010), but the carbon positions could not be deduced. Accordingly, a three-dimensional Fourier synthesis was calculated, again with signs assigned to the structure factors on the basis of the ruthenium position. The carbon positions were now immediately apparent; the compound was indeed a sandwich molecule with the ruthenium atom bonded to the five-membered rings.

ii) Refinement.

The atomic positional parameters as determined from the three-dimensional electron-density map were refined through several structure-factor least-squares cycles on the Burroughs 220 computer; the complete set of data was used. In all structure-factor calculations, the atomic scattering curve for carbon was taken as an average of the curves given by Berghuis et al. (8) and Hoerni-Ibers (9). The atomic scattering curve for ruthenium was taken from Thomas and Umeda (10);

the $\Delta f'$ correction for dispersion (Dauben and Templeton, 11) was included after a few least-squares cycles. Hydrogen atoms were ignored in the early stages of refinement, but when they were included in the later calculations, the scattering curve of McWeeny (12) was used.

Estimated isotropic temperature factors of the ruthenium and carbon atoms were included in the first set of calculated structure factors, which led to an R factor of 0.185. (The R factor is given by $R = \frac{\sum ||F_o| - |F_c||}{\sum |F_o|}$, the sums being over the observed reflections; the quantity minimized in the least-squares calculations is $\sum w (F_o^2 - F_c^2)^2$.) After the first cycle the weighting function was changed from function I to function II, table 2. Refinement was continued through the fourth cycle with the agreement between the F_o 's and F_c 's improving with each cycle.

For the fifth cycle two changes were made: anisotropic temperature factors were assigned to the ruthenium atoms, and the form factor curve for ruthenium was partially corrected for dispersion (11) by subtracting 0.5 electrons but ignoring the $\Delta f'$ correction. By the end of the seventh cycle, the R factor was down to 0.094; at this point we converted isotropic temperature factors of the carbon atoms to anisotropic ones and proceeded with the refinement. The resulting shifts led to negative temperature factors for some of the carbon atoms, and at the eleventh cycle the refinement was diverging rather than converging.

Table 2. Weighting functions for least-squares.

(The quantity minimized is $\sum_{hkl} \omega (F_o^2 - F_c^2)^2$.)

$$\omega = \omega_e \omega_i$$

ω_e is a subjective external weight based on the quality of an observation. The usual ω_e is 1.00. If there was only one observation, $\sqrt{\omega_e}$ was taken as 0.7. If there were two observations, $\sqrt{\omega_e}$ ranged from 0.5, for poor agreement between the two, to 1.1, for very good agreement, unless there was reason for thinking the observation should not be included at all--in which case, $\omega_e = 0$.

I
$$\omega_i = 1/f^2$$

W. Cochran (13) has shown that the weighting function, $\omega = 1/f$ will make the least-squares minimization of $\sum \omega (F_o - F_c)^2$ to determine atomic coordinates equivalent to determination by Fourier synthesis. The weakness in this function, just as in Fourier synthesis, is that there is no dependence on the quality of observation of F_o .

II
$$\omega_i = \frac{1}{P + Q F_o + R F_o^2}$$

This expression can be used to construct a function which reflects the experimentally observed pattern of reliability of F_o (14). In this work R was set equal to 0, and the function was used to vary the dependence on F_o . As refinement proceeded, more dependence was placed on F_o by increasing the ratio of Q to P .

III
$$\omega_i = \frac{1}{F_o^2} \quad \text{for } F_o > 4F_{\text{minimum}}$$

$$\omega_i = \frac{1}{4F_o F_{\text{min}}} \quad \text{for } F_o < 4F_{\text{minimum}}$$

This is the square root of weighting function IV. This, of course, gives more weight to large F_o 's than IV. This very closely approximates the Hughes (15) scheme for minimization of $\sum \omega (F_o - F_c)^2$.

Table 2. (continued)

$$\text{IV} \quad \omega_i = \frac{1}{F_o^4} \quad \text{for } F_o > 4F_{\min}$$

$$\omega_i = \frac{1}{16 F_o^2 F_{\min}^2} \quad \text{for } F_o < 4F_{\min}$$

Hughes (15) used a weighting function based on $\sigma(F_o) = F_o$ for $F_o > 4F_{\min}$, where F_{\min} is the smallest F_o which can be estimated, and $\sigma(F_o) = 4F_{\min}$ for $F_o < 4F_{\min}$ in minimizing $\sum \omega (F_o - F_c)^2$. To minimize $\sum \omega (F_o^2 - F_c^2)^2$, our uncertainties should be based on F_o^2 , and we have $\sigma(F_o^2) = 2 F_o \sigma(F_o)$. Therefore, the converted Hughes weighting scheme is based on $\sigma(F_o^2) = 2F_o^2$ for $F_o > 4F_{\min}$ and $\sigma(F_o^2) = 8F_o F_{\min}$. We remove the factor of 2 and get the weighting function as listed.

To halt this divergence, we restored the isotropic temperature factors for the carbon atoms as given by the seventh cycle and took the atomic coordinates as given by the tenth cycle. Refinement was continued, and after two cycles the complete list of observed and calculated structure factors was examined for serious discrepancies. In the course of examining 2710 reflections, 37 were found to be weighted improperly; all these were reflections which were covered on only one set of films and which should have been weighted as being less than some estimable minimum, in which case they enter the least-squares process only if $F_o > F_c$. Their effect on the refinement must have been small because the agreement was generally good and because they entered the refinement with $\sqrt{w_e} = 0.7$. There were two errors due to scaling the intensities to the wrong film in a set, and, hence, the F_o 's were small by a factor of approximately 2. The two worst errors were in the reflections (9 10 1), $F_o/F_c = 16/52$, and ($\overline{13}$ 11 2), $F_o/F_c = 54/13$. Errors in transcription were found, and the F_o 's were corrected to 54 and 20.

Further refinement led to convergence at the sixteenth cycle with the result depicted by part A of figure 2; the R factor was 0.085. The weighting function was changed to function III, table 2; after three least-squares cycles the structure had converged to that illustrated in part B of figure 2, with $R = 0.087$.

We were not, however, satisfied with the carbon framework given by either refinement and decided to calculate a difference-Fourier synthesis with coefficients $F_o - F_{Ru}$ in hope of getting a more satisfactory structure. The result of the difference-Fourier synthesis is given in figure 3. The points of maximum electron density were determined by least-squares, assuming the distribution of density in the neighborhood of the maximum is given by (16)

$$\log(\rho) = p + ax^2 + by^2 + cz^2 + dx + ey + fz + gxy + hyz + ixz .$$

The least-squares fit for each point was to a $3 \times 3 \times 3$ grid centered as closely as possible to the point of apparent maximum density. The resulting structure is given in part C of figure 2. In the three-dimensional plot of the electron density the carbon atoms were clearly defined even in the presence of the heavy atom. The definition of the carbon atoms suggested that the hydrogen atoms might be resolvable and that their contributions might be significant in the structure-factor calculations. No attempt was made to locate the hydrogen atoms by a difference-Fourier synthesis, but we did calculate their positions and included their contributions in the ensuing structure-factor calculations but not in the least-squares refinement. A hydrogen atom was placed 1.06 \AA from each carbon atom, except C_8 and C_9 , on line with that atom and the center of the ring. The temperature factor of a hydrogen

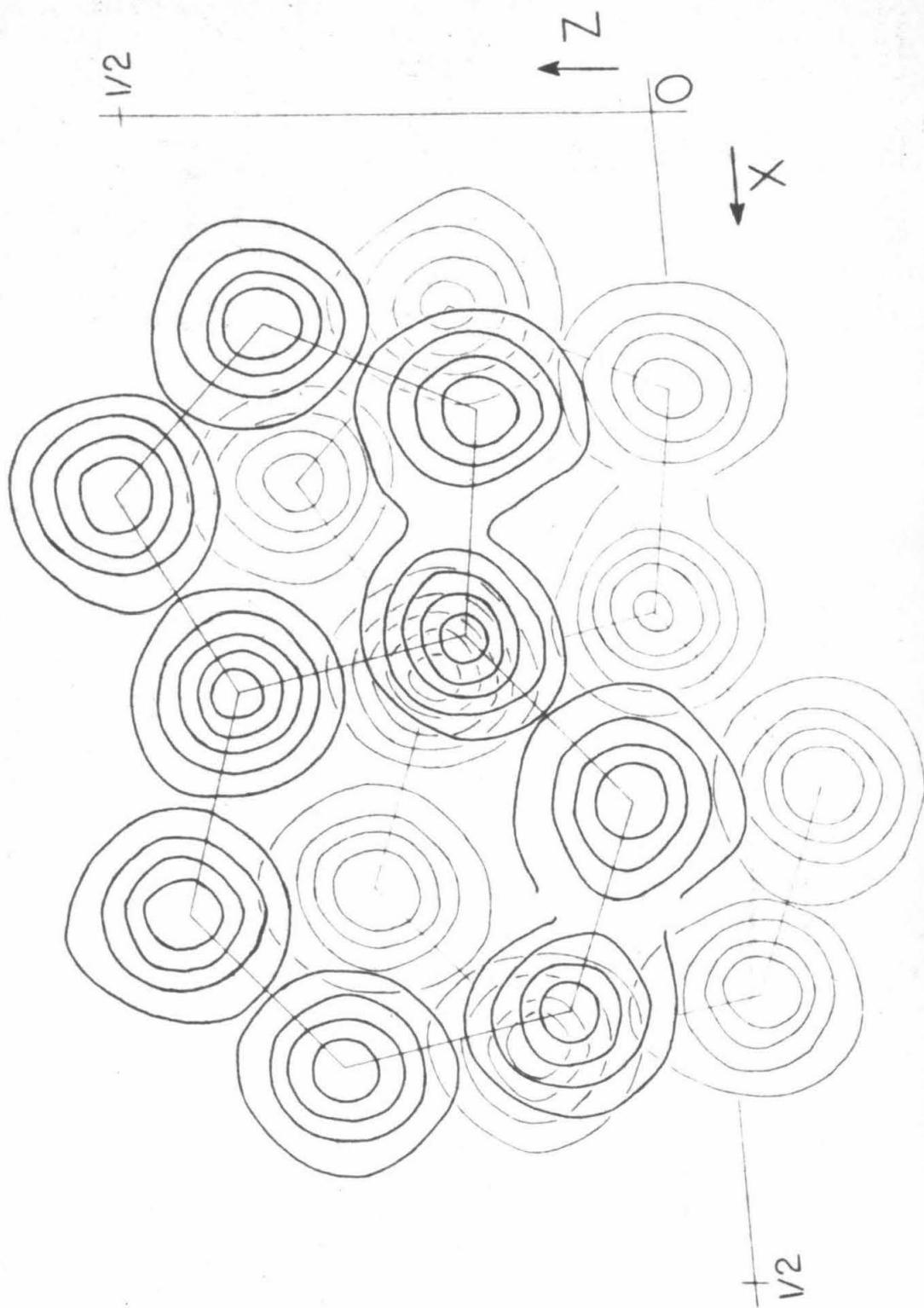


Figure 3. Composite difference Fourier. The Fourier was calculated in sections perpendicular to b with $0.01 b$ ($.14 \text{ \AA}$) between sections. The contours are drawn in sections nearest the corresponding atomic centers at intervals of $2 e. \text{ \AA}^{-3}$ beginning at $2 e. \text{ \AA}^{-3}$.

atom was taken as one unit greater than that of its attached carbon atom. Both the temperature factors and the coordinates of the hydrogen atoms were duly changed in parallel with the carbon atoms as the refinement proceeded.

Least-squares refinement was continued, starting with the atomic coordinates given by the difference-Fourier synthesis, with the temperature factors as given by the last least-squares cycle, and with weighting function I of table 2; however, some of the shifts seemed to be in the wrong direction. (At this point we felt that we knew approximately how the structure should change, for although we did not know what the bond distances should be, we felt that the molecule should have mm symmetry.) We also discovered and corrected a serious error, the F_o of reflection (9 1 2) being changed from 13.9 to 81.9 ($F_c = 64.3$). This error, which had been made in converting intensities to structure factors, was simply overlooked in the previous checks.

We changed to weighting function III of table 2 and again started the refinement with the coordinates from the difference-Fourier synthesis. The R factor of the first cycle was 0.071--a significant improvement from 0.085, the R factor before the difference-Fourier. After four more cycles (numbers 21-24), the refinement had converged ($R = 0.064$) to structure D, figure 2. This structure, however, did not approach mm symmetry as closely as that given by the difference-

Fourier synthesis; for that reason we changed to weighting function IV of table 2 and continued refinement.

After five more least-squares cycles all shifts were below about 10% of the standard deviations, and we stopped refinement with $R = 0.0596$. The final atomic coordinates and temperature factors and their standard deviations are given in the last two columns of table 3, which is a summary of the course of refinement. The bond distances and bond angles calculated from these atomic coordinates are shown in figure 4.

It seems that there are four places where we could have stopped refinement; each possible stopping point is represented by a structure in figure 2. We felt at each of the first three stages, however, that the actual structure was slightly different from the one at hand, and we acted accordingly.

iii) Behavior of unobserved reflections .

Of about 670 reflections which were too weak to be observed, 74 calculated larger than the observable minimum, F_{\min} . All the unobserved reflections are included in the list of observed and calculated structure factors in table 4. The largest observed structure factor is for the (111) reflection, 196 electrons out of 663 in the unit cell; the average value of F_{\min} is 7.24 electrons with a maximum of 11.30 and a minimum of 3.07. The average ΔF for these 74 reflections is 1.11 electrons, and the largest ΔF is 3.82 electrons. The average $\Delta F/F_0$ ratio is 0.18, and the largest is 0.80 (2.95/3.69).

Table 3. Summary of refinement.

Cycle	ΣF_o	ΣF_c	R	ΣwF_o^{4*}	ΣwF_c^{4*}	R'	N**	$(w_e/w)^{1/2***}$
6	69778	68777	.094	2341	2362	.056	2185	2.0+.05 F_o
12	66788	67446	.090	1964	2242	.065	2174	1.8+.05 F_o
16	68678	67135	.085	2217	2214	.039	2136	1.8+.05 F_o
19	68821	66995	.087	2941	2902	.049	2132	F_o
24	68453	67344	.064	2907	2894	.020	2122	F_o
29	66385	65926	.060	1320	1324	.025	2111	F_o^2

* ΣwF_o^4 and ΣwF_c^4 are on the same arbitrary scale for cycles 6, 12, and 16, on the absolute scale for times 10^3 for 19 and 24, and on the absolute scale for the final cycle (29).

**The number of reflections in the least-squares refinement.

***The weighting function remained constant between the designated cycles.

$$R' = \Sigma w(F_o^2 - F_c^2)^2 / \Sigma wF_o^4$$

In the remainder of the table the parameters given are those produced by the designated cycle. The decimal points in the fractional coordinates are omitted except in the final coordinates and the standard deviations. The coordinates in the cycle column labelled S were obtained from the first three-dimensional Fourier synthesis, and in the column labelled DF, from the difference-Fourier synthesis. The isotropic temperature factors, B, are in \AA^{-2} units, and the anisotropic temperature factors, in the form

$$T = \exp - [\alpha h^2 + \beta k^2 + \gamma l^2 + \delta hk + \epsilon hl + \eta kl],$$

of the ruthenium atom are dimensionless and multiplied by 10^5 . Atoms which would be equivalent if the molecule has mm symmetry are grouped together.

The primed positions are in ring II, the unprimed in ring I.

Table 3 (continued - 2)

	S	6	12	16	19	DF	24	Final	σ
Ru									
x	166	1651	1651	1652	1652		1652	.16520	.00003
y	036	0348	0346	0346	0346	same	0346	.03459	.00003
z	252	2638	2636	2637	2637	as	2636	.26366	.00008
α		231	258	256	261	19	236	242.7	2.7
β		275	269	264	255		271	279.0	3.2
γ		1420	1550	1590	1634		1667	1796.2	16.7
δ		9.4	14.2	7.5	4.7		8.5	10.0	4.1
ϵ		116	109	129	147		60	55.9	8.2
η		0.7	-35	-27	-20		-16	-9.0	9.3
C(2)									
x	084	0854	0854	0850	0861	0905	0882	.09037	.00060
y	148	1511	1514	1524	1529	1541	1541	.15444	.00061
z	421	3863	3838	3830	3824	3840	3840	.38416	.00135
B	3.00	3.08	3.24	3.71	3.59	3.59	4.12	3.677	.222
C(2)'									
x	078	0807	0799	0818	0861	0834	0797	.08117	.00064
y	-094	-0944	-0941	-0936	-0940	-0925	-0918	-.09186	.00071
z	248	2128	2063	2058	2110	2060	2000	.20492	.00146
B	3.00	3.16	3.68	4.71	4.86	4.86	4.22	4.232	.251

Table 3 (continued - 3)

	S	6	12	16	19	DF	24	Final	σ
C(1)									
x	127	1216	1217	1221	1237	1277	1246	.12619	.00062
y	175	1813	1817	1811	1808	1809	1815	.18084	.00066
z	209	1873	1871	1874	1876	1896	1885	.18817	.00142
B	3.00	3.17	3.55	3.81	3.72	3.72	4.04	4.006	.236
C(1)'									
x	121	1210	1189	1178	1204	1192	1159	.11735	.00063
y	-067	-0649	-0645	-0641	-0641	-0645	-0646	-.06414	.00064
z	035	0130	0105	0083	0124	0087	0067	.00952	.00144
B	3.00	3.07	3.40	4.15	4.53	4.53	3.59	3.899	.245
C(3)									
x	163	1617	1613	1609	1614	1640	1628	.16338	.00055
y	130	1314	1314	1315	1309	1312	1316	.13054	.00055
z	529	5354	5382	5384	5382	5362	5386	.53986	.00126
B	3.00	2.93	2.73	2.56	2.61	2.61	3.09	3.282	.203
C(3)'									
x	157	1595	1590	1605	1621	1572	1553	.15601	.00052
y	-112	-1170	-1179	-1163	-1158	-1140	-1148	-.11442	.00057
z	355	3703	3729	3734	3751	3643	3616	.36053	.00124
B	3.00	2.89	2.62	2.46	2.61	2.61	2.47	3.213	.202

Table 3 (continued - 4)

	S	6	12	16	19	DF	24	Final	σ
C(8)									
x	232	2254	2236	2233	2235	2237	2216	.22317	.00052
y	170	1770	1791	1782	1776	1768	1783	.17820	.00056
z	211	2175	2195	2193	2199	2208	2190	.21882	.00119
B	3.00	2.94	2.69	2.13	2.19	2.19	2.49	3.091	.192
C(8)'									
x	226	2133	2138	2125	2120	2138	2139	.21512	.00054
y	-072	-0734	-0732	-0727	-0724	-0709	-0713	-.07173	.00056
z	037	0313	0331	0309	0305	0377	0336	.03456	.00124
B	3.00	2.93	2.77	1.95	1.87	1.87	2.12	3.155	.206
C(9)									
x	253	2535	2525	2517	2524	2483	2485	.24844	.00049
y	143	1477	1481	1470	1468	1460	1460	.14645	.00049
z	437	4446	4449	4434	4435	4353	4366	.43607	.00108
B	3.00	3.05	3.10	2.61	2.51	2.51	2.42	2.589	.181
C(9)'									
x	247	2333	2351	2367	2368	2387	2413	.24044	.00049
y	-098	-1032	-1018	-1018	-1021	-1017	-1024	-.10267	.00054
z	263	2511	2478	2490	2479	2523	2536	.25117	.00113
B	3.00	2.81	1.96	1.12	1.41	1.41	1.67	2.846	.182

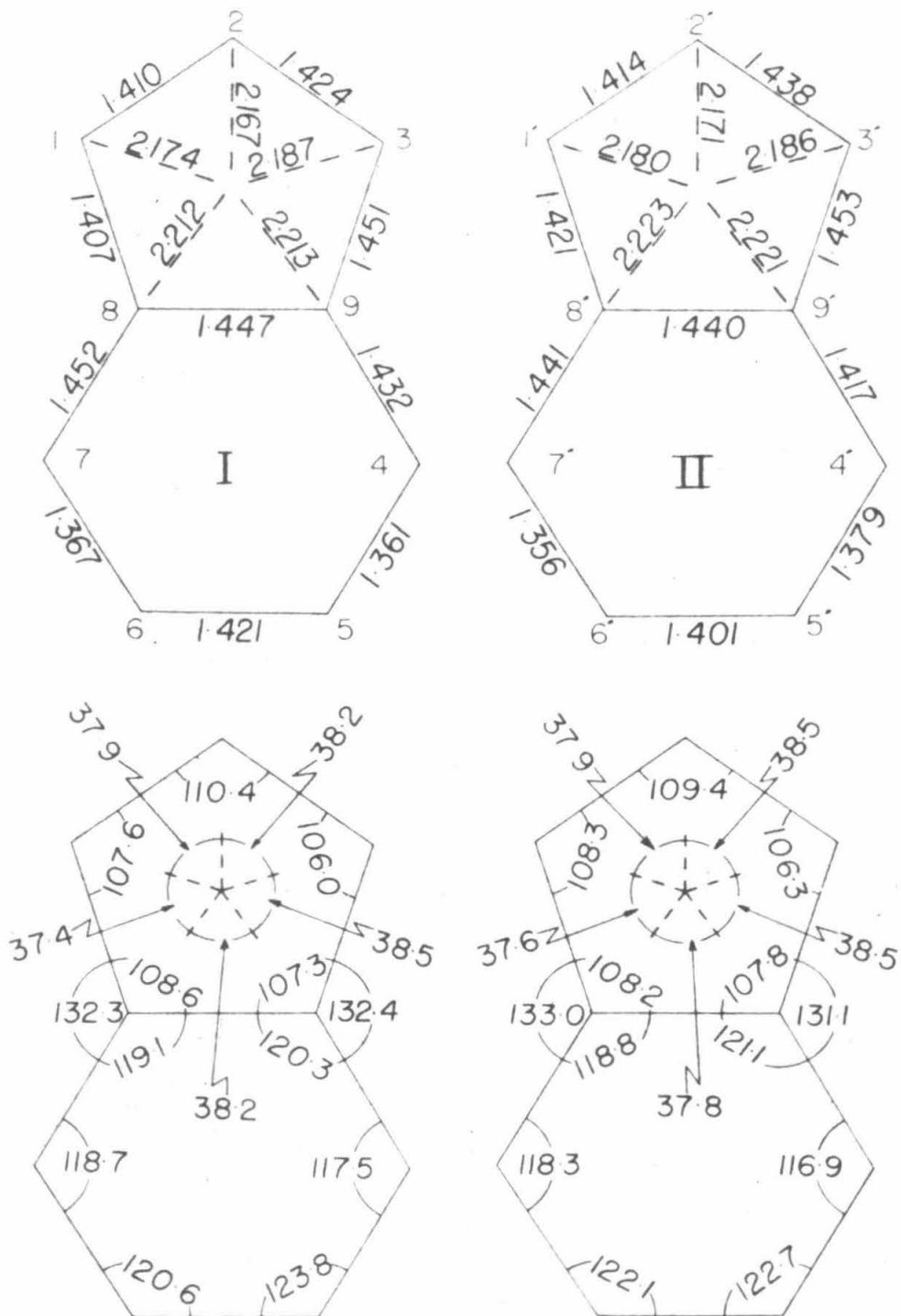
Table 3 (continued - 5)

	S	6	12	16	19	DF	24	Final	σ
C(7)									
x	302	2936	2931	2931	2925	2951	2957	.29553	.00058
y	197	1989	1989	1994	1990	1954	1984	.19810	.00057
z	059	0686	0685	0681	0683	0760	0749	.07593	.00134
B	3.00	3.00	3.00	3.01	3.24	3.24	3.45	3.688	.228
C(7)'									
x	296	2935	2933	2928	2928	2885	2883	.28715	.00052
y	-045	-0542	-0543	-0544	-0539	-0533	-0541	-.05290	.00056
z	-115	-1039	-1042	-1060	-1040	-1038	-1088	-.10734	.00119
B	3.00	2.93	2.62	2.07	2.19	2.19	2.81	3.472	.192
C(4)									
x	337	3497	3493	3493	3508	3434	3437	.34365	.00056
y	132	1346	1349	1345	1346	1354	1349	.13469	.00057
z	518	5178	5157	5140	5168	5061	5065	.50834	.00129
B	3.00	3.17	3.58	4.19	4.30	4.30	3.37	3.343	.206
C(4)'									
x	331	3299	3302	3314	3307	3320	3349	.33426	.00059
y	-110	-1165	-1162	-1167	-1165	-1157	-1165	-.11604	.00061
z	344	3206	3193	3227	3212	3221	3256	.32438	.00140
B	3.00	3.00	2.95	2.79	2.95	2.95	3.24	3.745	.226

Table 3 (continued - 6)

	S	6	12	16	19	DF	24	Final	σ
C(6)									
x	385	3831	3845	3849	3834	3845	3863	.38546	.00065
y	179	1857	1856	1858	1852	1845	1855	.18388	.00070
z	143	1441	1443	1449	1436	1479	1497	.14991	.00151
B	3.00	3.14	3.63	4.73	4.77	4.77	4.95	4.381	.254
C(6)'									
x	379	3826	3831	3830	3834	3771	3770	.37615	.00069
y	-063	-0677	-0668	-0666	-0662	-0653	-0662	-.06477	.00068
z	-029	-0165	-0177	-0212	-0204	-0282	-0292	-.02994	.00154
B	3.00	3.05	3.06	3.29	3.39	3.28	3.84	4.323	.268
C(5)									
x	411	4118	4125	4137	4131	4087	4102	.40774	.00061
y	147	1518	1525	1531	1527	1515	1533	.15253	.00067
z	362	3656	3640	3648	3656	3647	3643	.36423	.00141
B	3.00	3.15	3.65	4.32	4.03	4.03	4.48	3.921	.235
C(5)'									
x	405	4071	4046	4024	4001	4003	4002	.39957	.00065
y	-095	-0956	-0956	-0948	-0954	-0965	-0941	-.09459	.00070
z	188	1894	1834	1814	1904	1826	1789	.18158	.00151
B	3.00	3.21	3.89	5.22	5.50	5.50	4.18	3.937	.254

Figure 4. Final bond distances and angles.



iv) Possible sources of error:

a) Absorption and extinction.

We have made no correction for absorption or extinction.

Either absorption effects must be very small or compensation for absorption has been made by the temperature factors; we observe no systematic trends in the discrepancies between the F_o 's and F_c 's. Extinction is evident in two reflections, which are characterized as follows:

reflection	F_o	F_c	F/F_o	w_e
200	151.4	-187.7	.239	1.0
020	118.8	154.7	.294	0.6

Because of the weighting function employed in the last stages of refinement, $w \propto 1/F_o^4$, these reflections had a low weight compared to the average reflection (average $F_o = 32.6$), and their influence on the structure should be very small.

b) Scattering curve of ruthenium.

We compared the scattering curve of ruthenium used in our calculations (Thomas-Umeda, 10) with an empirical scattering curve which would fit our data. We did this by obtaining $|F_{Ru}|$ and $||F_o| - |F_c - F_{Ru}||$ for each reflection and collecting sums of both quantities as a function of $\sin^2\theta$, where F_{Ru} is the ruthenium contribution to F_c and $F_c - F_{Ru}$ is the sum of the carbon and hydrogen contribution to F_c . The two absolute quantities should be approximately equal and differences in their sums

should reflect systematic errors in the F_o 's or errors in the theoretical scattering curve, or both. We compiled table 5 during the last least-squares cycle and plotted the results in figure 5. We used the Thomas-Umeda scattering curve as a base and employed the corrections indicated by table 5 and figure 5 to derive an empirical scattering curve and plotted the curve in figure 6. The curve looks unreasonable in the region from 0.60 to 0.75 in $\sin^2\theta$; in this region the scattering power increases as $\sin^2\theta$ increases. This may be experimental error since this is the region of $\sin^2\theta$ where reflections began to be resolved into the α_1 and α_2 components.

Discussion of Results

- i) Molecular structure:
 - a) Bond distances and angles.

The final bond distances and bond angles have been given in figure 4. Tables 6 and 7 list the distances and angles along with their averages for a molecule of mm symmetry; other information to be discussed below is also given in table 6. Much more will be said about the bond distances in the discussions that follow. These tables are presented at this time primarily for reference.

Two features of the molecular structure should be emphasized. First, the ruthenium atom is not on the axis joining the centers of the two five-membered rings but is displaced by a small but significant

Table 5. Data for empirical scattering curve.

$\sin^2 \theta_{\text{Cu}}$	N	$\frac{\Sigma F_{\text{Ru}} }{N}$	$\frac{\Sigma D}{N}$	$\frac{\Sigma F_{\text{Ru}} / \Sigma D}{N}$
0-0.1	89	5718.4	5825.5	1.020*
0.1-0.2	160	8011.8	7955.3	.993
0.2-0.3	178	7405.7	7405.1	1.000
0.3-0.4	215	7750.4	7844.1	1.012
0.4-0.5	220	6970.1	7109.0	1.020
0.5-0.6	247	6685.1	6784.4	1.015
0.6-0.7	228	6001.3	5902.7	.983
0.7-0.8	252	5969.3	5585.5	.936
0.8-0.9	268	5344.0	5040.9	.943
0.9-1.0	181	3148.0	3260.3	1.035

N is the number of observed reflections in that region of $\sin^2 \theta$.

$$\frac{\Sigma D}{N} = \frac{\Sigma | |F_o| - |F_c - F_{\text{Ru}}| |}{N}$$

*If the (200) and (020) reflections are omitted, the ratio is 1.006 (see text).

Figure 5. A plot of the ratio of the theoretical to empirical scattering curves as a function of $\sin^2 \theta$.

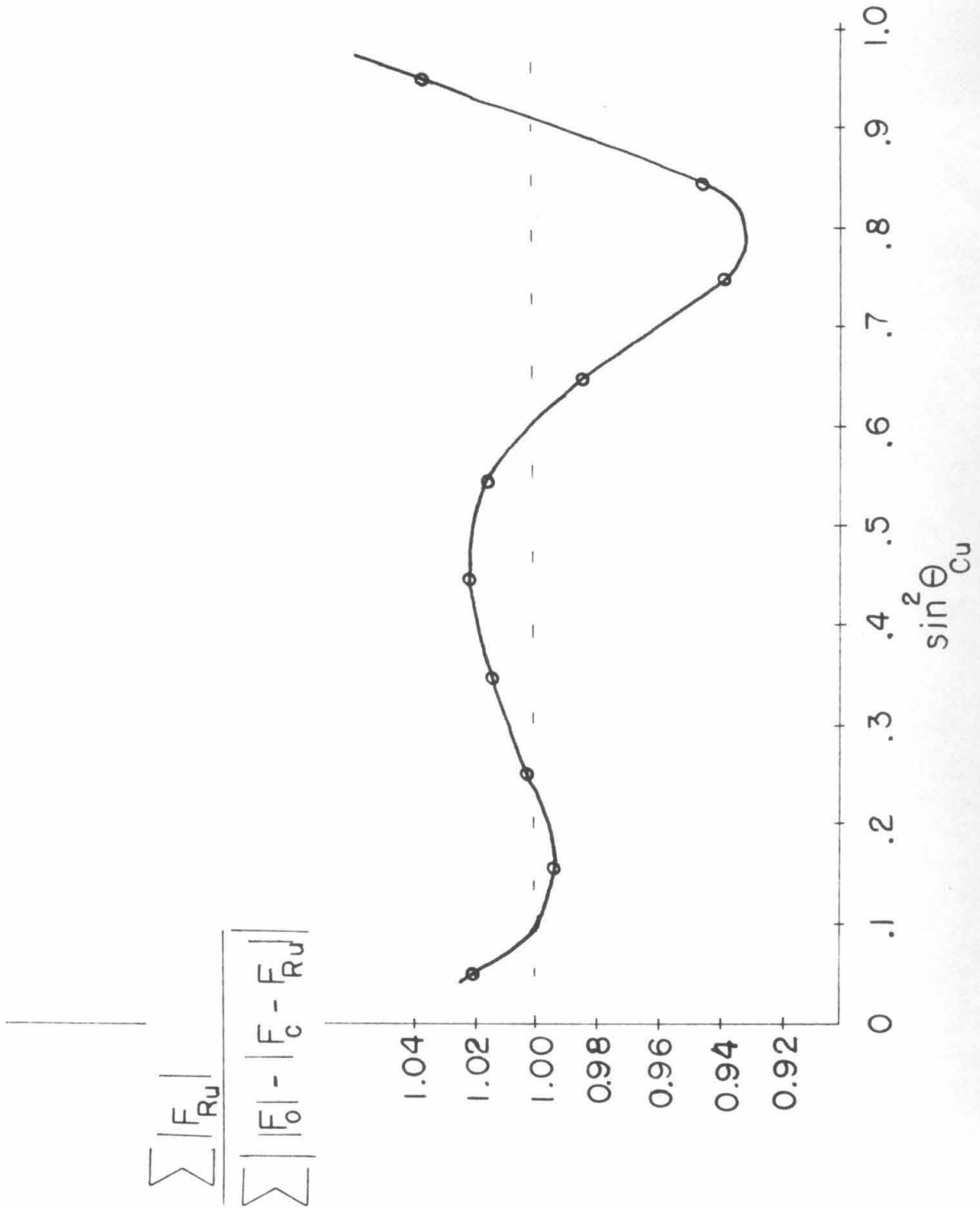


Figure 6. Theoretical and empirical scattering curves for ruthenium.

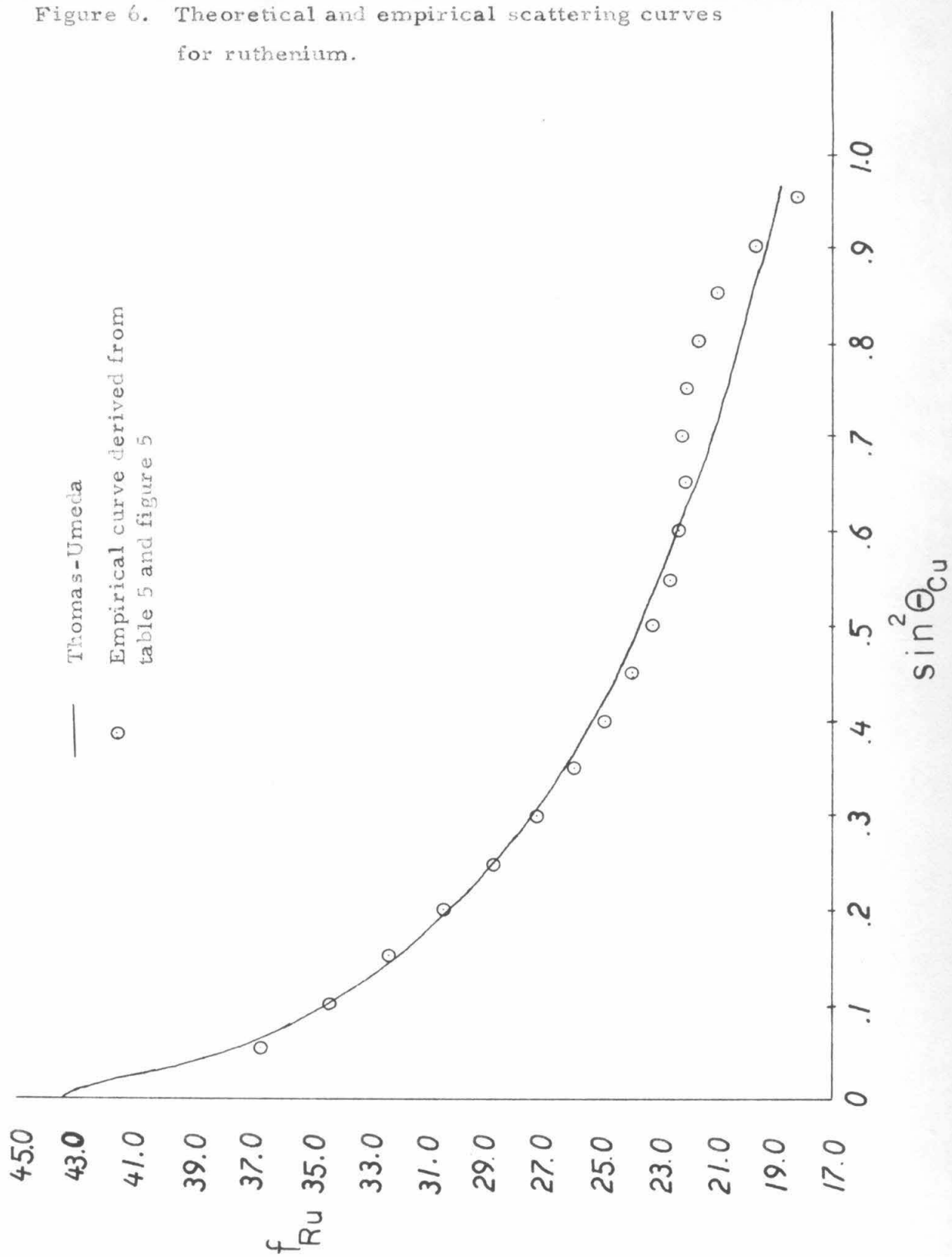


Table 6. Bond distances and bond numbers.

C-C	Distances (Å)			Predicted	Bond Numbers	
	Observed I	II	Mean		Obs.	Pred.
1-2	1.414	1.410				
			1.422 \pm .011	1.441	1.34	1.24
2-3	1.438	1.424				
8-1	1.421	1.407				
			1.433 \pm .018	1.457	1.28	1.18
3-9	1.453	1.451				
8-9	1.440	1.447				
			1.444 \pm .004	1.461	1.23	1.16
9-4	1.417	1.432				
			1.436 \pm .013	1.441	1.27	1.24
7-8	1.441	1.452				
4-5	1.379	1.361				
			1.366 \pm .009	1.365	1.71	1.71
6-7	1.356	1.367				
5-6	1.401	1.421				
			1.411 \pm .010	1.441	1.40	1.24
Ru-C						
C ₂	2.171	2.167				
			2.169 \pm .002	2.197	.51	.46
C ₁	2.180	2.174				
			2.182 \pm .005	2.159	.48	.53
C ₃	2.186	2.187				
C ₈	2.223	2.212				
			2.217 \pm .005	2.245	.42	.38
C ₉	2.221	2.213				

The standard deviations given reflect only the internal consistency among chemically equivalent distances; they are calculated by

$(\sum_i^n (m-x_i)^2/n)^{\frac{1}{2}}$. From the least-squares standard deviations of atomic coordinates, the standard deviation of a C-C distance is $\pm .012$ Å and of a Ru-C distance, $\pm .008$ Å.

Table 7. Bond angles.

C-C-C	I	II	Mean
1-2-3	109.4	110.4	109.5 \pm 0.5
2-3-9	106.3	106.0	107.1 \pm 0.9
2-1-8	108.3	107.6	
3-9-8	107.8	107.3	108.0 \pm 0.5
1-8-9	108.2	108.6	
3-9-4	131.1	132.4	132.2 \pm 0.7
1-8-7	133.0	132.3	
8-9-4	121.1	120.3	119.8 \pm 0.9
7-8-9	118.8	119.1	
9-4-5	116.9	117.5	117.9 \pm 0.7
6-7-8	118.3	118.7	
4-5-6	122.7	123.8	122.3 \pm 1.2
5-6-7	122.1	120.6	
C-Ru-C			
1-R-2	37.9	37.9	38.1 \pm 0.2
2-R-3	38.5	38.2	
3-R-9	38.5	38.5	38.0 \pm 0.5
1-R-8	37.6	37.4	
8-R-9	37.8	38.2	38.0 \pm 0.2

The standard deviations of the mean are taken equal to $\left(\frac{\sum_i^n (m-x_i)^2}{n}\right)^{\frac{1}{2}}$.

The least-squares standard deviations of atomic coordinates give a standard deviation of $\pm 0.7^\circ$ for a C-C-C angle and of $\pm 0.5^\circ$ for a C-Ru-C angle.

amount (approximately $.03 \text{ \AA}$) toward positions 2 (see figure 4). The agreement between the halves of the molecule and the estimated standard deviations, obtained as a by-product of the least-squares calculations and confirmed by the general agreement between structurally equivalent bond distances, make the differences in Ru-C bond lengths significant. The second feature is the shortness of the C_6-C_7 and C_4-C_5 bonds (see figure 4 and table 8). Trotter found the iron atom in bis-indenyliron to be displaced toward positions 2, but he found the short bond to be C_5-C_6 . Because Trotter worked with a disordered crystal, we feel our values of the molecular dimensions are more reliable. (He reports only the mean bond distances and gives no standard deviations.) In saying this, we imply that there is no reason for the indenyl groups to be different in the two compounds.

b) General features.

Within experimental error, the carbon atoms constituting an indenyl group are coplanar, and the planar indenyl groups are parallel. The indenyl groups are in the eclipsed configuration, and, within experimental error, the molecule has mm symmetry as in ruthenocene (17). In bis-indenyliron and ferrocene (18), however, the carbon atoms in the five-membered rings are staggered. If one considers only local symmetry in molecules of this type, one can say that an iron atom prefers to occupy a center of symmetry while a ruthenium atom prefers to lie in a mirror plane.

The least-squares plane of each indenyl group was calculated by the method of Blow (19) using a program written for the Burroughs 220 by Mr. Noel D. Jones. The out-of-plane distance of each atom and the direction cosines of a normal vector to each plane are given in table 8; the angle between the two normals is about 0.8° .

To determine if there is any departure from the eclipsed configuration of the indenyl groups we calculated an average vector from the carbon atoms in one plane to the corresponding atoms in the other; direction cosines of this average inter-ring vector are given in table 8. The direction cosines of the two normal vectors were also averaged and normalized to define an average-normal vector; the angle between this average-normal vector and the average inter-ring vector is 0.2° , which means that the indenyl groups are eclipsed, certainly within experimental error.

In calculating an average inter-ring vector, we also calculated each individual distance and averaged these for an average inter-ring separation (see table 8). The average separation is 3.665 \AA compared to 3.68 \AA for ruthenocene. The average separations in bis-indenyliron and ferrocene are 3.43 and 3.32 \AA .

c) Prediction of bond distances.

Let us employ a method used by Pauling (20a) to discuss the molecules of ruthenocene and ferrocene to predict a molecular structure

Table 8. Out-of-plane distances, inter-ring separation and direction cosines of a normal vector to each ring.

C	Out-of-plane distance		Separation
	Ring I	Ring II	
2	-.001	.002	3.636
1	-.020	-.010	3.617
3	-.010	-.015	3.618
8	.018	.013	3.694
9	.016	.009	3.684
7	.019	.008	3.706
4	.012	.019	3.704
6	-.015	-.008	3.669
5	-.018	-.018	<u>3.653</u>
Origin	2.817	0.812	3.665 (average)

All distances are in Angstrom units. The distance to the origin is the absolute distance. The out-of-plane distance is taken as negative if it is toward the ruthenium atom and as positive if it is out-of-plane away from the ruthenium atom, toward the outside of the molecule.

Direction Cosines*

	Ring I	Ring II	Normalized Average	Average Inter-ring (C-C)
cos x	.01012	.02175	.015935	.011653
cos y	.95040	.95156	.951004	.951023
cos z	.31085	.30667	.308768	.308902

In orthogonal systems whose axes are parallel to a, b, and c of the monoclinic cell.

for bis-indenyliron and bis-indenylruthenium. In doing so we will assume that the iron and ruthenium atoms use all nine of their valence orbitals for bond formation or for occupancy by unshared electrons or electron pairs. Hence, we expect corresponding bonds in the two compounds to have identical bond numbers, and the only difference in the two molecules will be in the metal-to-carbon bond distances, reflecting different sizes of the metal atoms. After Pauling, we consider the 1287 structures represented in figure 7. The horizontal bars represent double bonds that are basically part of the five-membered ring, and the vertical bars represent Ru-C bonds. The number below each diagram is the number of structures of that type. We can count the number of appearances of each canonical form, assuming equal weight; the counting is summarized in table 9.

In every canonical form each carbon-to-carbon bond is a single or a double bond. Therefore, to count the bond number we only have to count the number of times it appears as a double bond; we can also predict the Ru-C bond number by counting bonds. Both countings are summarized in table 10, and the comparison between predicted and observed C-C bond distances is also made there.

We see immediately that there is good agreement between the observed and predicted bond lengths for bis-indenylruthenium and that Pauling's treatment does indeed predict the shortness of the C_6-C_7 and

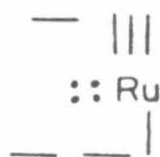
Figure 7. A representation of resonating-bond structures.



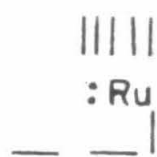
A 49



B 36



C 48



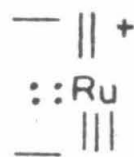
D 14



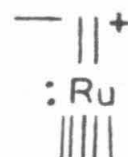
E 12



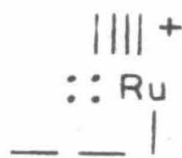
F 420



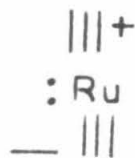
G 360



H 60



I 126



J 108



K 18



represents

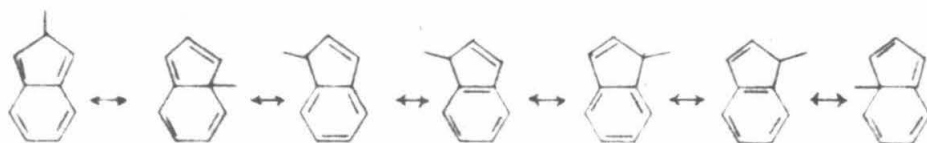


Table 9. Counting canonical forms.

Symbol							
Ru-C bonds	1	3	5	5	2	4	
Number of forms	7	6	1	30	9		
Number of times each appears in							
A	14						
B		12					
C	12	14					
D	2		14				
E		2	12				
F	60				14		
G		60			12		
H			60		2		
I	18					14	
J		18				12	
K			18			2	
							Totals
Subtotals	106	106	104	28	28	372	
Number of forms	742	636	104	840	252	2574	
Ru-C bonds	742	1908	520	1680	1008	5858	
Double bonds	2968	1908	208	2520	504	8108	

Table 10. Prediction of carbon to carbon bond distances and ruthenium to carbon bond numbers.

		C_3-C_9	C_2-C_3		C_6-C_7	C_7-C_8
Double bonds in		C_8-C_1	C_1-C_2	C_9-C_8	C_4-C_5	C_9-C_4
Type*	Weight*					C_5-C_6
1	106	2	3	2	5	2
3	106	1	1	1	5	1
5	104				1	
2	28	5	7	3	18	9
4	28				6	2
Weighted totals		458	620	402	1836	626
Double bond character**		.178	.241	.156	.713	.243
Predicted bond distances*** (Å)		1.457	1.441	1.461	1.365	1.441
Observed:						
bis-indenyl-ruthenium		1.433	1.422	1.444	1.366	1.428
bis-indenyl-iron		1.41	1.47	1.39	1.45	1.40
						(C_5-C_6 , 1.30)

Table 10 (continued)

Ru-C bonds in		C ₉	C ₈	C ₁	C ₃	C ₂
Type*	Weight*					
1	106	1	1	2	2	1
3	106	3	3	4	4	4
5	104	1	1	1	1	1
2	28	10	10	14	14	12
4	28	6	6	8	8	8
Weighted totals		976	976	1356	1356	1194
					(5858 total)	
Bond number		.379	.379	.527	.527	.464

* See table 9. Type is the number of Ru-C bonds.

**Fraction of total forms (2574) in which it appears as a double bond.

***See Pauling (20), tables 7-9.

C_4-C_5 bonds. That the C_6-C_7 and C_4-C_5 bonds are nearly double bonds (75%) is supported by Seus (21) who was able to hydrogenate bis-indenylruthenium to produce bis-4, 5, 6, 7-tetrahydroindenylruthenium. If, on the other hand, the double bond were in the C_5-C_6 position, as indicated by Trotter's work, one would expect hydrogenation to yield bis-5, 6-dihydroindenylruthenium.

To predict the Ru-C bond distances in the same way that Pauling treated ferrocene and ruthenocene, we must first calculate the d character of the ruthenium bond orbitals. If we assume that the unshared pairs occupy 4d orbitals and that the bonding electrons are distributed equally among the 5s, $5p^3$ and unoccupied 4d orbitals, then we calculate that the d character is 41.6%. We get the same d character for the iron atom in bis-indenyliron, except that we are referring to 3d orbitals. This amount of d character leads to the single-bond radii for ruthenium and iron of 1.313 and 1.137 Å (20b). An alternative is to use the single bond radii as given in Pauling's table of metallic radii (20c); from this table we get single bond radii of 1.264 and 1.165 Å for ruthenium and iron. Using a single bond radius of 0.770 Å for carbon and correcting for electronegativity difference (-0.056 Å for Fe-C and -0.024 for Ru-C), we calculate the following metal-to-carbon bond lengths (in Å) :

	<u>single bond radius used</u>		observed distance
	(<u>d</u> character)	(metallic)	
ferrocene	2.045	2.075	2.05
ruthenocene	2.246	2.188	2.21
bis-indenylruthenium	2.268	2.201	2.19
bis-indenyliron	2.060	2.088	2.10

There is better agreement between the observed and calculated bond lengths if one chooses the metallic radii; hence, the single bond radii of iron and ruthenium will be taken as 1.165 and 1.246 Å (the metallic radii) in all discussions that follow as well as in all tables and figures where it is necessary to use such radii.

In table 6 we have summarized the information on bond distances and bond numbers; we have assumed mm symmetry. Figure 8 shows the average bis-indenylruthenium and bis-indenyliron molecules as observed and also the predicted molecules to facilitate comparison.

We should point out that the predicted and observed structures agree well except for the metal-to-carbon bonds. We have predicted correctly that the longest metal-to-carbon bond is that to C₈ or C₉, but the relative lengths of the other bonds are not predicted correctly. The average metal-to-carbon bond distance, however, agrees well with the average of the observed distances.

From table 6 we can calculate the number of observed and predicted covalent bonds for each carbon atom, assuming the C-H bond number to be 1.000; the covalent bonds are listed:

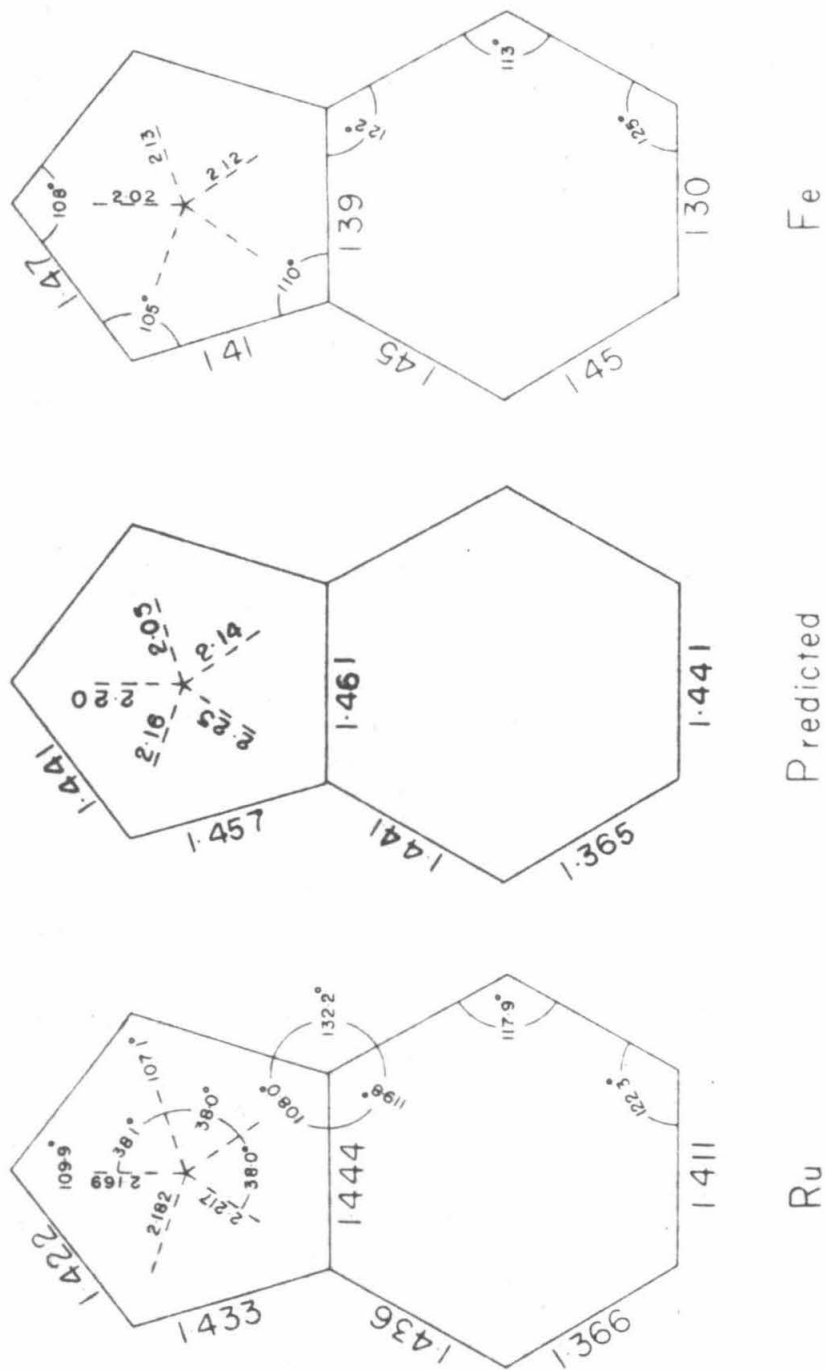


Figure 8. Observed and predicted bond distances (in Å) in bis-indenylruthenium, bis-indenyliron, ruthenocene, and ferrocene.

	C ₂	C _{1,3}	C _{8,9}	C _{4,7}	C _{5,6}
Observed	4.178	4.097	4.194	3.973	4.106
Predicted	3.946	3.946	3.956	3.956	3.956

We judge that we have observed more electrons than are available for bonds. (This was apparent earlier in table 6, where the expected bond numbers are less than those observed, which of course is a result of the observed distances being less than those predicted.) It may well be that some of our observed distances are shorter than those in the true structure because we have not attempted to correct for thermal motion of the atoms. But in our prediction of the bond numbers we have neglected any purely ionic molecules in which a negative charge would reside on the indenyl group or groups; this would increase the predicted bond numbers.

We can find no support for longer bond distances in the results of the three-dimensional difference-Fourier (see figure 2C and figure 3) or in an electron-density map drawn in the least-squares plane of each indenyl group (figure 9). If anything, these results indicate even shorter bond lengths than given by the least-squares refinement. We feel, however, that figure 9 may be a little misleading because the ruthenium may contribute to the electron density in the five-membered rings and by doing so displace the maxima toward the center of the ring; the ruthenium contribution has been removed in figure 3.

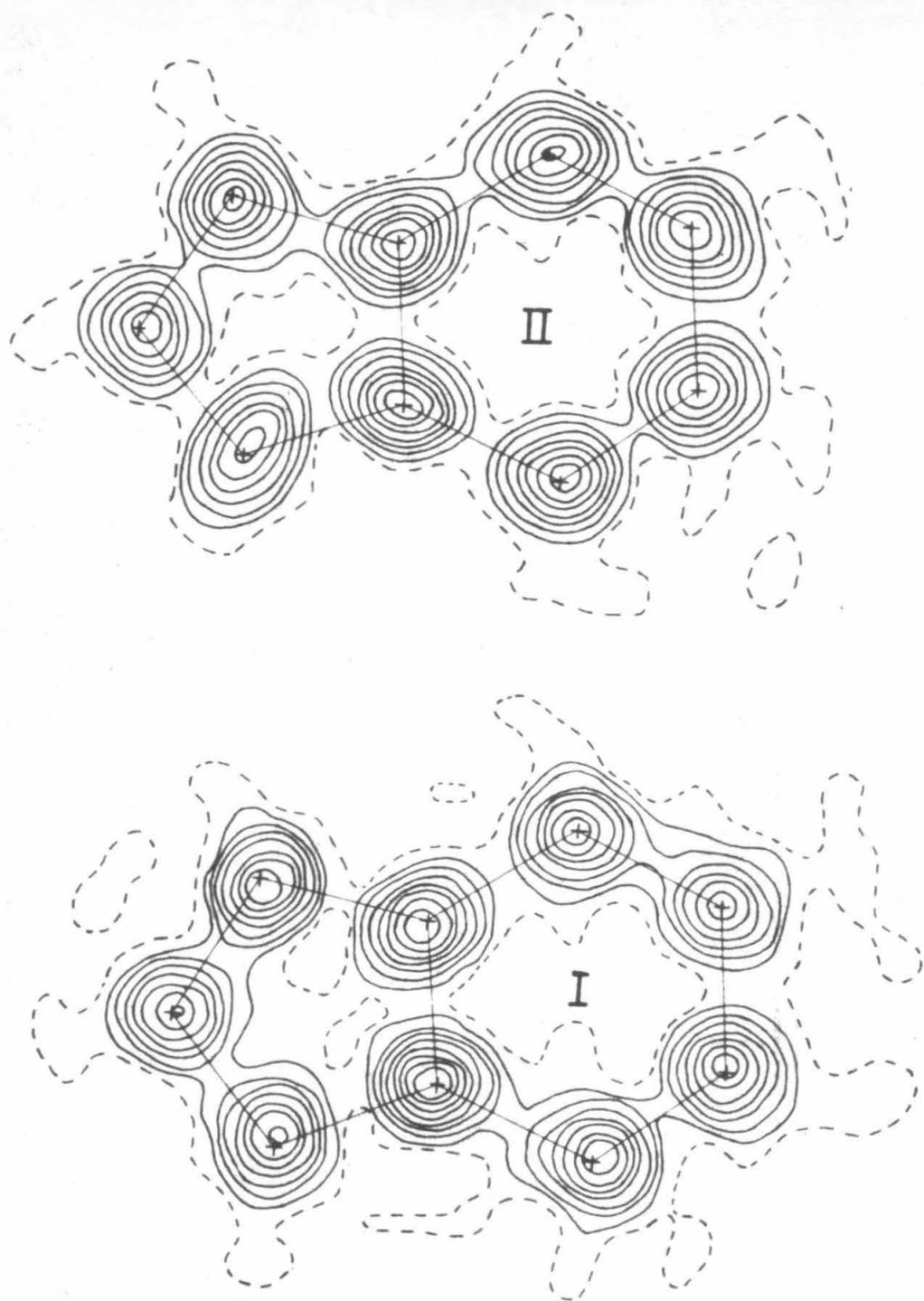


Figure 9. The electron density in the planes of the indenyl groups. Contours are drawn at intervals of 1 e. \AA^{-3} starting with the dashed line at 1 e. \AA^{-3} . The final positions are marked with an x.

d) Temperature factors.

We have said earlier that the final result as we present it is the "best" result that the investigation has yielded--because the agreement between the observed and calculated structure factors is the best and because this final molecule approaches mm symmetry more closely than any other. There is yet another reason for our feeling that the final result is the "best"; this reason is the pattern and agreement of temperature factors in the indenyl groups.

One can examine table 3 and see that in our final result the temperature factors of corresponding carbon atoms agree well and fit into the expected pattern of thermal motion better than in any other stage of refinement. Moreover, the range of temperature factors is smaller than at any other stage. The final temperature factors are given again in table 11; as expected, the thermal motions of the atoms on the ends of the indenyl groups are the largest while the smallest motions are by the atoms common to the two rings.

The anisotropic motion of the ruthenium atom is described by its vibrational ellipsoid, which is defined in table 12. The motion is essentially isotropic.

ii) Packing of the molecules in the unit cell.

The packing of the molecules in the unit cell is illustrated in figures 10 and 11. There are only six non-bonded distances which are short enough to mention.

Table 11. Isotropic temperature factors (B) .

	I	II	Mean
C ₂	3.677	4.232	3.955
C ₁	4.006	3.899	3.601
C ₃	3.284	3.213	
C ₈	3.091	3.155	2.920
C ₉	2.589	2.846	
C ₇	3.688	3.472	3.562
C ₄	3.343	3.745	
C ₆	4.381	4.322	4.140
C ₅	3.921	3.937	

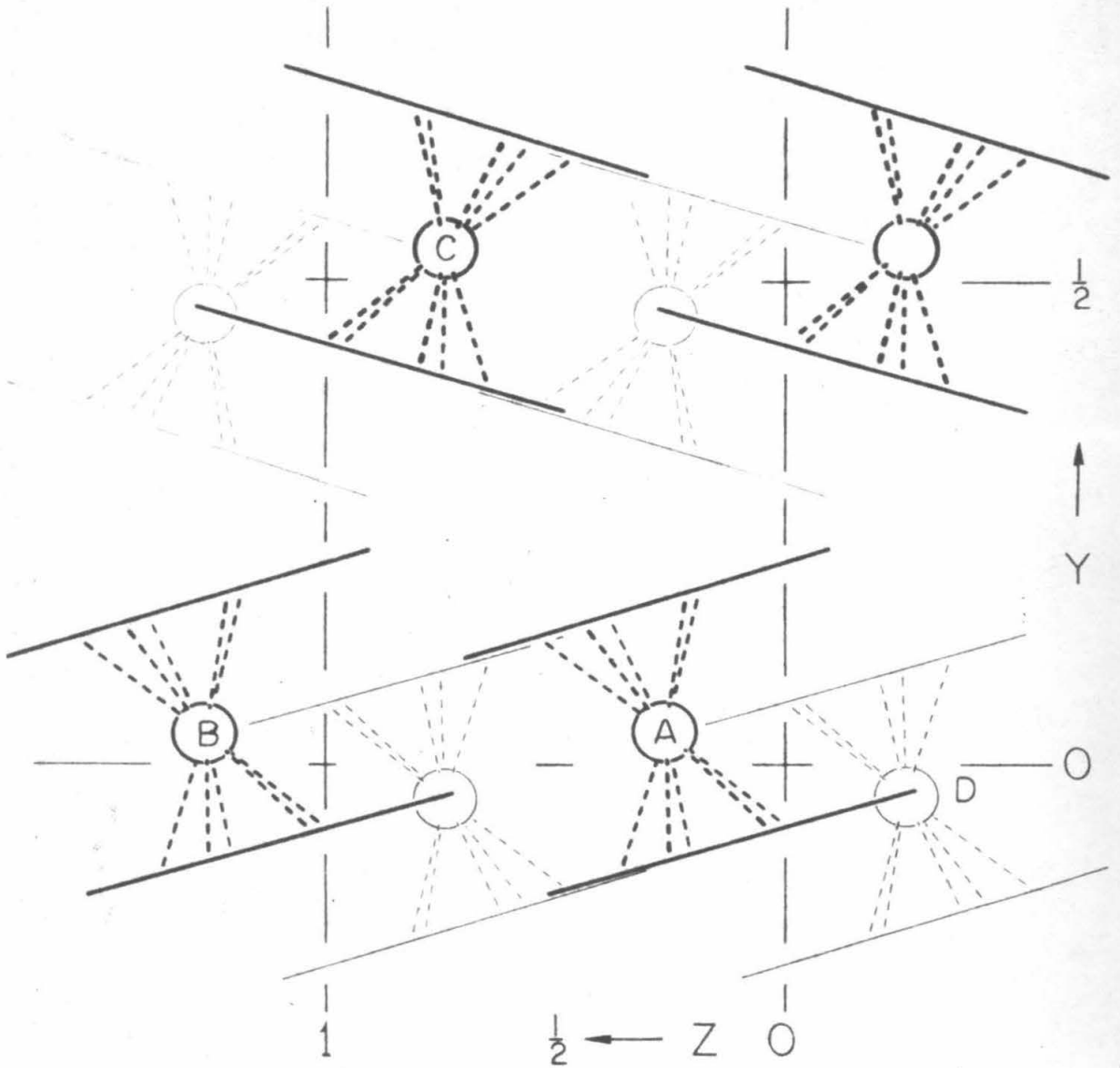
The standard deviations as given by the least-squares treatment are about $\pm 0.22 \text{ \AA}^{-2}$, ranging from ± 0.18 to $\pm 0.27 \text{ \AA}^{-2}$ (see table 3).

Table 12. Vibration ellipsoid of the ruthenium atom.

axis i	B_i	Direction cosines		
		cos x	cos y	cos z
1	2.787	-.1327	-.0363	.9905
2	2.212	.2075	.9762	.0636
3	2.023	.9692	-.2139	.1220

The direction cosines are relative to a Cartesian coordinate system which has two axes identical to a and b of the monoclinic cell of bis-indenylruthenium; the third axis is parallel to c.*

Figure 11. A representation of the structure viewed down a.



The ruthenium atom is approached by three hydrogen atoms. The ruthenium atom of molecule A, figure 11, is 3.3 Å from the hydrogen atom on C(7)' of molecule B, 3.6 Å from the hydrogen on C(1) of molecule D, and 3.6 Å from the hydrogen on C(3) of the molecule displaced minus one unit along z (This molecule is not pictured; the relationship is the same as that between Ru_B and the hydrogen on C(3)_A. In this discussion, the primed positions are for that indenyl group (II) having the less positive y coordinates.). This packing effect with the hydrogen atoms approaching the ruthenium atom is also observed in ruthenocene (17). The distances from C(7) of molecule B to C(8)' and C(9)' of molecule C are 3.48 and 3.31 Å. The distance from the hydrogen atom on C(7) of molecule B to C(8)' of molecule C is 2.7 Å.

A little more will be said about the packing in discussing a disordered crystal. We feel that the packing is adequately described in figures 10 and 11 and that words would not enlighten the reader.

iii) Accuracy of the molecular geometry.

The standard deviations in individual atomic coordinates obtained by inversion of the normal equation matrices lead to mean standard deviations of .008 Å for Ru-C bond lengths and of .012 Å for C-C bonds. The root-mean-square (rms) deviations of chemically equivalent bonds agree with these expected uncertainties. All three groups of chemically equivalent Ru-C bonds have a rms deviation of

less than $.006 \text{ \AA}$. All six sets of C-C bonds have a rms deviation of less than $.019 \text{ \AA}$, and only two sets have a rms deviation larger than the expected $.012 \text{ \AA}$. There is no doubt that the Ru-C₈ and Ru-C₉ bonds are significantly longer ($.03 \text{ \AA}$) than the other Ru-C bonds and that the C₆-C₇ and C₄-C₅ bonds are significantly longer than any other C-C bonds. Bond distances and rms deviations are listed in table 6.

In a recent investigation of the crystal structure of the dimer of rhodium chloride 1,5-cyclooctadiene, Ibers and Snyder (22) attempted "to answer the question: How well can carbon ring geometry be defined in the presence of second-row transition metals, if intensity data collected at room temperature and estimated visually are used?" In that investigation they expressly took into account anisotropic thermal motions of the heavy atoms.

The molecular structure of the dimer of rhodium chloride 1,5-cyclooctadiene and of bis-indenylruthenium are suitable for comparison. Rhodium and ruthenium are adjacent, second-row transition elements, and the rhodium atoms are bonded to four carbon atoms and to two chlorine atoms while the ruthenium atom is bonded to ten carbon atoms. Furthermore, mm symmetry can be logically assumed for both molecules, though this symmetry is not crystallographic.

Ibers and Snyder report $.03 \text{ \AA}$ for the standard deviation of a Rh-C bond and $.08 \text{ \AA}$ for the standard deviation of a C-C bond. In particular, let us compare the C_5-C_6 and C_1-C_2 bonds, the double bonds, of rhodium chloride 1,5-cyclooctadiene with the C_1-C_8 and C_3-C_9 bonds (which is the most inconsistent set of four bonds within the molecule) of bis-indenylruthenium. The four bonds, which should be equal within each molecule, are (in \AA):

rhodium chloride 1,5- <u>cyclooctadiene</u>		bis-indenylruthenium	
C-C		C-C	
1-2	1.52	8-10	1.42
5-6	1.42	3-9	1.45
1'-2'	1.36	8'-10'	1.41
5'-6'	1.44	3'-9'	1.45
Mean	1.44		1.43
σ	.06		.02

From the results of their investigation, Ibers and Snyder conclude "that the ring geometry is difficult to define even when anisotropic thermal motions of the heavy atoms are incorporated into the theoretical model." However, we feel that the ring geometry can be well defined, certainly to within $.02 \text{ \AA}$ in the bonds within the ring.

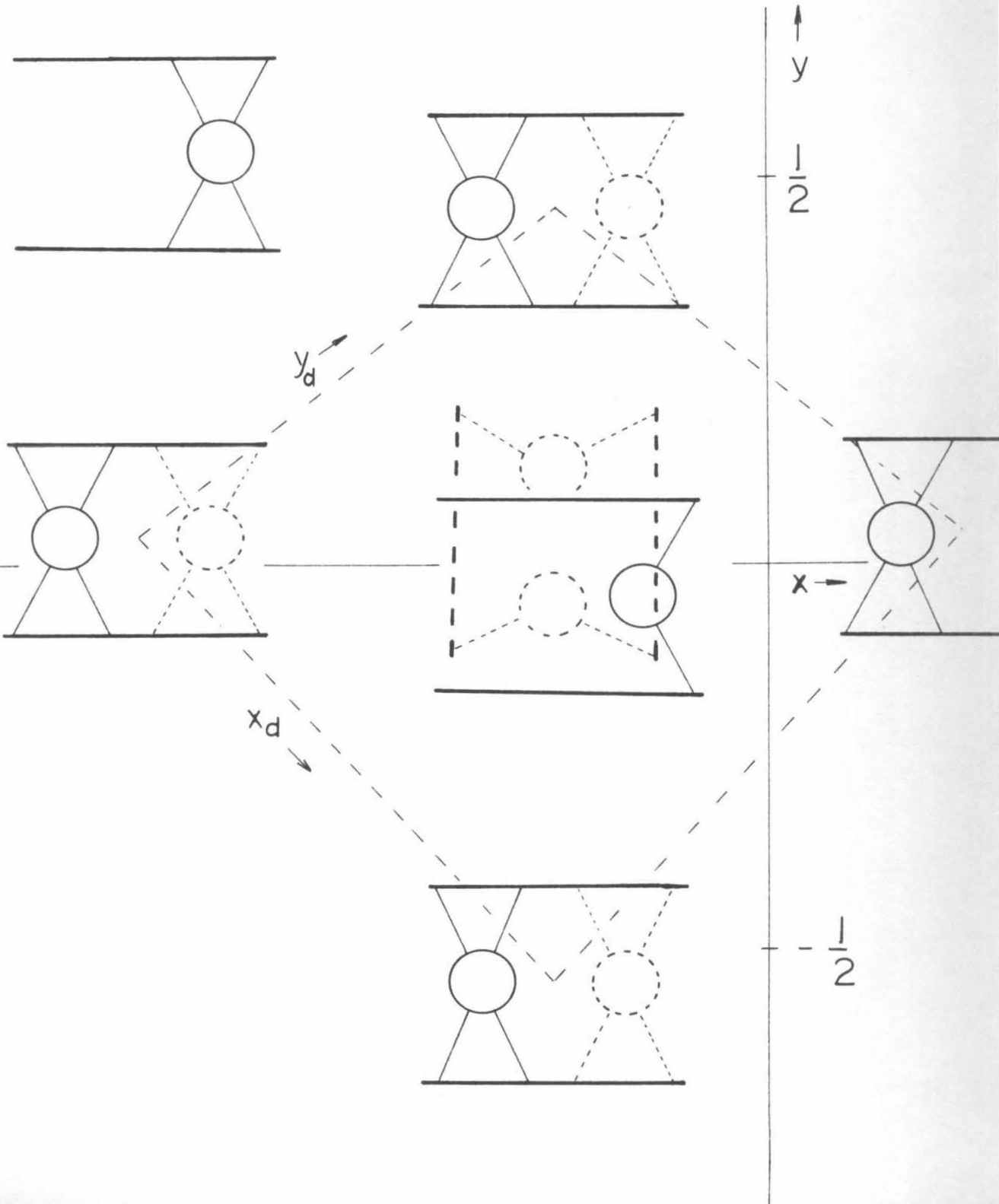
Disordered Bis-indenylruthenium

As stated in the experimental part, the first crystal of bis-indenylruthenium gave photographs indicating a unit cell only half as large as the one whose structure we determined and also suggesting disorder. The size of the unit cell indicates that there are only two molecules per unit cell and therefore, that the ruthenium atoms must occupy special positions (000) and $(\frac{1}{2} \frac{1}{2} 0)$ --that is, at the centers of symmetry of the molecule, indicating that the six-membered rings are trans.

Intensity data for the $hk0$ reflections were collected and corrected for Lorentz-polarization effects and then were used in generating the (001) Patterson projection. The Patterson map, however, did not show the ruthenium atoms to be in special positions; seemingly, there were four half ruthenium atoms in the unit cell. Trotter (6) encountered a similar problem in his investigation of the structure of bis-indenyliron.

In the same way that Trotter proposed a structure for disordered bis-indenyliron, we propose a disordered structure of bis-indenylruthenium. Around a special position there can be two orientations, equally probable, related by a center of symmetry so that the structure appears to have a center. This packing and unit cell of the disordered structure are shown in relation to the packing and unit cell of the ordered structure in figure 12. One can mentally construct the average

Figure 12. Comparison of packing in the ordered and disordered structures. The ordered unit cell is given by the solid lines and the disordered by the dashed. Compare to figure 10.



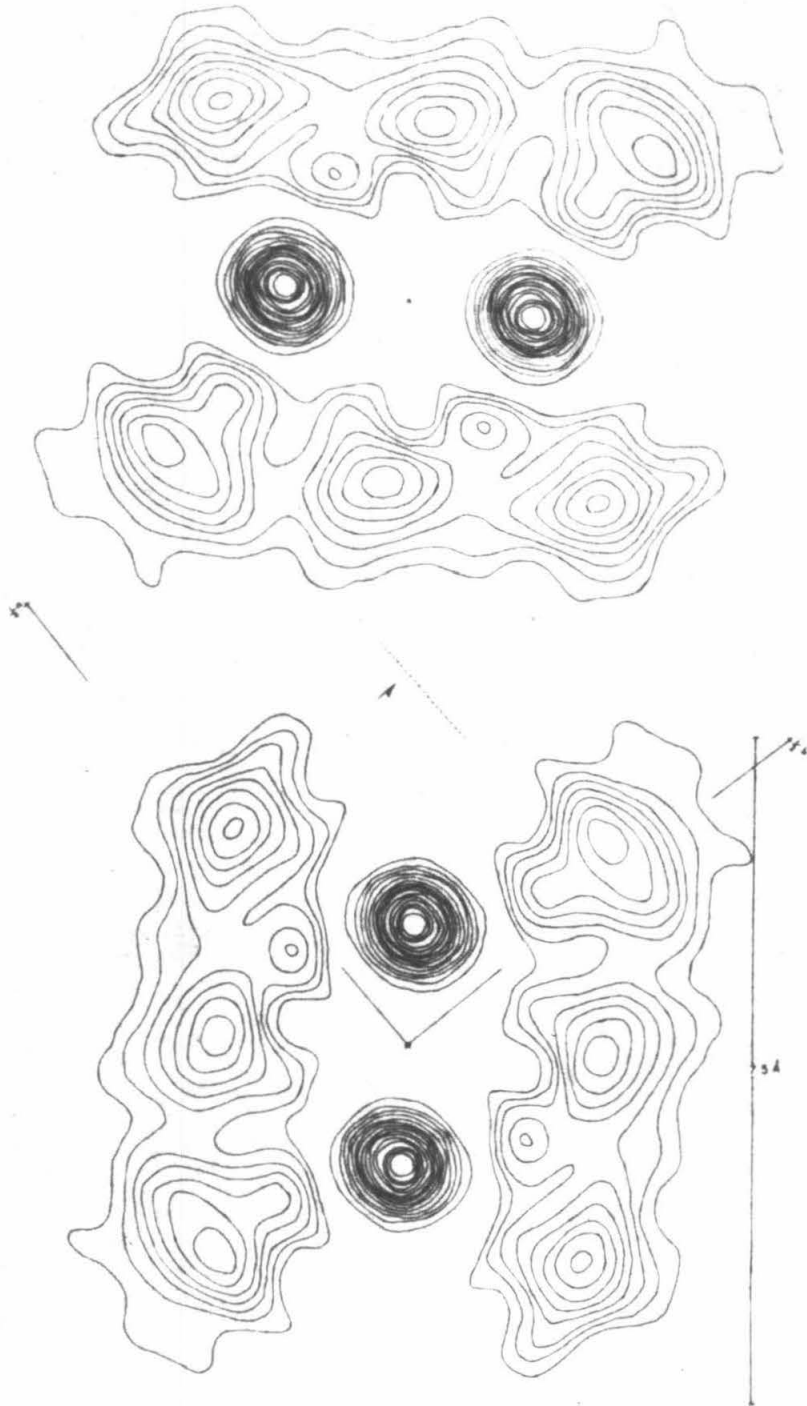
disordered structure by putting half ruthenium atoms at (xyz, \overline{xyz}) and half carbon atoms, to complete the half-molecules, in two planes with the five- and six-membered rings of one half-molecule occupying the general region of the six- and five-membered rings of the other half-molecule, the two half-molecules being related by a center of symmetry.

The positions of the ruthenium atom, obtained from the Patterson map, were used to assign signs to the F_o 's and an electron density projection onto (001) showed that the planar indenyl groups are almost perpendicular to the xy plane. The x and y coordinates of the carbon atoms were guessed on the basis of the ordered structure, and the $hk0$ structure factors were calculated. The signs of these F_c 's were then used to get an electron density projection onto (001); this electron density map is shown in figure 13.

Lattice constants calculated from Weissenberg photographs indicate that the packing of the ordered crystal is more efficient than the disordered; the ratio of ordered to disordered density is calculated to be 1.02. The c axes of these two forms are essentially the same, and the a axis and the b axis of the disordered crystal are such that the diagonal in the xy plane is essentially the same length as the a axis of the ordered crystal ($\sqrt{a_d^2 + b_d^2} = \sqrt{123 + 87} = 14.5 \text{ \AA}$, $a_o = 14.5 \text{ \AA}$), see figure 12.

In view of the disorder, no accurate structure determination seems possible and the work on this modification was abandoned.

Figure 13. Electron density projection onto (001) of the disordered modification of bis-indenylruthenium.



PART II

"Ni₅ Cd₂₁"

INTRODUCTION

In his examination of the nickel-cadmium system Voss (1) observed a binary intermetallic compound which he called NiCd_4 . Twenty-three years later (in 1931) Ekman (2) observed the same phase but reported the composition to be $\text{Ni}_5\text{Cd}_{23.6}$. His powder photographs indicated a cubic structure with the edge of the unit cell equal to $a_0 = 9.761 \text{ k} \times (9.781 \text{ \AA})$. Since the diffraction pattern was very similar to that of γ brass, he concluded that the structure was isotypic with that of this latter phase.

Prior to this work Ekman had discovered that the ratio between the number of valence electrons and the number of atoms, the so-called electron-to-atom ratio, in the two isostructural compounds Cu_5Zn_8 and Cu_9Al_4 , is 21/13, if copper is assigned the valence one, zinc the valence two, and aluminum the valence three. The same electron-to-atom ratio, he said, could be obtained for the nickel-cadmium phase if it were assigned the composition $\text{Ni}_5\text{Cd}_{21}$ and if nickel were assumed to have zero valence.

In 1934 Swartz and Phillips (3) reported that in the nickel-cadmium system the compound of highest cadmium content had the composition NiCd_7 .

The most recent report on nickel-cadmium alloys, which appeared in 1955, is that of Lihl and Buhl (4). These authors found the γ phase to exist at about 18.5 at. % Ni, which corresponds to $\text{Ni}_5\text{Cd}_{22}$, but stated that their powder photographs could be indexed only on the basis of a face-centered cubic cell of edge $a_0 = 19.545 \text{ \AA}$, which is twice the value reported by Ekman (loc. cit.). They believed that the structure of this phase is very closely related to that of γ brass, and again, referring to the electron-to-atom ratio 21/13, they assigned the "ideal" composition $\text{Ni}_5\text{Cd}_{21}$ to this phase.

The name " $\text{Ni}_5\text{Cd}_{21}$ " shall be retained provisionally until the actual composition is more firmly established.

The object of the present investigation is to find an explanation for the doubling of the cube edge and, furthermore, to test the validity of the assumption made by previous investigators. Another reason for our interest in this structure is that it may provide a basis for the formulation of structures of intermetallic compounds of very high complexity. Such structures have many interatomic distances which are functionally independent from one another, and, therefore, provide considerable information about interatomic distances.

Experimental

i) Preparation of single crystals.

An alloy of composition 17.8 at. % Ni and 82.2 at. % Cd was prepared from Baker Analyzed reagent nickel of 99.5% purity and Mallinckrodt analytical reagent grade cadmium sticks of 99.94% purity. Nickel shot and pieces of cadmium were melted together in an alundum crucible by induction heating in argon gas at atmospheric pressure; the melt was allowed to solidify slowly. The ingot was found to contain a very large number of crystals, most of which seemed to be fragments of cubes and square prisms. Since the cubes were too large to yield intensity data unaffected by absorption, a small fragment with an approximately rectangular cross section was selected to be used for X-ray photography.

Laue photographs indicated O_h Laue symmetry. Rotation and Weissenberg photographs indicated a cubic face-centered lattice with $a_0 = 19.6 \text{ \AA}$, in accord with the results of Lihl and Buhl (4). Each one of the observable reflections on the Weissenberg photographs had either all indices even or all indices odd with no systematic absences; the probable space groups are, accordingly, O^3 , T_d^2 , and O_h^5 .

ii) Intensity data.

An almost complete three-dimensional set of intensity data was obtained from equi-inclination Weissenberg photographs taken with MoK_α radiation. The $[110]$ direction of the cube was chosen as rotation axis. Since the identity period along this direction is only $a_0/\sqrt{2}$, where a_0 is the edge of the cubic unit cell, the complete sphere of reflection can be recorded with considerably fewer photographs than with a crystal rotated about $[100]$. This method, furthermore, yields cross correlations between even and odd layers, which is not possible with the latter method for cubic face-centered crystals.

The intensities were estimated visually by comparing the diffraction spots with those on a calibrated scale. The multiple-film technique was used, and the films were interleaved with nickel foil .001 inches thick. Corrections were made for Lorentz and polarization effects but not for absorption or extinction. Absorption corrections were not necessary because of the very small size of the crystal, which was $.060 \times .023 \times .017 \text{ mm}^3$. The maximum μR was of the order 0.8.

For this investigation 623 symmetry independent reflections were used, 340 of which were either too weak to be observed or too weak to be estimated with reasonable accuracy. These 340 reflections were treated as being weaker than an estimated maximum value.

Data were obtained from the equator and from layer lines two through six, the rotation axis being the $[110]$; the first layer was omitted by accident. Because of this omission, 13 reflections were not covered. The observed structure factors are listed in table 5 at the end of this part.

The Derivation of the Structure

i) General considerations.

The smallest unit cube is of edge $a_0 = 19.6 \text{ \AA}$ and contains approximately 400 atoms, of which roughly one-fifth are nickel and four-fifths are cadmium. The probable space groups are O^3 , T_d^2 and O_h^5 .

Since the total number of distance vectors in the unit of structure is approximately proportional to the square of the number of atoms, the application of Patterson maps to the solution of the structure seemed hopeless. The stochastic method as defined by Pauling (5) seemed to be the only one that offered promise for a successful attack.

Of the three probable space groups given above, T_d^2 is the only one that has the symmetry elements necessary to describe an atomic arrangement similar to that of γ brass. This space group, therefore, was the one that had to be considered in the first place, at

least to test the correctness of the assumptions made by Ekman (2) and independently by Lihl and Buhl (4).

The procedure developed by Samson (6) was used to explore this space group. A fairly detailed description of his method is given below.

ii) Samson's method to derive trial structures of complex cubic intermetallic compounds.

Practically all of this section is quoted from an early draft of a paper to be submitted for publication by Dr. Samson. The figures included here were prepared for that paper; I have supplied the legends for them. These will be referred to in later discussions.

Introduction

Cubic crystals of metals and intermetallic compounds have always been observed to incorporate atoms in special positions. This feature probably arises from the difficulty or perhaps impossibility to achieve a cubic space-filling structure by utilizing general positions alone. One may profitably begin with the hypothesis that a special position is always needed to define the center of a coordination shell described solely or partially by a general position. Hence, if in a cubic crystal the configuration of atoms is known around each point that can be defined by a special position, the atomic arrangement of the crystal is completely determined.

In the subsequent discussion it is understood that the origin of coordinates of the cube is placed in accordance with the Space Group Tables given in the International Tables (7). The (100) plane and the (110) plane referred to below are always those passing through the origin of the cube.

In each one of the space groups T^2 , T^4 , T_h^4 , T_h^6 , O^3 , T_d^2 , and T_d^5 , every special position places at least one point on the (110) plane. To determine a structure having one of these space groups it is necessary only to determine the coordination shell around each single atom or available site that is located on the (110) plane.

A similar rule applies to structures of the space groups O^4 , O^6 , O^7 , O_h^7 , O_h^8 except that the special positions of the kind $\frac{1}{8}$, X , $\frac{1}{4} \pm X$, etc., eventually may have to receive special treatment. These positions are of such a nature, however, that they most likely will represent vertices of coordination shells around single atoms or available sites on the (110) plane, as will be seen in the following chapter.

For most of the remaining cubic space groups it will be necessary to determine the coordination shells around single atoms on both the (100) plane and the (110) plane. In some rare cases it may be necessary to investigate one specially chosen additional plane.

The symmetry chart

A means of recognizing the possible configurations of atoms around single atoms on a plane is the symmetry chart, an example of

which is shown in figure 1. This chart has been drawn for the (110) plane of a crystal of space group O_h^7 and cube edge $a_0 = 30.6 \text{ \AA}$, scale $1 \text{ \AA} = 1 \text{ cm}$. The points a and b are defined by the two 8-fold positions, 000 etc., and $00\frac{1}{2}$, etc., respectively; c and d are points of the two 16-fold positions $\frac{1}{8} \frac{1}{8} \frac{1}{8}$, etc., and $\frac{1}{8} \frac{1}{8} \frac{5}{8}$, etc., respectively, which are centers of symmetry. The letters correspond to the notations used for this space group in the International Tables (7), page 340. The same notations are referred to below.

If each point were replaced by a rigid sphere of a radius $r = 1.40 \text{ \AA}$ equal to one-half the average interatomic distance assumed in the crystal, then the centers of such spheres on the (110) plane are confined as indicated in figure 1. The lines e and f are the loci of points of one degree of freedom, XXX etc. and 00X etc., positions e and f. The points with two degrees of freedom, XXZ etc., position g, are confined within the areas limited by solid lines. The indentation t is a result of the center of symmetry at c. If a point XXZ is at G, its surrounding sphere of radius $r = 1.40 \text{ cm}$ is then in contact with two other equivalent contiguous spheres, one above (ZXX) and one below (XZX) the point $\underline{+}G$, since e is a 3-fold axis of symmetry. The point G is accordingly at a distance $\frac{1}{\sqrt{3}} r$ and the point $\underline{+}G$ at a distance $\frac{1}{2\sqrt{3}} r$ from the line e. Points of the kind $\underline{+}G$, representing the projection of the centers of two spheres, one above and one below the

Figure 2. Symmetry chart of the (110) plane, space group T_d^2 , see text.

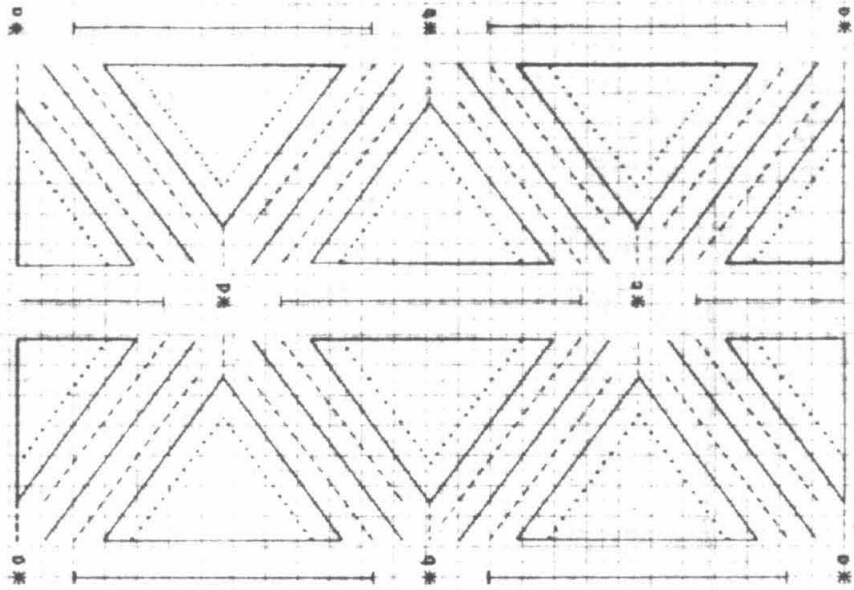
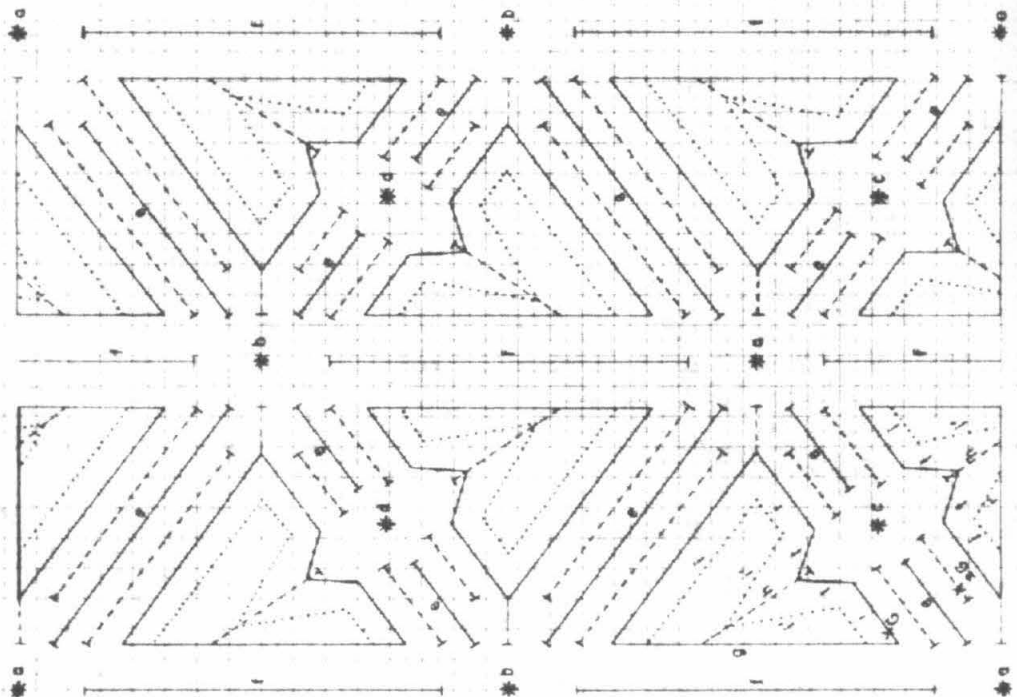


Figure 1. Symmetry chart of the (110) plane, space group O_h^7 , see text.



(110) plane are referred to as "plus-minus" points. The broken and dotted lines are accordingly loci of "plus-minus" points of contiguous spheres and are referred to as "plus-minus" lines.

The areas limited by the dotted lines i and i' and the solid line g are "plus-minus" fields for the general position $192i$. The isosceles triangle of the sides i' is forbidden for this position as a result of the center of symmetry at point c .

Position $96h$ ($\frac{1}{8}, X, \frac{1}{4} - X$, etc.) describes plus-minus points located on the broken lines h . These points are at the vertices of a hexagon around c , the size of which is determined by X .

Figure 2 represents a symmetry chart of the (110) plane of a cube of edge $a_0 = 25.8 \text{ \AA}$, space group T_d^2 , $r = 1.25 \text{ \AA}$ (smallest assumed distance). Figure 3a shows the (110) plane and figure 3b the (100) plane of the same cube but for space group O_h^5 .

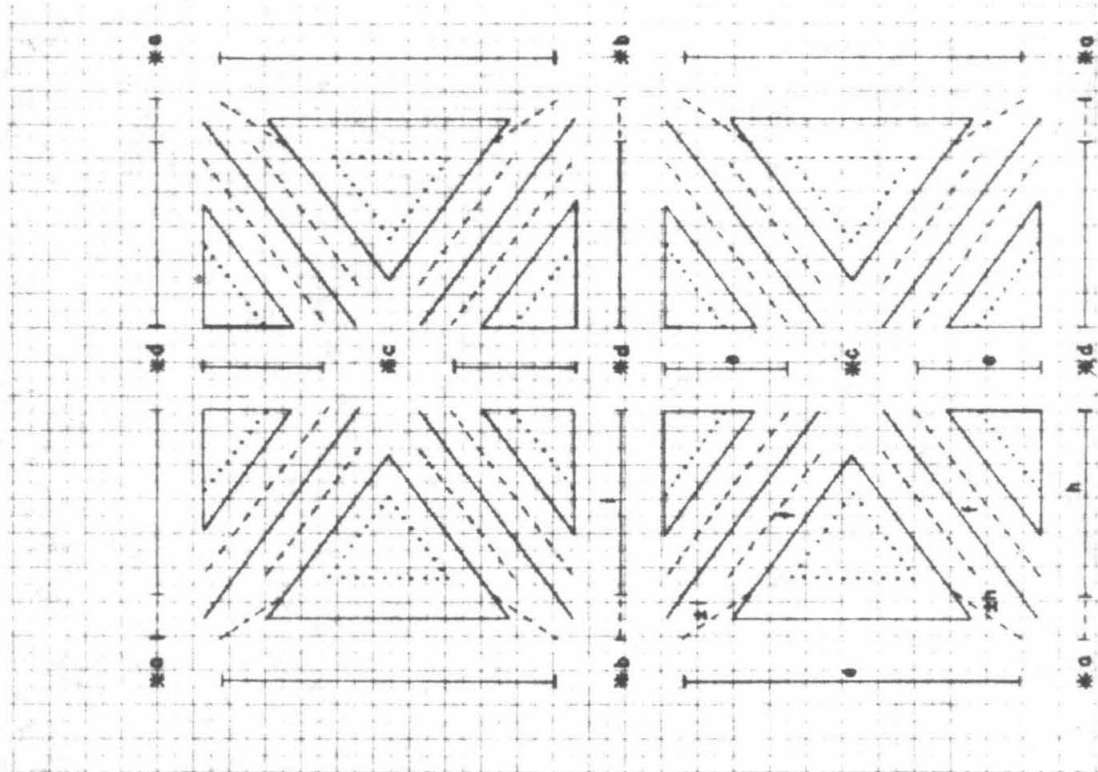
The representation of coordination polyhedra

A few examples of how coordination polyhedra may be represented for their immediate recognition on the symmetry chart are given below.

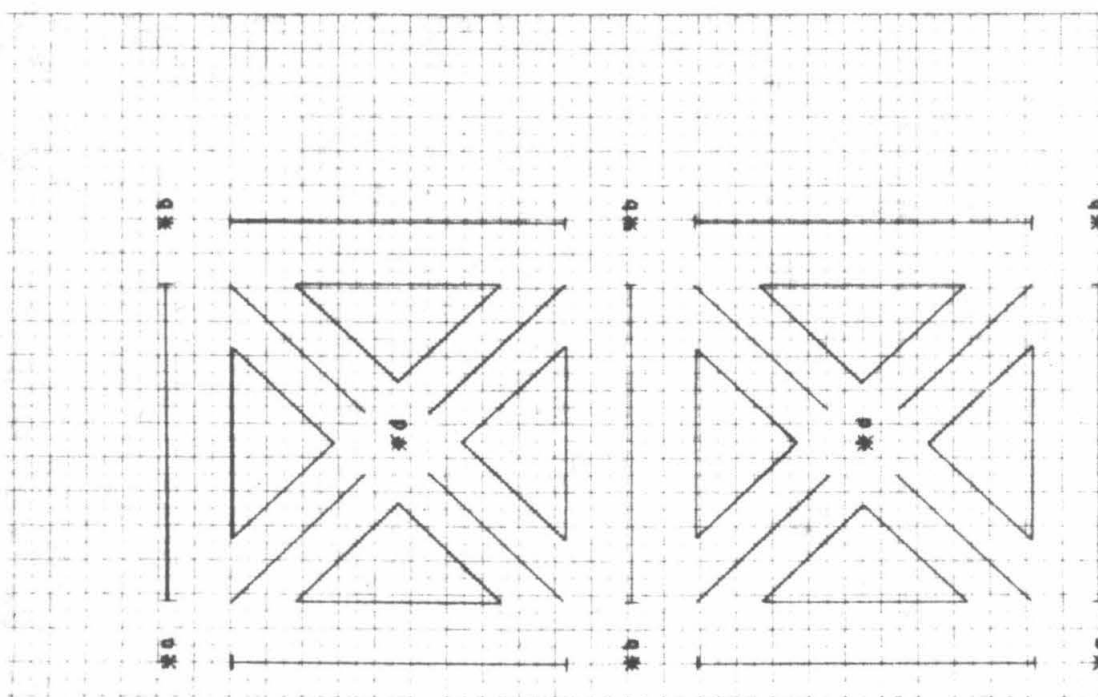
A very frequently observed coordination polyhedron is the truncated tetrahedron bounded by four hexagons and four triangles, figure 4a. A section through the (110) plane is shown in figure 4b and c. The packing of atoms around such a polyhedron is explored by describing

Figure 3. Symmetry charts for a cube of edge $a_0 = 25.8 \text{ \AA}$, space group O_h^5 , with a smallest assumed distance of 1.25 \AA .

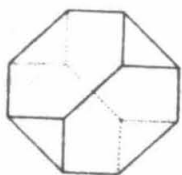
3a) (110) plane



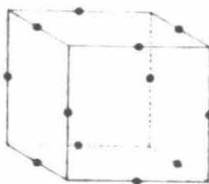
3b) (100) plane



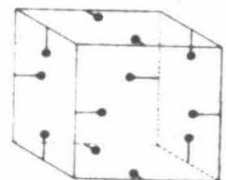
Figures 4, 5 and 6. For explanation, consult text.



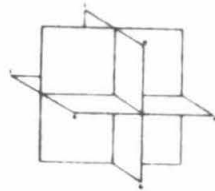
a



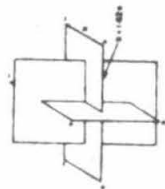
a



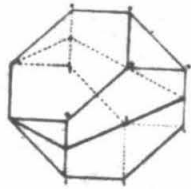
a



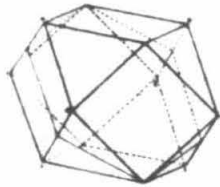
b



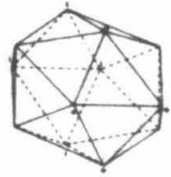
b



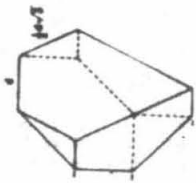
b



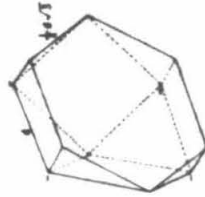
c



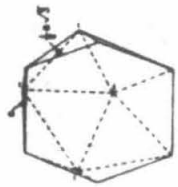
c



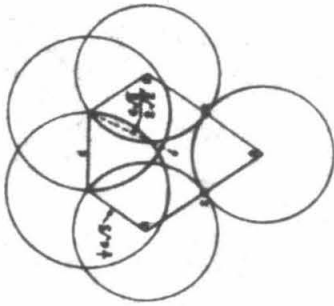
c



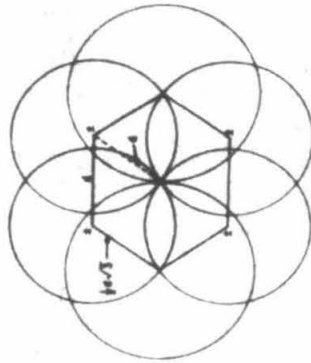
d



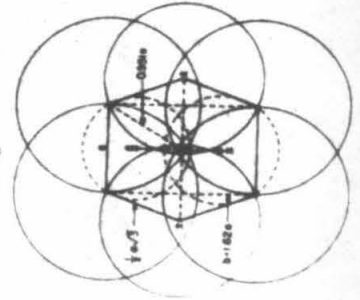
d



d



e



e

Figure 4

Figure 5

Figure 6

around each vertex a sphere of a radius equal to the distance d between the vertex and the center of its assumed nearest neighbor outside the polyhedron. A (110) section through such an arrangement of spheres is shown in figure 4d. The center of any circle of $r = d$ is allowed to lie upon the circumference of any other circle but not inside it, while the center of any "plus-minus" circle representing two "contiguous" atoms is allowed to be as close as $r = \frac{1}{2}d\sqrt{3}$ to the center of a circle of $r = d$.

Figure 5 shows a cubo-octahedron which is represented according to the same principles. Figure 6 demonstrates how the icosahedron can be derived through deformation of a cubo-octahedron. The three mutually perpendicular squares in figure 5b have been substituted by rectangles, figure 6b, the sides of which are a and $b = 1.62a$, where b is also the diameter of a pentagon of side a . This representation of the icosahedron was found to be the most perspicuous one with regard to symmetry charts so far explored. An example of the usefulness of this representation can also be found in an earlier paper (Samson, 8) which, however, does not show the symmetry chart.

It is seen that the circles around the vertices of the polyhedron shown in figure 4d leave a free area around the center, while in figure 5d the circles intersect at the center and in figure 6d overlap at the

center. This feature demonstrates the metrical nature of these polyhedra. With twelve contiguous spheres of equal size at the vertices of the truncated tetrahedron, it is possible to accommodate a sphere 34.5% larger in radius at the center, since $\frac{r_{\text{cent}}}{r_{\text{vert}}} = \frac{\sqrt{11}}{\sqrt{2}} - 1 = 1.345$, figure 4d, while for the icosahedron the central sphere is nearly 10% smaller.

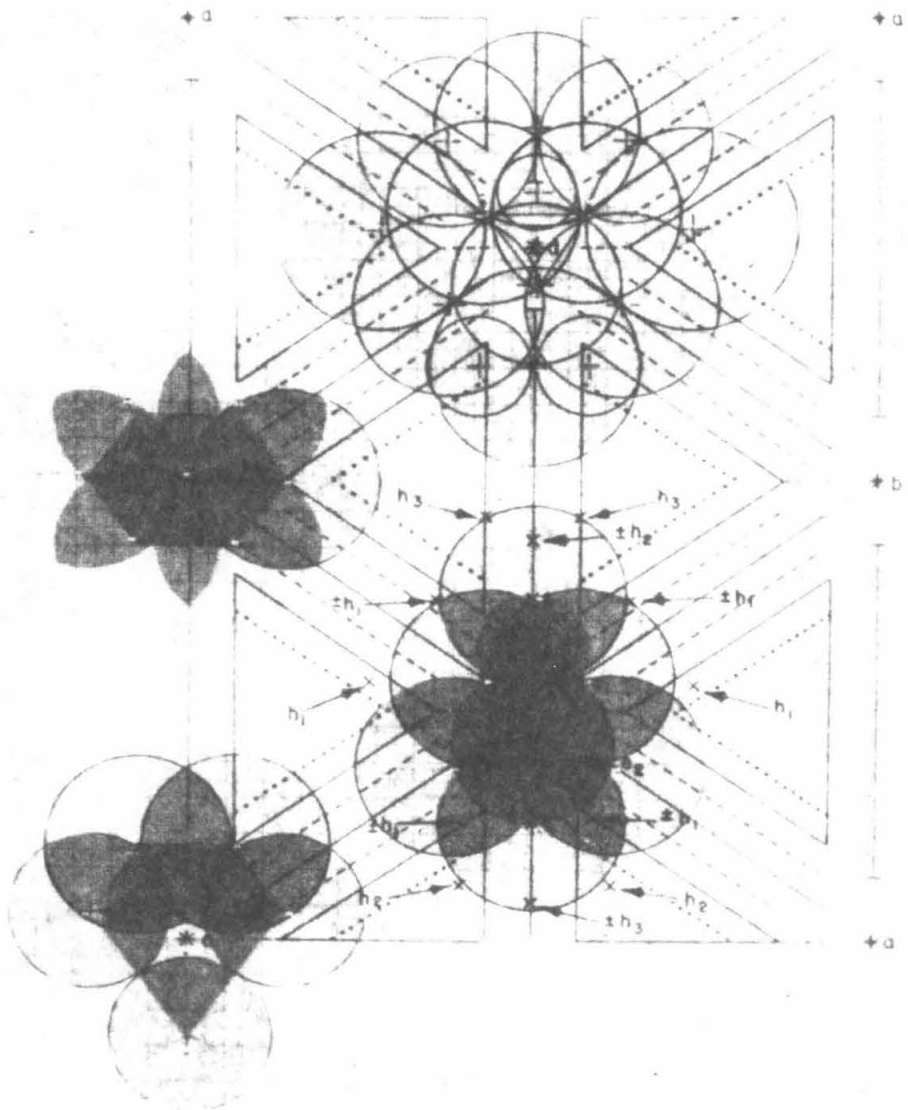
Packing of coordination polyhedra

Figure 7 represents the same symmetry chart as figure 2. Transparent templates of polyhedra such as are shown in figures 4 and 5 are held in position with pins.

The discs around e_1 and $\pm e_1$, figure 7, represent a positive tetrahedron, which is surrounded by a negative tetrahedron (e_2 and $\pm e_2$). The disc at f_1 is at the vertex of an octahedron. If more atoms are added at the points h_1 , $\pm h_2$ and $\pm h_3$, as is indicated with arrows, the arrangement of points around f_1 is similar to that shown in figure 6d, i. e., f_1 is at the center of an icosahedron.

It is obvious that transparent templates of sections through large atom complexes commonly observed in complex metal structures may appreciably facilitate the search for a reasonable structural motif. Such a template, which represents an atom complex characteristic for γ -brass type structures is placed at point d, figure 7.

Figure 7. An illustration of the use of templates for representing polyhedra and atom complexes.



A symmetry chart that has been filled with circles representing sections through spheres to show the packing of atoms, as well as the structural motif, shall hereafter be referred to as a packing chart.

iii) Definitions

a) Centers

Space group T_d^2 is non-centrosymmetric. The word center shall be used to refer to the points a, c, b and d in figure 2. These points are defined by the special positions 4a, 4c, 4b, and 4d, respectively, in accord with the space group tables given in the International Tables, Vol. I (7); they correspond accordingly to 000, etc., $\frac{1}{2} \frac{1}{2} \frac{1}{2}$, etc., $\frac{1}{2} \frac{1}{2} \frac{1}{2}$, etc., and $\frac{3}{4} \frac{3}{4} \frac{3}{4}$, etc. The symmetry elements around each such point are $\bar{4} 3m$.

There are consequently four independent centers, each one of which may be chosen as the origin of the cube, the translations being $\frac{1}{2} \frac{1}{2} \frac{1}{2}$, $\frac{1}{2} \frac{1}{2} \frac{1}{2}$, or $\frac{3}{4} \frac{3}{4} \frac{3}{4}$, respectively. Such translations do not alter the magnitude of calculated structure factors, $F_c = A^2 + B^2$, but they affect the values of A and B for certain classes of reflections and consequently also the phase angles.

b) Polyhedra, positions, and complexes.

The structure is conveniently described and discussed in terms of four polyhedra: the octahedron, the tetrahedron, the cubo-octahedron, and the icosahedron. The position of X00 etc., describes a regular

octahedron. The points defined by position e, XXX, etc., are at the vertices of a regular tetrahedron. The cubo-octahedron just referred to is bounded by two sets of four equilateral triangles each and six 4-sided faces. This polyhedron is described by position h, XXZ, etc. If the parameter Z is chosen to be exactly 0, $\frac{1}{4}$, $\frac{1}{2}$, or $\frac{3}{4}$, the cubo-octahedron will be bounded by eight equilateral triangles of equal size and six squares, such as is shown in figure 5. In this structure, however, the cubo-octahedron has a shape such as is shown in figure 10. A regular icosahedron is shown in figure 6. In space group T_d^2 this polyhedron has to be described with the use of several point positions. The four polyhedra are also shown in part in figure 7.

More complicated arrangements of atoms will be referred to as complexes. The arrangement of atoms shown in figure 7 shall be called the γ -complex, because it is observed in all the γ -brass type structures that so far have been established. It consists of two tetrahedra, one of which is negative with respect to the other, one octahedron, and one cubo-octahedron. Each atom complex arranged about a point a, b, c or d shall be called according to this point--for instance, a-complex, b-complex, etc. The outermost shell of any such complex is always a cubo-octahedron of T_d symmetry, i. e., it has two sets of four equilateral triangles.

iv) Least-squares calculations.

In the least-squares refinement, the quantity $\sum w (F_o^2 - F_c^2)^2$ was minimized. The shifts in atomic positional parameters were calculated from the diagonal matrix elements of the normal equations. Refinement of the temperature factors and the scale factor was based on a set of complete normal equations which took into account the coupling between each possible pair of temperature factors, and between each temperature factor and the scale factor.

The scattering curves for nickel and cadmium were used as given by Thomas and Umeda (9) in all of the structure-factor calculations.

v) The γ -brass type trial structure.

The overall diffraction pattern of Ni_5Cd_{21} has great similarity with that observed for Ag_5Zn_8 , which has a γ -brass type structure (10); therefore, it seemed likely that the atomic arrangement is similar to that in γ brass, Cu_5Zn_8 (11). Accordingly, a symmetry chart representing the (110) plane passing through the origin of the cube was explored with the aid of templates representing atom complexes such as observed in γ brass (see fig. 7). It was quickly recognized that eight subcells of a γ -brass type structure could be accommodated in the unit cell, and the approximate atomic coordinates could be obtained from the packing chart. The initial assumption was made that the

doubling of the cube edge was due to variations in the occupancy of the subcells. This assumption arose from the observation that the diffraction pattern indicates pseudo-body-centering. The reflections hkl with $h + k + l = 2n + 1$ were, in general, much weaker than the reflections with $h + k + l = 2n$.

The structure-factor least-squares calculations based on several variations of this atomic arrangement indicated that doubling is due to a more complicated phenomenon than a change in population. We were gradually forced to assume that the arrangements of atoms around some of the centers were not γ -complexes.

vi) Other trial structures.

With the use of the symmetry chart we explored several other structural motifs. Our second idea was to investigate the possibility of combining two γ -complexes, one at 000 and the other at $\frac{1}{2} \frac{1}{2} \frac{1}{2}$, with another kind of complex at the remaining two centers. A reasonable arrangement of atoms was obtained by placing Friauf polyhedra at $\frac{1}{4} \frac{1}{4} \frac{1}{4}$ and $\frac{1}{4} \frac{1}{4} \frac{3}{4}$; a Friauf polyhedron is a 17-atom complex consisting of an atom, in this case at $\frac{1}{4} \frac{1}{4} \frac{1}{4}$ and at $\frac{1}{4} \frac{1}{4} \frac{3}{4}$, surrounded by 4 atoms at the vertices of a tetrahedron and by 12 atoms at the vertices of a truncated tetrahedron. The regular tetrahedra which form an integral part of the Friauf polyhedron are related to the tetrahedra around a and b by translations of $\frac{1}{2} \frac{1}{2} \frac{1}{2}$. In carrying out calculations on this trial structure, we obtained our second clue to

the structure, the first being the γ -brass type arrangement. The very high values of some of the temperature factors resulting from the least-squares shifts suggested that the truncated tetrahedra of the Friauf polyhedra had to be omitted. The temperature factors for the atoms of the regular tetrahedra were normal, thus indicating that these were actually part of the structure.

Another idea was to fit γ -complexes together with close-packed arrangements. These can be obtained by placing atoms at the vertices of a regular octahedron. The equilateral triangles form the first two layers A and B. The third layer, C, is then provided by a cubo-octahedron as the next outer shell. This idea led to the third clue to the structure: one octahedron in the structure is a small one.

I cannot give full details of this investigation. Many structures were designed on paper with the aid of the symmetry chart. A few of these included the 96-fold position. Several were combinations of γ -complexes, Friauf polyhedra, and other more or less regular coordination shells. The space group, O_h^5 was also explored. When this search led to a well-packed atomic arrangement with pseudo-body-centering, structure-factor and least-squares calculations were used to test the trial structure.

vii) A working model.

The attempt to derive a structure which seemed to demand one small octahedron, tetrahedra, and γ -complexes led to a trial structure based on three γ -complexes and one 22-atom complex which we call an o-complex. This latter one consists of six atoms at the vertices of an octahedron, which is surrounded by four atoms at the vertices of a tetrahedron, the next outer shell being a cubo-octahedron. This trial structure we call $\text{o}\gamma\gamma\gamma$.

A series of least-squares cycles led us to believe that the structure is of the type $\text{o}\gamma\text{o}\gamma$, with o-complexes at the points a and b and with γ -complexes at the points c and d. The proposed $\text{o}\gamma\text{o}\gamma$ structure is described by 14 crystallographically different positions. The overall agreement between observed and calculated structure factors was reasonably good. After a few least-squares cycles, the agreement index dropped from $R = 0.40$ to $R = 0.26$ for 157 reflections with $\sin \theta$ less than 0.33. An electron-density map of the (110) plane calculated on the basis of these reflections suggested that an atom had to be placed at $\frac{3}{4} \frac{3}{4} \frac{3}{4}$ inside the tetrahedra of a γ -complex and, furthermore, that some of the sites were occupied by a different kind of metal atom than we initially assumed. Some minor changes of the atomic coordinates also had to be made. Subsequent to these changes, four additional refinement cycles were carried out. These improved the

agreement to $R = 0.16$. A few changes based on another electron density map and a few more least-squares cycles reduced the agreement index to $R \approx 0.13$.

The structure had by then changed considerably from our initial postulate. The first electron-density map had indicated an atom at $\frac{3}{4} \frac{3}{4} \frac{3}{4}$ inside a γ -complex; the positive and negative tetrahedra of this γ -complex had become almost equal in size to form a distorted cube. The atomic arrangement around $\frac{3}{4} \frac{3}{4} \frac{3}{4}$ had gradually come to resemble a body-centered cube. After examining the structure by means of the symmetry chart, Dr. Samson had suggested that an atom be placed at point b , since the octahedron around that point had become large enough to accommodate an atom. Moreover, the second electron-density map had indicated that the position c is occupied 30 percent of the time and that for the other 70 percent of the time point c is surrounded by a tetrahedron. Refinement calculations based on such a disordered structure led to no improvement in the agreement index; only the reflections with $\sin \theta$ less than 0.36 were used in these calculations.

At this point we decided to use the full set of three-dimensional data. We started refinement using the weighting function

$$\sqrt{w} \propto \frac{\sqrt{w_e}}{1000 + 0.1 F_o^2} \quad \text{where } F_o \text{ is based on one-fourth of the unit}$$

cell, the asymmetric unit. The minimum observable F_o , F_{\min} , is

such that the weighting function is approximately that of Hughes (12) (refer to table 2 in part I). From time to time we changed the weighting function to $\sqrt{w} \propto \frac{\sqrt{w_e}}{100 + F_o}$, but used the one above for most of the refinement. Changes of the weighting function seemed to have very little effect on the results.

The first refinement cycle based on the full set of data was disappointing. The agreement index at the beginning was $R = 0.22$. A few cycles reduced it to $R = 0.195$.

A difference map of the (110) plane was calculated; it is shown in figure 8. This map indicates disorder around all four centers. The positions a , f_1' , f_2' , e_6' , f_1 , f_2 , and e_6 , in addition to e_5 and c , appear to be partially occupied. In order to fully describe this kind of disorder, 21 crystallographic positions are needed. Subsequent least-squares refinement cycles of this structure yielded $R = 0.155$; the atomic parameters at this stage of the refinement are listed in tables 1 and 2. The refinement was still converging, and the shifts in temperature and population factors indicated that the occupancy of some of the sites was far from being determined.

Refinement of this disordered structure was interrupted because of insufficient information regarding the magnitude of the off-diagonal matrix elements. It seems possible that in a situation like this the omission of the off-diagonal matrix elements may keep the

Figure 8. Difference Fourier of the (110) plane. Solid contours at 4, 8, 12 and 16 $e. \text{\AA}^{-3}$. Dashed lines = $-4 e. \text{\AA}^{-3}$, dotted line = $-8 e. \text{\AA}^{-3}$.

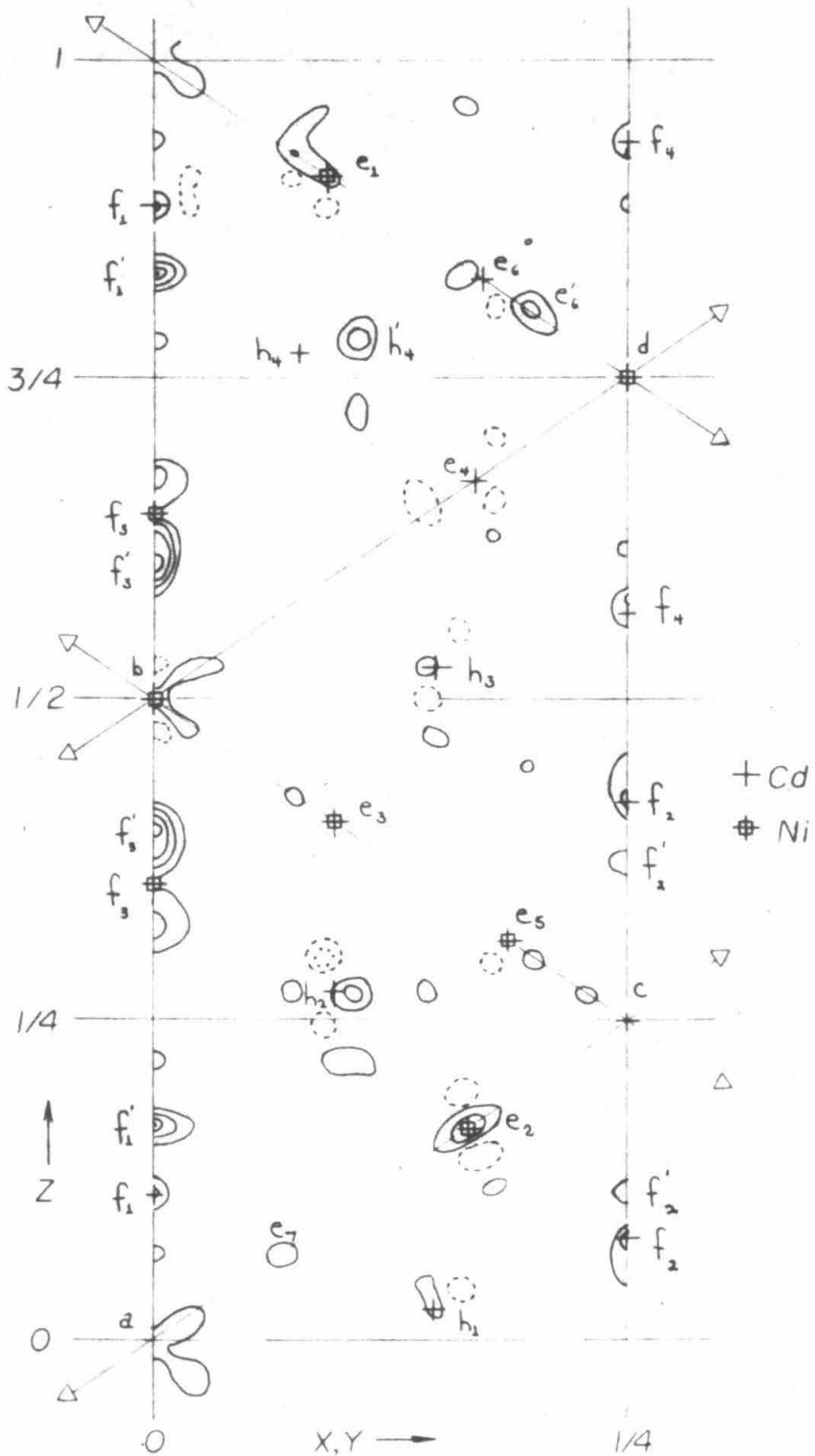


Table 1

Comparison of trial structures for " $\text{Ni}_5\text{Cd}_{21}$." Atomic parameters and standard deviations. If a position is partially occupied, the percent occupancy is given beside the atomic symbol. Pairs of positions such as e_6 and e_6' are used to describe disorder.

Position		Ordered	Disordered	
		16 positions	17 positions	21 positions
e_1	x	$-.0908 \pm .0011$	$-.0897 \pm .0019$	$-.0910 \pm .0011$
	B	0.04 ± 0.4	0.96 ± 0.8	0.86 ± 0.4
		Ni	Ni	Ni
e_2	x	$.1658 \pm .0013$	$.1659 \pm .0012$	$.1646 \pm .0014$
	B	0.84 ± 0.4	3.90 ± 0.4	1.23 ± 0.4
		Ni	Cd	Ni
e_3	x	$.4063 \pm .0016$	$.4071 \pm .0017$	$.4065 \pm .0015$
	B	2.21 ± 0.6	1.73 ± 0.6	2.45 ± 0.5
		Ni	Ni	Ni
e_4	x	$.6706 \pm .0008$	$.6704 \pm .0009$	$.6704 \pm .0008$
	B	1.41 ± 0.3	0.96 ± 0.2	2.09 ± 0.3
		Cd	Cd	Cd
e_5	x	$.3115 \pm .0022$	$.3129 \pm .0024$	$.3100 \pm .0021$
	B	3.85 ± 0.9	1.32 ± 0.9	1.96 ± 0.8
		Ni	Ni	Ni, 70%
e_6	x	$.8260 \pm .0012$	$.8260 \pm .0012$	$.8267 \pm .0010$
	B	3.30 ± 0.4	3.08 ± 0.4	2.44 ± 0.3
		Cd	Cd	Cd, 90%
e_6'	x			$.8050^{**} \pm .0156$
	B			$2.00^* \pm 5.3$ Ni, 10%
f_1	x	$.1138 \pm .0007$	$.1116 \pm .0008$	$.1135 \pm .0007$
	B	2.03 ± 0.2	1.93 ± 0.3	1.70 ± 0.2
		Cd	Cd	Cd, 88%
f_1'	x			$.1672 \pm .0051$ $2.00^* \pm 1.7$ Cd, 12%
f_2	x	$.4206 \pm .0010$	$.4210 \pm .0011$	$.4210 \pm 0.0009$
	B	4.37 ± 0.4	4.43 ± 0.4	4.46 ± 0.3
		Cd	Cd	Cd

Table 1 (continued)

Position		Disordered		
		Ordered 16 positions	17 positions	21 positions
f_3	x	.6479 + .0016	.6495 + .0017	.6513 + .0014
	B	2.88 + 0.6 Ni	2.60 + 0.6 Ni	1.86 + 0.5 Ni, 90%
f_3'	x			.6244 + .0065
	B			2.00* + 2.2 Cd, 10%
f_4	x	.9347 + .0010	.9343 + .0011	.9339 + .0009
	B	4.32 + 0.3 Cd	4.15 + 0.4 Cd	4.56 + 0.3 Cd
h_1	x	.1475 + .0006	.1472 + .0006	.1475 + .0006
	B	.0264 + .0006 2.74 + 0.2 Cd	.0261 + .0006 2.36 + 0.2 Cd	.0261 + .0005 2.85 + 0.2 Cd
h_2	x	.4059 + .0006	.4058 + .0007	.4059 + .0005
	B	.2731 + .0007 4.69 + 0.3 Cd	.2734 + .0007 4.00 + 0.3 Cd	.2732 + .0006 4.45 + 0.3 Cd
h_3	x	.6487 + .0005	.6482 + .0005	.6483 + .0005
	B	.5230 + .0005 2.05 + 0.2 Cd	.5235 + .0005 1.73 + 0.2 Cd	.5233 + .0004 2.14 + 0.1 Cd
h_4	x	.9252 + .0005	.9254 + .0005	.9251 + .0004
	B	.7696 + .0005 2.94 + 0.2 Cd	.7693 + .0006 2.76 + 0.2 Cd	.7693 + .0005 2.84 + 0.2 Cd
a				0, 0, 0 13.3 + 18.0 Ni, 6%
c			$\frac{1}{2}, \frac{1}{2}, \frac{1}{2}$ 1.77 + 2.9 Ni, .30, e_5	$\frac{1}{2}, \frac{1}{2}, \frac{1}{2}$ 2.38 + 2.0 Cd, 30%
b		$\frac{1}{2}, \frac{1}{2}, \frac{1}{2}$ 10.9 + 3.8 Ni	$\frac{1}{2}, \frac{1}{2}, \frac{1}{2}$ 8.92 + 3.8 Ni	$\frac{1}{2}, \frac{1}{2}, \frac{1}{2}$ 3.97 + 1.8 Ni, 80%

Table 1 (continued)

Position	Ordered	Disordered	
	16 positions	17 positions	21 positions
d	$\frac{3}{4}, \frac{3}{4}, \frac{3}{4}$ 4.65 + 2.1 Ni	$\frac{3}{4}, \frac{3}{4}, \frac{3}{4}$ 4.14 + 2.0 Ni	$\frac{3}{4}, \frac{3}{4}, \frac{3}{4}$ 2.99 + 1.6 Ni, 90%
Atomic % Ni	24.5	19.7	23.1
$\Sigma F_o $	50045	53033	49134
$\Sigma F_c $	49766	53196	47933
N	323†	332	324
R	.164	.176	.155
$\Sigma \omega F_o^4$ ***	145	153	142
$\Sigma \omega F_c^4$ ***	178	198	159
R'	.13	.17	.10

N is the number of reflections, of 623 total, in the sums and in least-squares cycle.

$$R' = \frac{\Sigma \omega (F_o^2 - F_c^2)^2}{\Sigma \omega F_o^4}$$

* Shifts led to negative B.

** Shifts made bond distances within tetrahedron less than 2.2 Å.

*** On an arbitrary scale.

† Does not include 18 reflections which have an index greater than 25.

Table 2. Comparison of trial structures and of similar positions.

Position		Ordered	Disordered	
		16 positions	17 positions	21 positions
e_1	x	-.0908	-.0897	-.0910
	B	0.04	0.96	0.86
	Ni		Ni	Ni
e_2	$x-\frac{1}{4}$	-.0842	-.0841	-.0854
	B	0.84	3.90	1.23
	Ni		Cd	Ni
e_3	$x-\frac{1}{2}$	-.0937	-.0929	-.0935
	B	2.21	1.73	2.45
	Ni		Ni	Ni
e_4	$x-\frac{3}{4}$	-.0794	-.0796	-.0796
	B	1.41	0.96	2.09
	Cd		Cd	Cd
e_5	$x-\frac{1}{2}$.0615	.0629	.0600
	B	3.85	1.32	1.96
	Ni		Ni, 70%	Ni, 70%
e_6	$x-\frac{3}{4}$.0760	.0760	.0767
	B	3.30	3.08	2.44
	Cd		Cd	Cd, 90%
e_6'	$x-\frac{3}{4}$.0550**
	B			2.00*
				Ni, 10%
f_1	x	.1138	.1116	.1135
	B	2.03	1.93	1.70
	Cd		Cd	Cd, 88%
f_1'	x			.1672
	B			2.00*
				Cd, 12%
f_2	$x-\frac{1}{4}$.1706	.1710	.1710
	B	4.37	4.43	4.46
	Cd		Cd	Cd
f_3	$x-\frac{1}{2}$.1479	.1495	.1513
	B	2.88	2.60	1.86
	Ni		Ni	Ni, 90%
f_3'	$x-\frac{1}{2}$.1244
	B			2.00*
				Cd, 10%

Table 2 (continued)

Position		Ordered	Disordered	
		16 positions	17 positions	21 positions
f_4	$x-\frac{3}{4}$.1847	.1843	.1839
	B	4.32	4.15	4.56
	Cd		Cd	Cd
h_1	x	.1475	.1472	.1475
	z	.0264	.0261	.0261
	B	2.74	2.36	2.85
	Cd		Cd	Cd
h_2	$x-\frac{1}{4}$.1559	.1558	.1559
	$z-\frac{1}{4}$.0231	.0234	.0232
	B	4.69	4.00	4.45
	Cd		Cd	Cd
h_3	$x-\frac{1}{2}$.1487	.1482	.1483
	$z-\frac{1}{2}$.0230	.0235	.0233
	B	2.05	1.73	2.14
	Cd		Cd	Cd
h_4	$x-\frac{3}{4}$.1752	.1754	.1751
	$z-\frac{3}{4}$.0196	.0193	.0193
	B	2.94	2.76	2.84
	Cd		Cd	Cd

* Shifts led to negative B.

** Shifts made bond distances in tetrahedron less than 2.2 Å.

refinement calculations from converging. With our present computer program we do not have the means of estimating the magnitudes of the off-diagonal terms. Further refinement, therefore, has been postponed to await an adequate program for the IBM 7090 computer which will allow us to carry out full-matrix calculations. Furthermore, we feel that we should be very cautious in interpreting the difference-Fourier map. The small isolated peaks may be due to disorder, but we are rather hesitant in assigning significance to them and will discuss our reasons for this in another section after we have presented pertinent information.

Several attempts were made to escape the acceptance of a disordered structure through systematic consideration of various kinds of ordered arrangements. The only reasonable trial structures other than those that correspond very closely to the γ -brass type structures were the ones discussed below.

viii) Ordered structures.

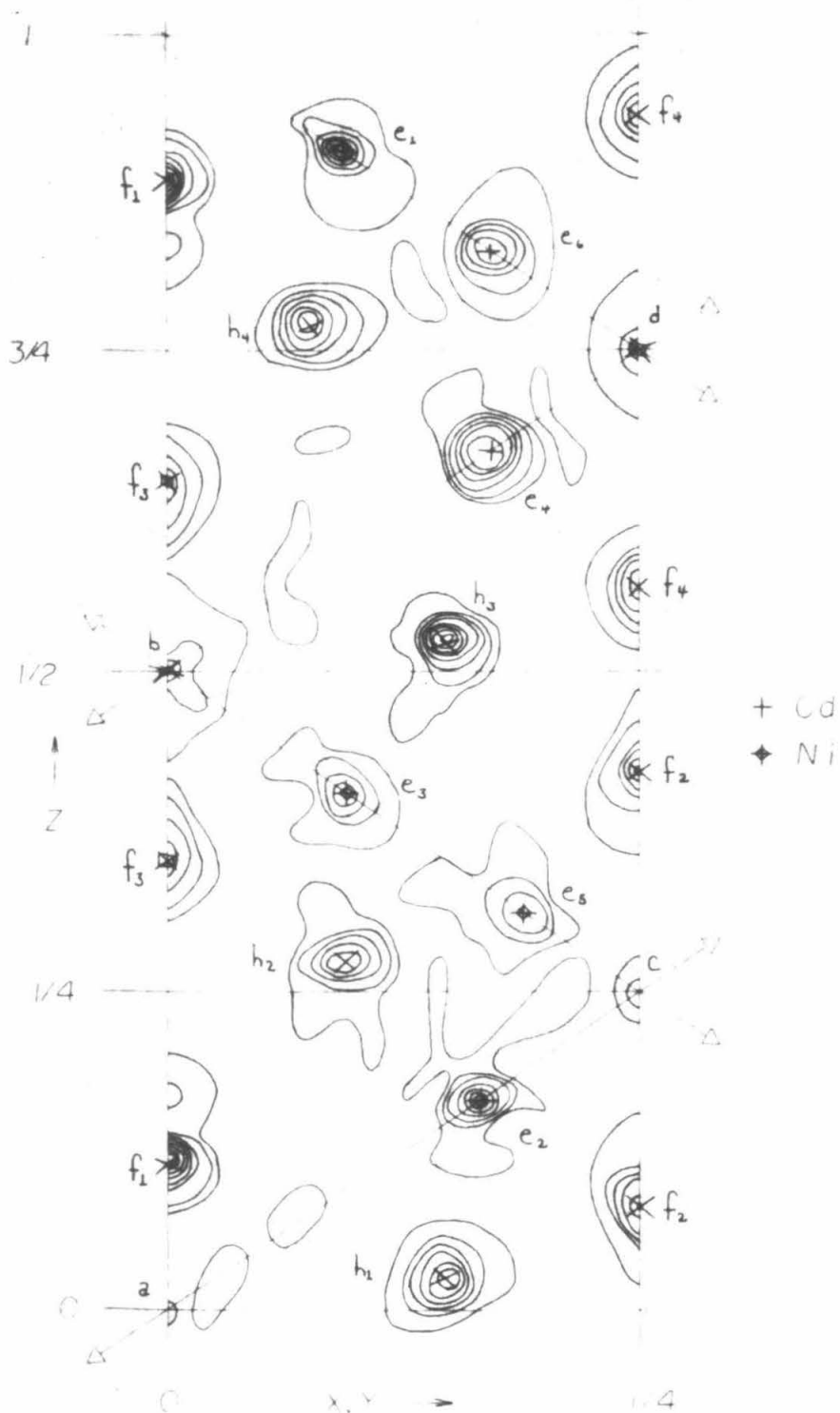
The initial structure may be described in terms of the atom complexes arranged about the four independent centers a, c, b, and d. At center a is a complex of 22 atoms which we have called a σ -complex; around center c is a complex of 26 atoms which we have called a γ -complex. The arrangement around b is very much like that around a except that the octahedron is large enough to accommodate

an atom at *b* such as to produce a complex of 23 atoms. The arrangement around *d* resembles a body-centered cube and is a 27 atom complex. These four complexes with the cubo-octahedra omitted are shown in figures 11, 12, 13, and 15. A cubo-octahedron is shown in figure 10.

A series of refinement cycles led to convergence with $R \cong 0.175$ and to a structure defined by the parameters listed in tables 1 and 2. The electron-density map calculated on the basis of these parameters is shown in figure 9. This electron-density map and the temperature factors of the nickel atoms at positions e_1 and e_2 indicate that the scattering power is the same as for most of the positions to which we have assigned cadmium atoms. The electron-density map also indicates scattering matter at point *c* and near position f_1 , and rather broad regions of scattering at positions f_2 and f_3 .

We assumed that the occupancy at position e_2 is cadmium rather than nickel. In view of the relatively short nearest-neighbor distances around position e_1 , it seemed likely that this position was occupied by nickel atoms, which have a metallic radius about 17 percent smaller than cadmium atoms. This assumption is not in accord with the electron-density map but, on the other hand, the structure is not sufficiently well refined to permit the actual scattering power to be truly represented on the electron-density map. In order to test if the

Figure 9. Electron-density map of the (110) plane. Contours at intervals of 20 e. \AA^{-3} , beginning with 0 e. \AA^{-3} .



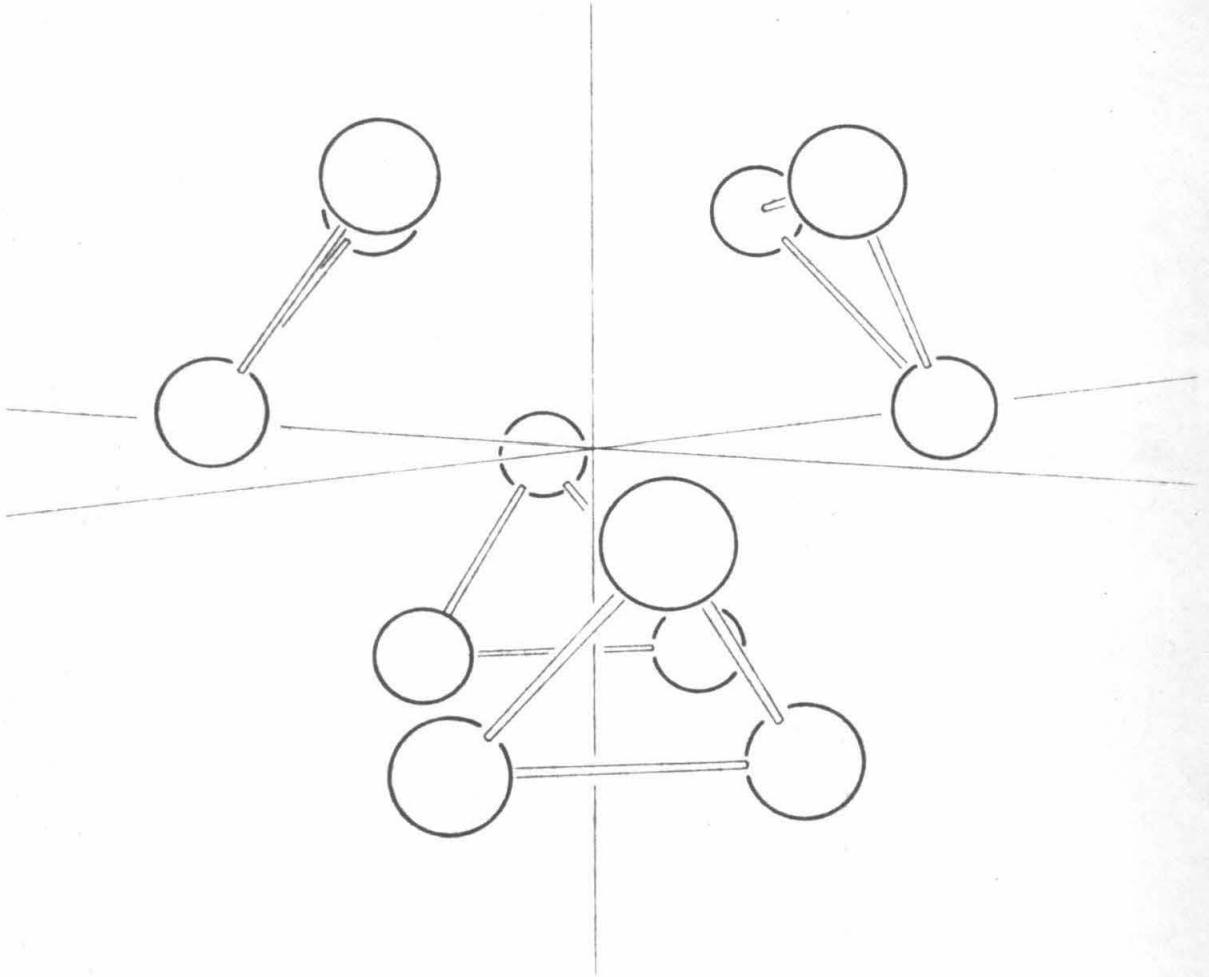
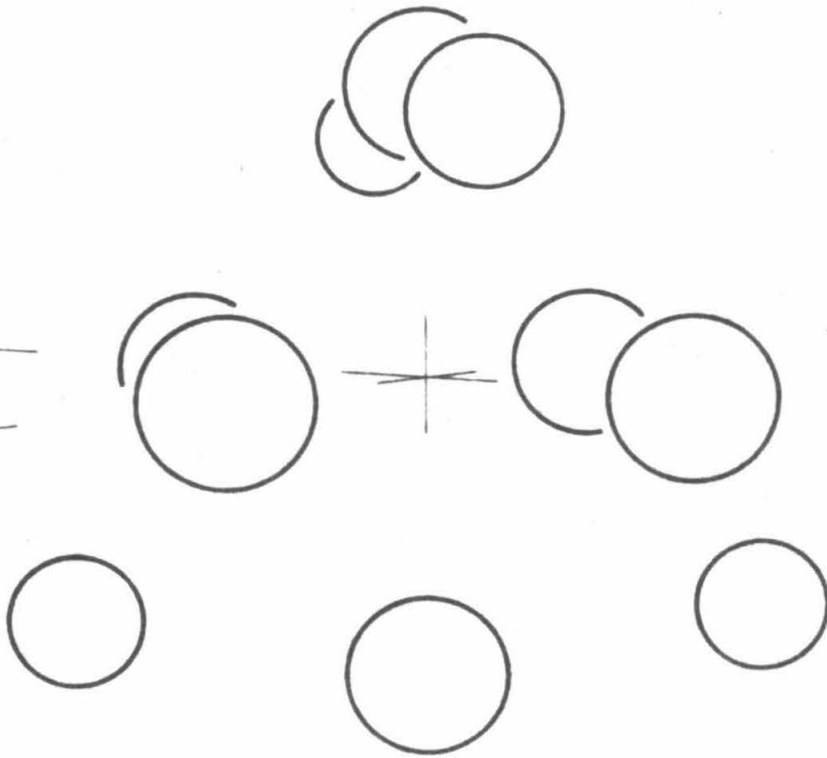


Figure 10. A representation of atoms arranged about the vertices of a distorted cube-octahedron. The atom complexes shown in figures 11, 12, 13, and 15 fit inside this polyhedron.

Figure 11. The atomic arrangement around the points 000, etc., defined by position 4a. This 10-atom complex consists of a tetrahedron and an octahedron.



a

Figure 12. Atom complexes around the points $\frac{1}{4} \frac{1}{4} \frac{1}{4}$, etc., defined by position 4c. This arrangement of atoms at the vertices of two tetrahedra and one octahedron is also observed in the structure of γ brass.

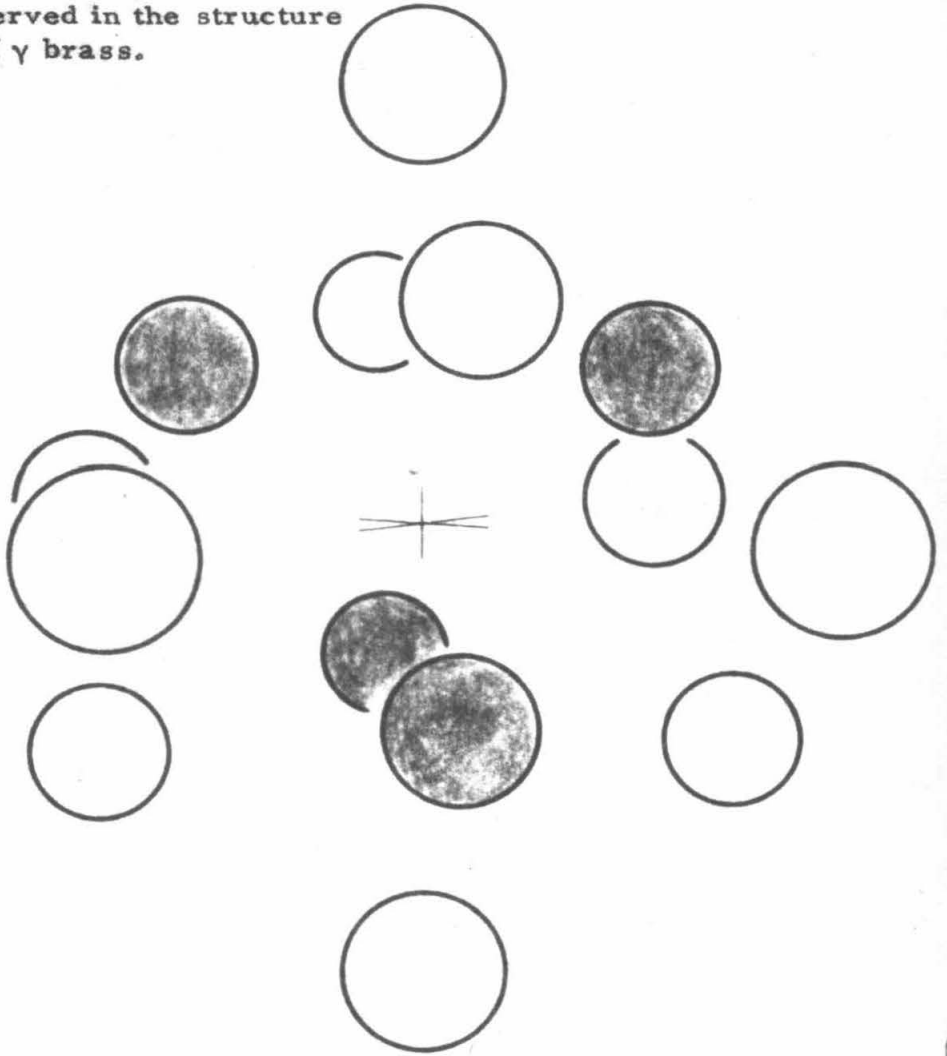


Figure 13. Arrangement of atoms around the points $\frac{1}{2} \frac{1}{2} \frac{1}{2}$, etc., defined by position 4b. Atoms at the vertices of a tetrahedron and an octahedron surround the atom at point b.

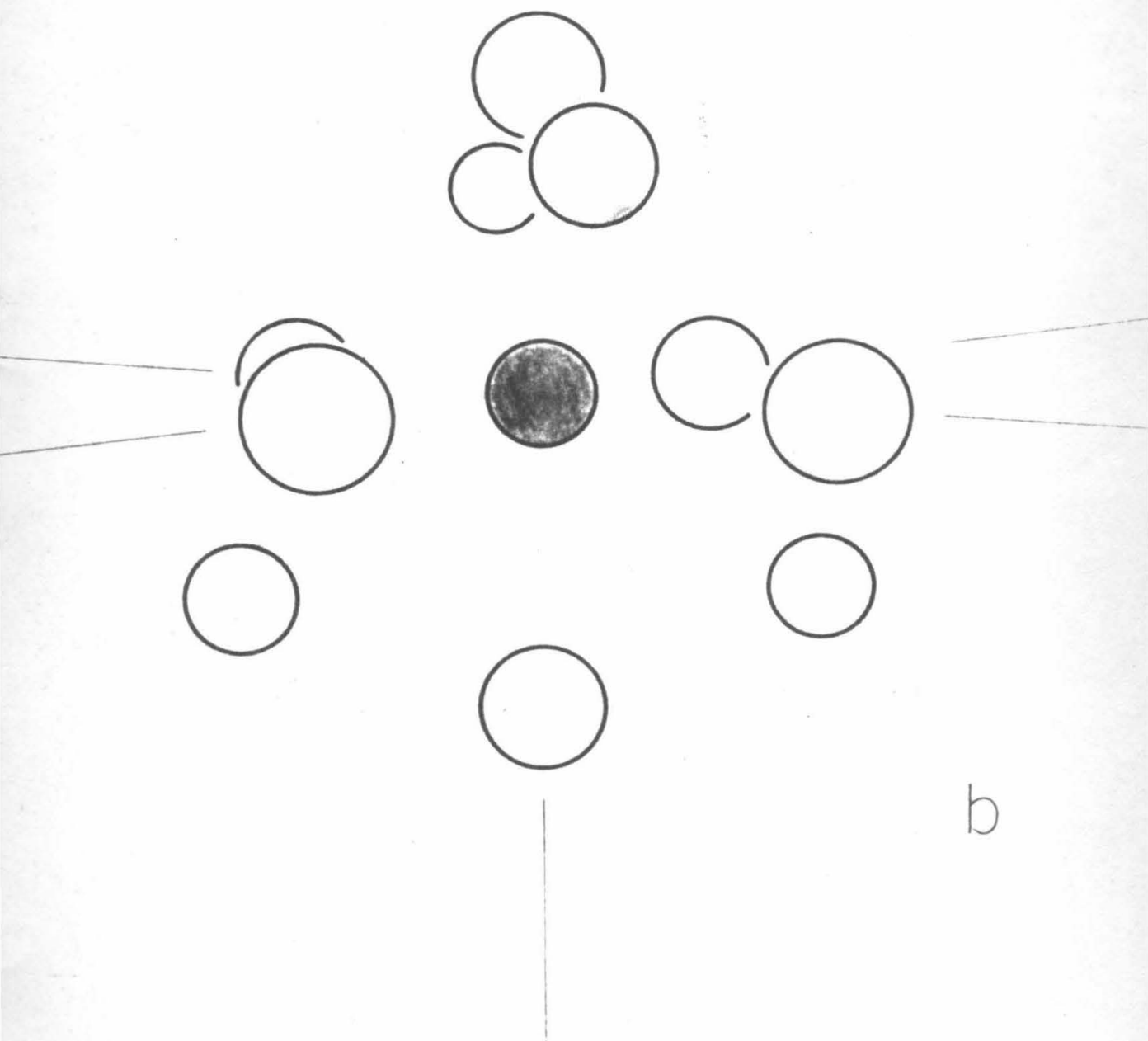


Figure 14. The packing around $\frac{1}{2} \frac{1}{2} \frac{1}{2}$ in more detail.

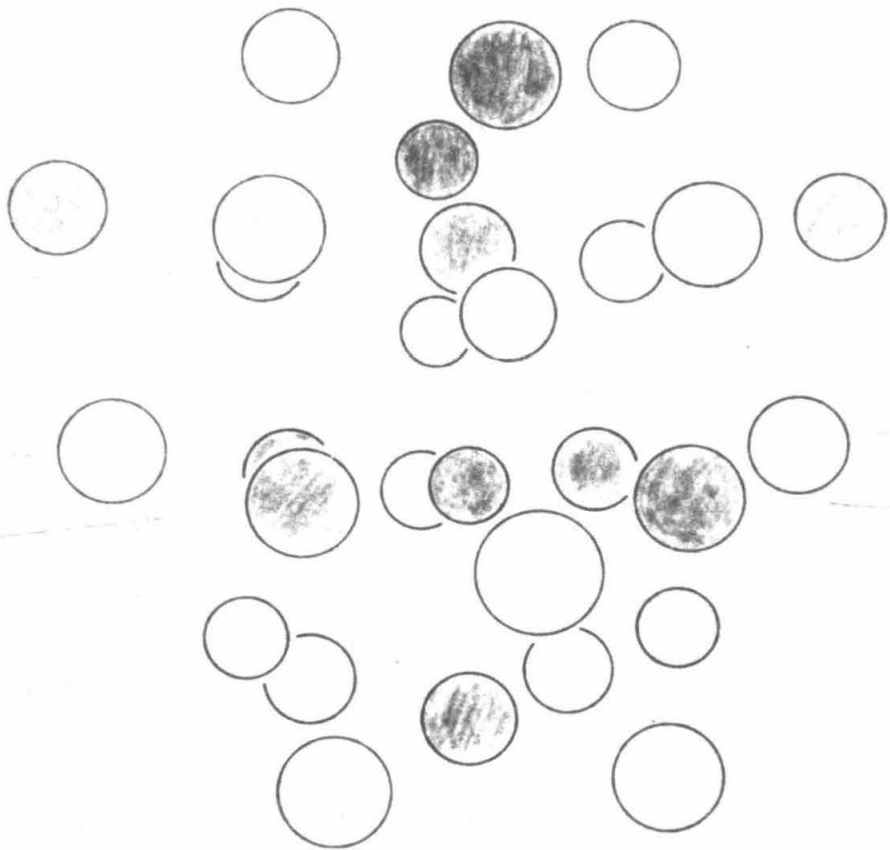
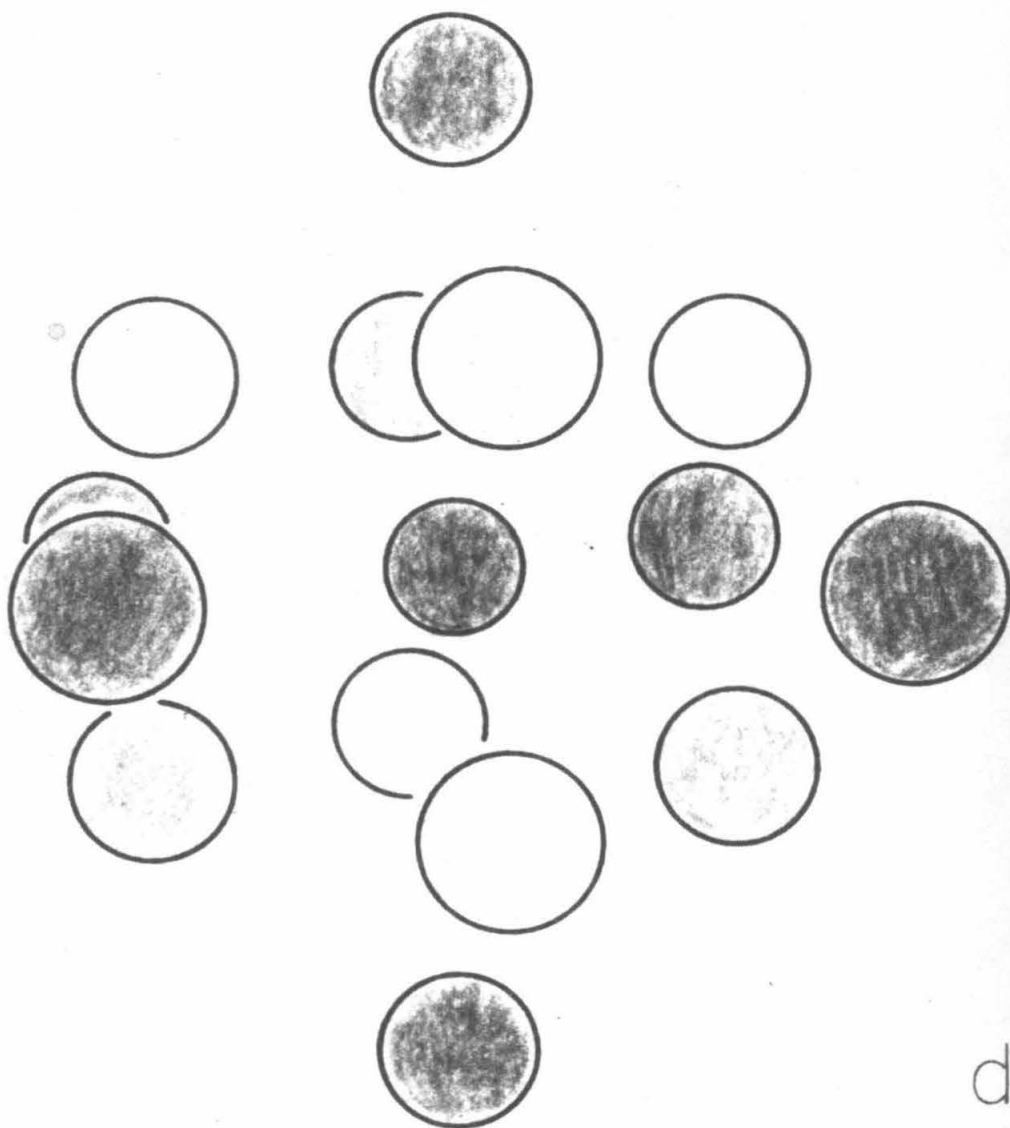


Figure 15. The arrangement of atoms around $\frac{3}{4} \frac{3}{4} \frac{3}{4}$, etc., resembling a body-centered cube.



d

disorder between positions c and e_5 is real, we assumed a fraction x of a nickel atom at point c and a fraction $1-x$ at position e_5 . Refinement calculations based on this assumption did not lead to improved agreement. The parameters obtained are given in tables 1 and 2.

The atom complexes around the four independent centers are similar to one another. The positions of the atoms of each complex relative to its center can be compared with the aid of table 2.

There may be intimate coupling between the parameters for positions related to each other by translations of approximately $\frac{1}{4} \frac{1}{4} \frac{1}{4}$, $\frac{1}{2} \frac{1}{2} \frac{1}{2}$ or $\frac{3}{4} \frac{3}{4} \frac{3}{4}$. It is possible that our neglect of an eventual coupling may have prevented a proper refinement. The phase angles may accordingly be incorrect by amounts large enough to cause false maxima on the Fourier maps. The peak near position f_7 in figure 9 gives the impression that the positions f_2 , f_3 and f_4 have been superimposed on position f_1 .

Discussion of the Structure

Because of the as yet questionable validity of the maxima that indicate disorder, the structure will provisionally be discussed as if it were ordered. A more detailed discussion will have to await the results of very extensive calculations based on complete matrices.

The assumed ordered structure is described by the sixteen crystallographically different positions listed in table 1. The positional

parameters are also included in this table. The interatomic distances calculated on the basis of these parameters are listed in table 3. The distribution of the nickel and cadmium atoms over the occupied positions, as given in table 3, was provisionally assumed on the basis of nearest-neighbor distances. Although the scattering power of the atoms in positions f_3 and b as indicated by the Fourier map and by the least-squares calculations corresponds at present to nickel, the nearest-neighbor distances correspond to cadmium atoms, which have a metallic radius about 20% larger than that of nickel. The short nearest-neighbor distances around position e_1 indicate nickel atoms at that position, whereas the electron-density maps indicate cadmium atoms. The assignment of cadmium atoms to position e_2 is compatible with the electron-density maps. Nearest-neighbor distances indicate the same occupancy for each of the other positions as indicated by the electron-density maps and by the least-squares refinement. The nearest-neighbor distances may not be reliable indicators of the occupancy reported in metal structures since extremely short bonds, as well as vacancies, have been reported in metal structures. Furthermore, the uncertainty in the distances is of the order 0.1 or 0.2 Å.

The composition of this idealized crystal structure corresponds to $\text{Ni}_{13}\text{Cd}_{85}$ or, roughly, $\text{NiCd}_{6.5}$, and the idealized unit cell contains 392 atoms. The calculated density is 9.12 g/cm^3 ; the density of nickel

Table 3. Approximate interatomic distances for the assumed ordered structure. Cube edge = 19.6 Å. For ligancy 12 the expected distances are 2.49 Å for Ni-Ni, 2.75 Å for Cd-Ni, and 3.02 Å for Cd-Cd (13).

Position	Kind of atom	Ligancy	Distance (Å)	Position	Kind of atom	Ligancy	Distance (Å)		
e ₁	Ni	3 Cd(h ₄)	2.77	h ₂	Cd	1 Ni(e ₅)	2.72		
		3 Cd(f ₁ ⁴)	2.56			1 Cd(e ₂)	2.89		
		3 Cd(h ₁ ¹)	2.78			2 Cd(f ₂ ²)	3.10		
		1 Cd(e ₆)	2.82			2 Cd(h ₂ ²)	2.99		
		10					1 Ni(e ₃)	2.61	
f ₁	Cd	4 Cd(h ₁)	3.01			1 Cd(f ₃)	3.03		
		2 Ni(e ₁)	2.56			2 Cd(h ₃)	3.43		
		2 Cd(h ₄)	3.09			2 Cd(h ₄ ³)	3.44		
		4 Cd(f ₁)	3.15			12			
		12				e ₃	Ni	3 Cd(h ₂)	2.61
h ₁	Cd	1 Ni(e ₁)	2.78			1 Ni(e ₅)	3.22		
		2 Cd(f ₁)	3.01			3 Cd(f ₃)	2.81		
		1 Cd(e ₂)	2.78	3 Cd(h ₃)	2.75				
		1 Cd(f ₂)	3.02	1 Cd(b ₃)	3.18				
		1 Cd(f ₂ ²)	3.36	11					
		2 Cd(h ₄ ⁴)	2.93	f ₃	Cd	2 Ni(e ₁)	2.81		
		2 Cd(h ₄)	2.99	2 Cd(h ₂ ³)	3.03				
		2 Cd(h ₁ ²)	3.36	4 Cd(h ₂)	2.95				
		12		2 Cd(h ₃)	3.16				
e ₂	Cd	3 Ni(e ₅)	2.93	1 Cd(b ₄)	2.90				
		3 Cd(f ₂)	2.88	11					
		3 Cd(h ₂)	2.78	h ₃	Cd	2 Cd(f ₃)	2.95		
		3 Cd(h ₁ ²)	2.89	1 Ni(e ₃)	2.75				
		12		1 Cd(e ₄)	2.96				
e ₅	Ni	3 Cd(e ₂)	2.93	1 Cd(f ₄)	2.93				
		3 Cd(f ₂)	2.79	2 Cd(h ₄ ⁴)	2.96				
		3 Cd(h ₂)	2.72	2 Cd(h ₄)	3.43				
		1 Ni(e ₃)	3.22	2 Cd(h ₂)	3.48				
		10		1 Cd(f ₂)	3.51				
f ₂	Cd	2 Ni(e ₅)	2.79	12					
		2 Cd(e ₂)	2.88	b	Cd	4 Ni(e ₁)	3.18		
		2 Cd(h ₂)	3.02	6 Cd(f ₃)	2.90				
		4 Cd(h ₁)	3.10	10					
		1 Cd(f ₄)	2.84						
		2 Cd(h ₃)	3.51						
		13							

Table 3 (continued)

Position	Kind of atom	Ligancy	Distance (Å)	Position	Kind of atom	Ligancy	Distance (Å)
e ₄	Cd	3 Cd(h ₃)	2.96				
		3 Cd(f ₃)	3.02				
		3 Cd(e ₄)	3.05				
		3 Cd(h ₄)	3.29				
		1 Cd(Ni)	2.70				
		13					
e ₆	Cd	3 Cd(e ₄)	3.05				
		3 Cd(f ₄)	3.00				
		3 Cd(h ₄)	2.96				
		1 Ni(e ₄)	2.82				
		1 Ni(d)	2.57				
		11					
f ₄	Cd	2 Cd(e ₄)	3.02				
		2 Cd(e ₆)	3.00				
		2 Cd(h ₃)	2.93				
		1 Cd(f ₃)	2.84				
		2 Cd(h ₂)	3.36				
		4 Cd(h ₄)	3.46				
		13					
h ₄	Cd	1 Cd(e ₄)	3.29				
		1 Cd(e ₆)	2.96				
		1 Cd(f ₁)	3.09				
		1 Cd(f ₃)	3.16				
		1 Cd(e ₁)	2.77				
		2 Cd(h ₃)	2.96				
		2 Cd(h ₃)	2.93				
		2 Cd(h ₁)	3.44				
		2 Cd(f ₄)	3.46				
		13					
d	Ni	4 Cd(e ₄)	2.70				
		4 Cd(e ₆)	2.57				
		(6 Cd(f ₄))	3.61				
		8					

is 8.90 g/cm^3 and of cadmium, 8.65 g/cm^3 . Figure 16 is a packing chart drawn for the ordered structure according to table 1. Figure 17 represents the structure and may be easier to follow than figure 16.

The atoms in the four positions f_2 , e_4 , f_4 , and h_4 have ligancy 13; the type of coordination shell around these four positions is illustrated in figure 18a. The atoms in the five positions f_1 , h_1 , e_2 , h_2 , and h_3 have ligancy 12; the coordination polyhedra around these positions are irregular. However, the atoms at position e_2 are surrounded by atoms at the vertices of a nearly regular icosahedron. The atoms in the three positions f_3 , e_3 , and e_6 have ligancy 11, and their coordination shells are illustrated in figures 18b and 18c. Around the three positions e_1 , e_5 , and b are 10 ligands, and around point d are 8 ligands.

Future Experimental Work

The determination of an accurate value of the cube edge was postponed until all the intensity data had been measured. In the meantime, the crystal deteriorated either due to corrosion or due to a phase transformation. A number of other crystals which had been mounted earlier had undergone the same deterioration.

Supplementary investigations to determine the homogeneity range of this phase and to determine how the cube edge and density vary with composition will soon be started. At the time the above

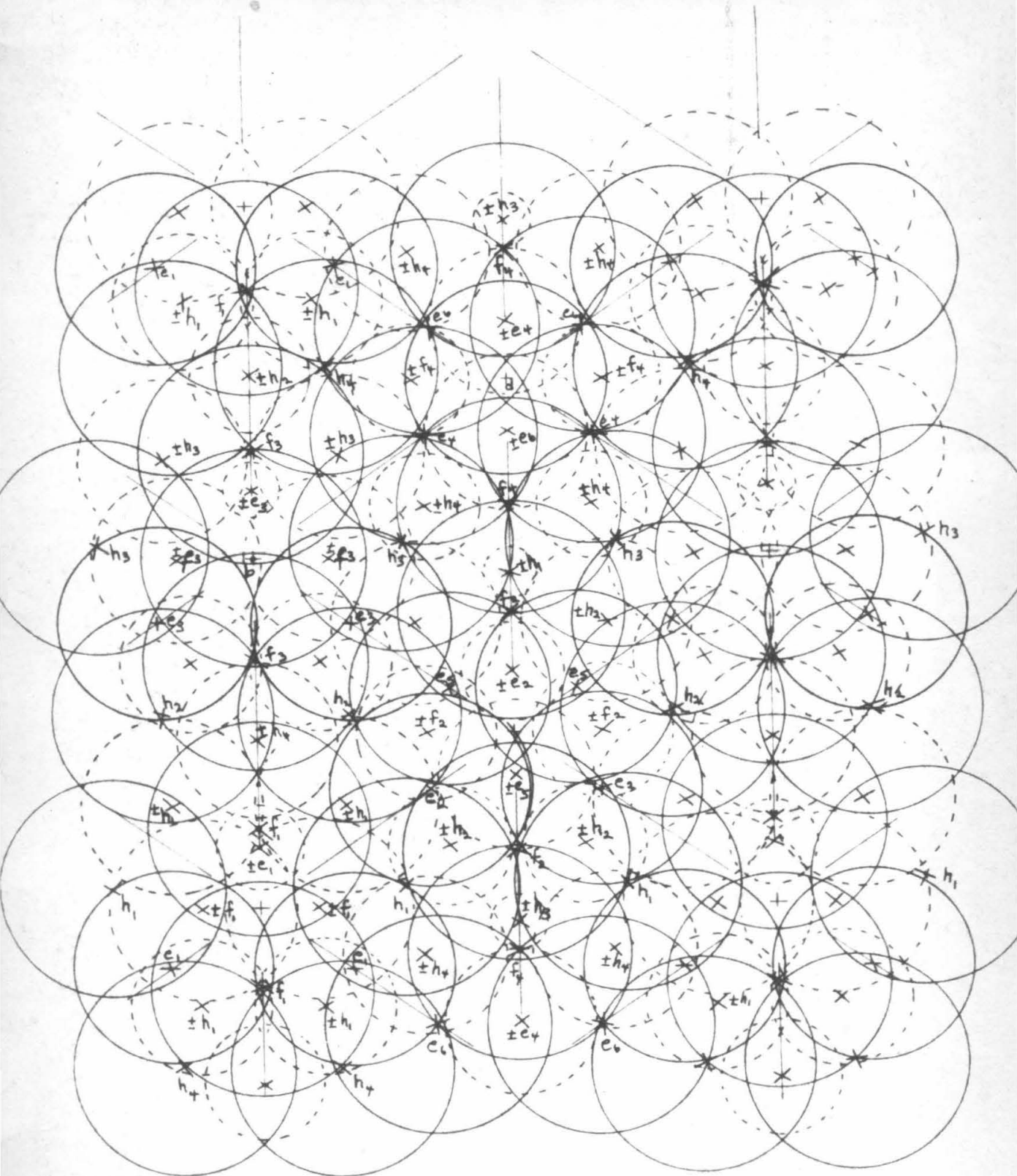


Figure 16. Packing chart of the (110) plane defining all 16 positions.

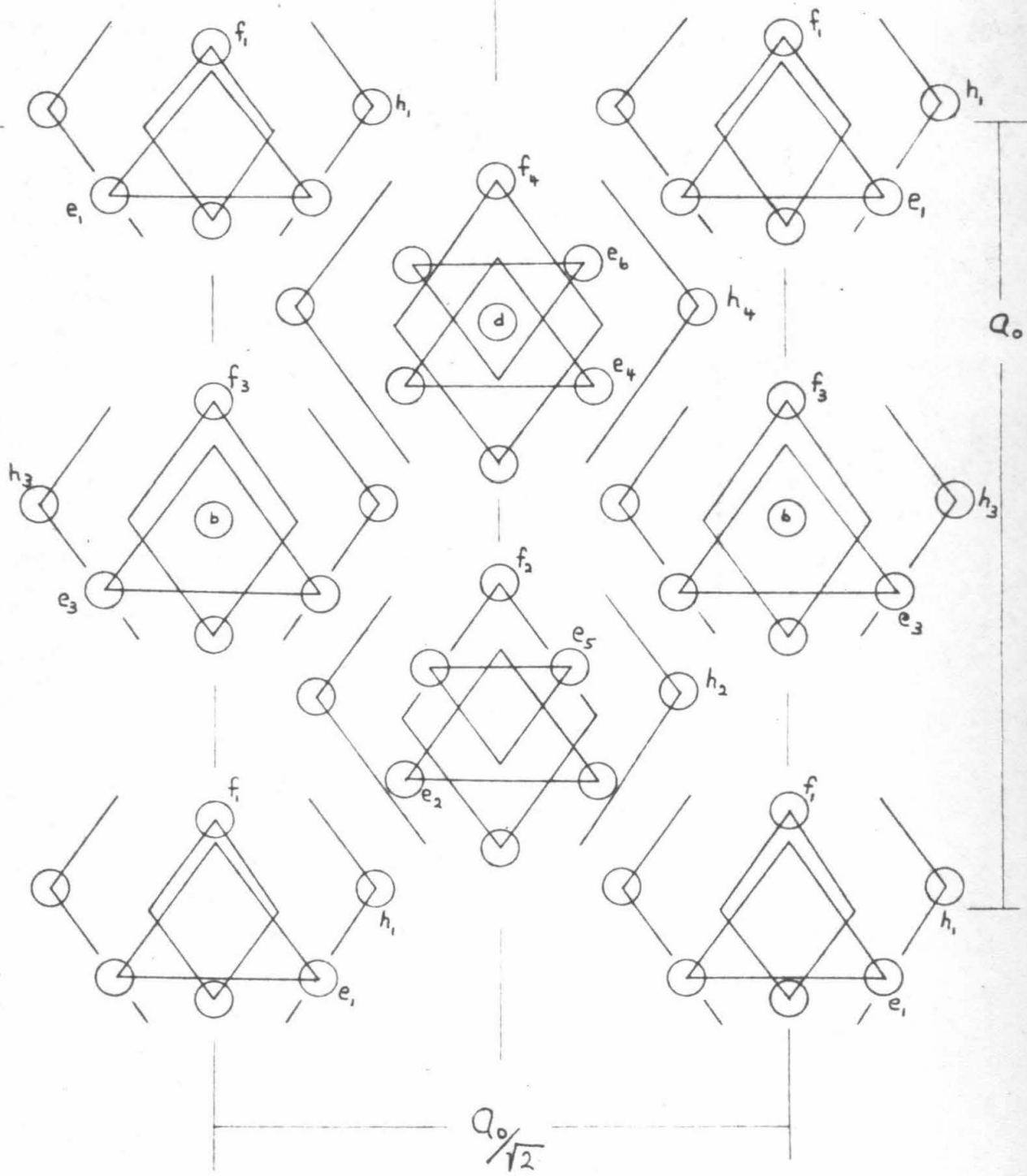
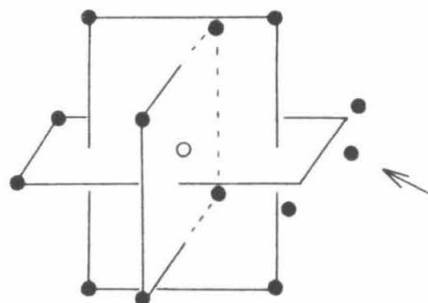


Figure 17. A schematic representation of the atom complexes and of the packing in the asymmetric unit. A circle represents an atom on the (110) plane. The end of a straight line or the intersection of two lines not encircled represents two atoms, one above and one below the (110) plane. A tetrahedron is outlined by a triangle, an octahedron by a rhombus, and a cubo-octahedron by straight lines.

Figure 18. Some illustrations of irregular coordination polyhedra.

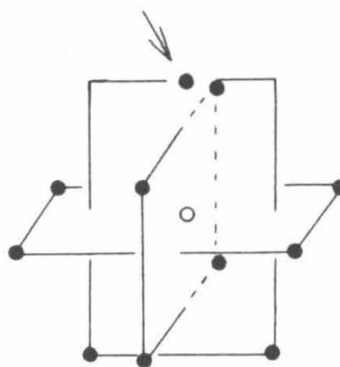
18a) For ligancy 13.

The coordination shell around f_2 , f_4 , e_4 , and h_4 . Ideally, one atom spreads apart two atoms of an icosahedron to become bonded to the central atom.



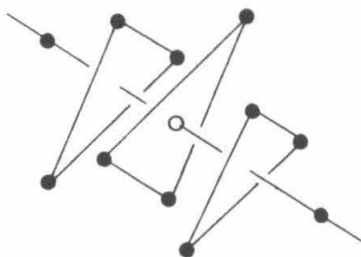
18b) For ligancy 11.

The coordination shell around f_3 . Ideally, one atom has replaced two atoms of an icosahedron.



18c) For ligancy 11.

The coordination shell around e_3 and e_6 .



investigations were done, facilities to carry out this kind of work were not available. A laboratory has now been set up which will enable us to conduct adequate experimental work.

Future Least-Squares Refinements

Refinement of the structure was postponed because of inadequate computing facilities. An adequate program has to allow a solution of the complete set of normal equations. Such a program is being written for the IBM 7090 computer and is expected to be available in a few months.

During the present work we have solved for the temperature- and population-factor shifts in three different ways. The first method took into account the coupling of each temperature factor with the scale factor and with all the other temperature factors, and treated the population factors as being completely independent. The second method took into account coupling between the temperature factor and the population factor of the same atom only; the shifts were based on a 2×2 matrix. The third method was like the second one with the scale factor added to couple with all temperature factors but not with any population factors. Usually the first and second methods gave population-factor shifts in the same direction, but the temperature-factor shifts were often in opposite directions. At times, both shifts from the third method had signs opposite to those of the shifts from one of the other two methods.

From this we can infer that some of the off-diagonal terms representing coupling between atomic coordinates may be large. All along we have been especially concerned about coupling between atoms separated by translations of $\frac{1}{2} \frac{1}{2} \frac{1}{2}$ or $\frac{1}{2} \frac{1}{2} \frac{1}{2}$ or $\frac{2}{4} \frac{2}{4} \frac{2}{4}$. In table 4 we have given the geometrical part of the structure expressions for an atom with coordinates $x_i, 00$ and for atoms related by translations of $\frac{1}{2} \frac{1}{2} \frac{1}{2}$, $\frac{1}{2} \frac{1}{2} \frac{1}{2}$, and $\frac{2}{4} \frac{2}{4} \frac{2}{4}$; in this table we have also indicated $\frac{\partial A_i}{\partial x_i}$. The derivative with respect to the temperature factor is the structure-factor expression multiplied by $\frac{-\sin^2 \theta}{\lambda^2}$.

From table 4 we can see that for the reflections with $h + k + l = 4n$ it makes no difference if an atom is at $x00$ or if it has been translated. Likewise, in a Fourier synthesis the structure would appear as a composite of the structures around the origin and around all the other centers. Reflections of the type $h + k + l = 4n + 2$ can differentiate atoms that are separated by a translation of $\frac{1}{2} \frac{1}{2} \frac{1}{2}$ or $\frac{2}{4} \frac{2}{4} \frac{2}{4}$, but not by $\frac{1}{2} \frac{1}{2} \frac{1}{2}$. Both types of reflections $h + k + l = 4n + 1$ and $h + k + l = 4n + 3$ are sensitive to all of the translations, but taken together as the type $h + k + l = 2n + 1$, they can differentiate atoms that are separated by a translation of $\frac{1}{2} \frac{1}{2} \frac{1}{2}$. The off-diagonal terms representing coupling between atomic coordinates have the same form as the off-diagonal terms that are important in the refinement of the temperature factors; therefore, they have to be important for the refinement of atomic coordinates. On a purely statistical basis,

Table 4. Geometrical structure factors and derivatives with respect to x for atoms at $x00 + (000, \frac{1}{4} \frac{1}{4} \frac{1}{4}, \frac{1}{2} \frac{1}{2} \frac{1}{2}, \frac{3}{4} \frac{3}{4} \frac{3}{4})$.

$$\begin{aligned} \text{Let } C &= 8(\cos 2\pi hx + \cos 2\pi kx + \cos 2\pi lx), \\ S &= 8(\sin 2\pi hx + \sin 2\pi kx + \sin 2\pi lx), \\ S' &= 16\pi(h \sin 2\pi hx + k \sin 2\pi kx + l \sin 2\pi lx), \\ \text{and } C' &= 16\pi(h \cos 2\pi hx + k \cos 2\pi kx + l \cos 2\pi lx). \end{aligned}$$

Geometrical structure factors.

Class of reflections	$x00 +$			
	000	$\frac{1}{4} \frac{1}{4} \frac{1}{4}$	$\frac{1}{2} \frac{1}{2} \frac{1}{2}$	$\frac{3}{4} \frac{3}{4} \frac{3}{4}$
$h + k + l$	000	$\frac{1}{4} \frac{1}{4} \frac{1}{4}$	$\frac{1}{2} \frac{1}{2} \frac{1}{2}$	$\frac{3}{4} \frac{3}{4} \frac{3}{4}$
$4n$	C	C	C	C
$4n + 1$	C	S	-C	-S
$4n + 2$	C	-C	C	-C
$4n + 3$	C	-S	-C	S

Derivatives with respect to x .

$h + k + l$	$x00 +$			
	000	$\frac{1}{4} \frac{1}{4} \frac{1}{4}$	$\frac{1}{2} \frac{1}{2} \frac{1}{2}$	$\frac{3}{4} \frac{3}{4} \frac{3}{4}$
$4n$	-S'	-S'	-S'	-S'
$4n + 1$	-S'	C'	S'	-C'
$4n + 2$	-S'	S'	-S'	S'
$4n + 3$	-S'	-C'	S'	C'

however, the terms correlating the different atoms are expected to be zero; there should be no coupling. We anticipate that the awaited program which will calculate off-diagonal matrix elements will enable us to analyze the interactions between parameters in more critical detail.

If one class of reflections happens to include systematic errors or if it is assigned a higher weight in the least-squares refinement than another class, then one may expect false peaks to occur in the electron-density maps. We are, therefore, very hesitant to accept disorder.

During the refinement of the assumed ordered structure we collected $\Sigma |F_o|$, $\Sigma |F_c|$, and $\Sigma |\Delta F|$ as a function of $\sin \theta$. In general, we found that the best agreement was within the range of $\sin \theta = 0.2$ to 0.3 . The ratio $\Sigma |F_o| / \Sigma |F_c|$ as well as the agreement indices, gradually increased with $\sin \theta$. This seemed to indicate that the temperature factors and the scale factor were too large, but the least-squares process tended to increase them still more. Invoking disorder by splitting a position to give two positions approximately 0.5 \AA apart should improve the agreement of the high order reflections without significantly affecting the low order region. To split the positions should reduce the temperature factors which will be reflected in larger F_c 's of the high order reflections and should also enable the least-squares process to adjust these positions to give even higher F_c 's.

Summary

We have found that the crystal structure of " $\text{Ni}_5\text{Cd}_{21}$ " is very complex. The structure is certainly not of the γ -brass type as reported by other investigators.

The investigation is far from complete, but the general atomic arrangement seems to be essentially correct.

Table 5. (2)

14 16	0082*	06 06	0255	11 15	0075*	11 15	0082*	12 16	0090
14 18	0087*	05 08	0114	11 17	0067*	11 17	0069*	12 18	0072*
14 20	0090*	06 10	0242	11 19	0068*	11 19	0072*	12 20	0087*
14 24	0082*	05 12	0562	11 21	0075*	11 21	0075*	12 22	0090
15 16	0105	05 14	0087	11 23	0075*	11 23	0077*	14 14	0080
15 18	0072*	06 15	0200	13 13	0205	13 13	0085	14 16	0073*
15 20	0075*	06 18	0062*	13 15	0105	13 15	0067*	14 18	0075*
15 22	0079*	06 20	0092	13 17	0070*	13 17	0083*	14 20	0078*
16 24	0082*	05 22	0107	13 19	0072*	13 19	0074*	14 22	0083*
18 18	0087*	05 24	0070*	13 23	0080*	13 21	0075*	16 16	0093
20 20	0107	06 26	0073*	13 25	0082*	13 23	0082*	16 18	0077*
22 22	0082*	06 28	0077*	15 15	0069*	15 15	0072*	18 18	0135
H 05		08 08	0357	15 17	0072*	15 17	0075*	18 20	0083*
05 05	0285	08 10	0143	15 19	0073*	15 19	0077*	H 13	
05 07	0050*	08 12	0167	15 21	0077*	15 21	0078*	13 13	0090
05 09	0047*	08 14	0152	17 17	0075*	17 17	0069*	13 15	0082*
05 11	0158	08 16	0072*	17 19	0077*	17 19	0080*	13 17	0085*
05 13	0157	08 18	0063*	19 19	0077*	17 21	0080*	13 19	0082
05 15	0175	08 20	0067*	H 08		19 19	0075*	13 21	0105
05 17	0098	10 10	0069	08 08	0772	H 10		15 15	0084*
05 19	0115	10 12	0062*	08 10	0210	10 10	0165	15 19	0079*
05 21	0065*	10 14	0064*	08 12	0140	10 12	0057*	17 19	0082*
05 23	0069*	10 16	0302	08 14	0057*	10 14	0062*	19 19	0085*
05 25	0070*	10 18	0082*	08 16	0184	10 16	0168	H 14	
07 07	0185	10 20	0070*	08 18	0193	10 18	0069*	14 14	0117
07 09	0058*	10 22	0094*	08 20	0075	10 20	0090*	14 16	0085*
07 11	0114	12 12	0132	08 22	0097	10 22	0092*	14 18	0089*
07 13	0087	12 14	0135	08 24	0114	12 12	0148	14 20	0247
07 15	0105*	12 16	0092	08 26	0120	12 14	0127	16 16	0072*
07 17	0060*	12 18	0245	08 28	0079*	12 16	0095	18 18	0077*
07 19	0113	12 20	0114*	10 10	0130	12 18	0087*	H 15	
07 21	0067*	12 22	0187	10 12	0092	12 20	0075*	15 15	0085*
07 23	0072*	12 24	0079*	10 14	0062*	12 22	0115*	15 17	0085*
09 09	0162	14 14	0065*	10 16	0142	14 14	0069*	15 19	0085*
09 11	0075	14 16	0097*	10 18	0180	14 16	0087*	15 21	0085*
09 13	0062*	14 18	0115	10 20	0070*	14 18	0094*	17 17	0085*
09 15	0093	14 20	0090*	10 22	0117*	14 20	0115	17 19	0085*
09 17	0065*	14 24	0083*	12 12	0065*	14 22	0080*	H 16	
09 19	0070*	16 16	0077*	12 14	0105	16 16	0075*	16 16	0128*
09 21	0072*	16 18	0110	12 16	0112	16 18	0077*	16 18	0077*
09 23	0077*	16 20	0077*	12 18	0107	16 20	0079*	16 20	0079*
11 11	0135	16 22	0140	12 20	0072*	16 22	0115*	16 22	0082*
11 13	0092	18 18	0140	12 22	0095*	18 18	0090*	16 24	0118*
11 15	0065*	18 20	0112*	12 24	0125*	20 20	0079*	18 18	0099*
11 17	0064*	18 22	0082*	14 14	0322	H 11		20 20	0082*
11 19	0084*	18 24	0147	14 16	0075*	11 11	0098	H 20	
11 21	0090	20 20	0075*	14 18	0097	11 13	0060*	20 20	0202
11 23	0075*	H 07		14 20	0075*	11 15	0075		
13 13	0165*	07 07	0357	14 22	0112*	11 17	0067*		
13 15	0070*	07 09	0045*	14 24	0083*	11 19	0095		
13 17	0070*	07 11	0107	16 16	0164	14 21	0075*		
13 19	0075*	07 13	0052*	16 18	0107	11 23	0077*		
13 23	0080*	07 15	0057*	16 20	0109*	13 13	0062		
13 25	0082*	07 17	0080	18 18	0112	13 17	0075*		
15 15	0065*	07 19	0127	18 20	0115	13 19	0075*		
15 17	0075*	07 21	0080	20 20	0150	13 21	0080*		
15 19	0090*	07 23	0069*	H 09		13 23	0082*		
15 21	0077*	09 09	0203	09 09	0094*	15 15	0069*		
17 17	0069*	09 11	0055*	09 11	0057*	15 17	0082*		
17 19	0075*	09 13	0057*	09 13	0063*	15 19	0099*		
17 21	0079*	09 15	0087*	09 15	0075*	15 21	0087*		
17 23	0082*	09 17	0098	09 17	0075*	17 17	0075*		
17 25	0085*	09 19	0067*	09 19	0070*	19 19	0075*		
19 19	0075*	09 21	0070*	09 21	0072*	H 12			
21 21	0078*	11 11	0060*	11 11	0067	12 12	0404		
H 06		11 13	0095	11 13	0062*	12 14	0100		

PART III

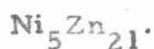
 $"Ni_5 Zn_{21}"$

Introduction

The intermetallic compounds $\text{Fe}_3\text{Zn}_{10}$, $\text{Ni}_3\text{Zn}_{10}$, and $\text{Mn}_3\text{Zn}_{10}$, commonly referred to as the Γ phases, are reported in the literature to be cubic with a cell edge of approximately $a_0 = 8.8 \text{ \AA}$ and space group O_h^9 . The structure proposed by Osawa and Ogawa (1) has been generally accepted and is described in handbooks such as Pearson, Handbook of Lattice Spacings and Structures of Metals (2); it has been assigned the type number 108_1 . Hume-Rothery (3) and Ekman (4) assumed that these compounds represented so-called electron-concentration phases with an electron-to-atom ratio of 21/13 and that, accordingly, the actual compositions were $\text{Fe}_5\text{Zn}_{21}$, $\text{Ni}_5\text{Zn}_{21}$, and $\text{Mn}_5\text{Zn}_{21}$, the transition metals being assigned the valency zero. Although the correctness of these assumptions has not been established through accurate experiments, the names $\text{Fe}_5\text{Zn}_{21}$, $\text{Ni}_5\text{Zn}_{21}$, and $\text{Mn}_5\text{Zn}_{21}$ shall be provisionally retained.

Dr. Samson felt that the structure proposed by Osawa and Ogawa (1) was not in accord with the fundamental structural principles that should apply in these three compounds. He, therefore, started a reinvestigation.

It proved to be extremely difficult to prepare iron-zinc and manganese-zinc compounds, whereas nickel-zinc phases were easy to obtain. The first compound to be investigated was, therefore,



Dr. Samson and his assistant, Dr. K. Lautsch, obtained a complete three-dimensional set of intensity data from an almost spherical single-crystal fragment of about 10 microns in diameter. Because of the very small size, copper radiation was used. Absorption correction was not necessary. The cube edge as determined from the diffraction maxima of this crystal was $a_0 = 8.897 \text{ \AA}$. These maxima had been recorded on a film placed in the asymmetric position in a precision Weissenberg camera of 10 cm diameter.

Since I was very much interested in this compound, Dr. Samson left to me the further prosecution of this work.

Experimental Work

The intensity data as supplied by Dr. Samson and Dr. K. Lautsch were processed by me. Lorentz and polarization corrections were applied and the data obtained from various sets of Weissenberg films were correlated with one another. The data for those reflections that had been recorded on n layers were given an external weight of $w'_e = 1.0 + 0.5(n-1)$. However, depending on a subjective evaluation of the quality of the data, w'_e was modified to give an overall external weight w_e . The evaluation was based mainly on the resolution of the α_1, α_2 doublet and on the agreement between different observations of the same reflection. The weights used in the least-squares refinements were $w \propto \frac{w_e}{40 + F_o}$.

The Trial Structure

i) Space group.

The single-crystal X-ray diffraction patterns obtained from $\text{Ni}_5\text{Zn}_{21}$ were very similar to those of Ag_5Zn_8 , the structure of which was found to be the same as that of γ brass, which is body-centered cubic, space group Td^3 . The structure of Ag_5Zn_8 was refined by Dr. Marsh in 1954 (5). He very kindly made his photographs available to me for comparison.

The Weissenberg photographs of $\text{Ni}_5\text{Zn}_{21}$ showed, however, in addition to the reflections of the kind $h + k + l = 2n$, three diffuse spots corresponding to the reflections 014, 122, and 113. The nature of these reflections, which correspond to a primitive lattice, has not been established. These reflections appear to have their origin in very small domains of primitive unit cells in the crystal.

If the diffuse reflections are ignored, the space groups which most likely apply to $\text{Ni}_5\text{Zn}_{21}$ are T_d^3 and O_h^9 .

ii) The derivation of the structure.

The atomic arrangement proposed by Osawa and Ogawa (1) was, as expected, quickly disproved by structure-factor and least-squares calculations. Symmetry charts of the (110) plane for the space groups O_h^9 and T_d^3 were then extensively explored. No reasonable structural motif could be found by assuming space group O_h^9 .

The next step was to start out with an atomic arrangement that corresponded closely to that of γ brass (space group Td^3).

A few least-squares refinement cycles based on such an arrangement led to convergence with an agreement index of $R = 0.28$. An electron-density map of the (110) plane, calculated on the basis of the structure given by the least-squares process, indicated that the vertices of the small tetrahedron, position e_2 , around the origin of the cube, were occupied only about 60 percent of the time and that

there was an atom at the origin, position a, the remaining 40 percent of the time (see figure 1). Structure-factor and least-squares calculations carried out for such a disordered atomic arrangement resulted in a drastic improvement of the agreement index which dropped to $R = 0.136$; the atomic parameters at this stage of the refinement are given in table 1. The complete list of observed and calculated structure factors is given in table 2.

Additional refinement cycles were carried out with the application of various types of weighting functions, but did not lead to any significant shifts in the parameters nor to an improved agreement. In all of these calculations the sum of the fractional occupancies of the two positions, a and e_2 , was kept equal to unity. Electron-density maps calculated in the course of these refinements differed only insignificantly from one another. However, they always indicated that the sum of the fractional occupancies of the positions a and e_2 was larger than unity.

Discussion of the Structure

The bond distances are given in table 3. The bond numbers were calculated with the use of the equation (6)

$$D_n = D_1 - 0.6 \log n$$

where D_1 has been taken as 2.31 \AA for a Ni-Ni bond, 2.37 \AA for a Ni-Zn bond, and 2.43 \AA for a Zn-Zn bond (6).

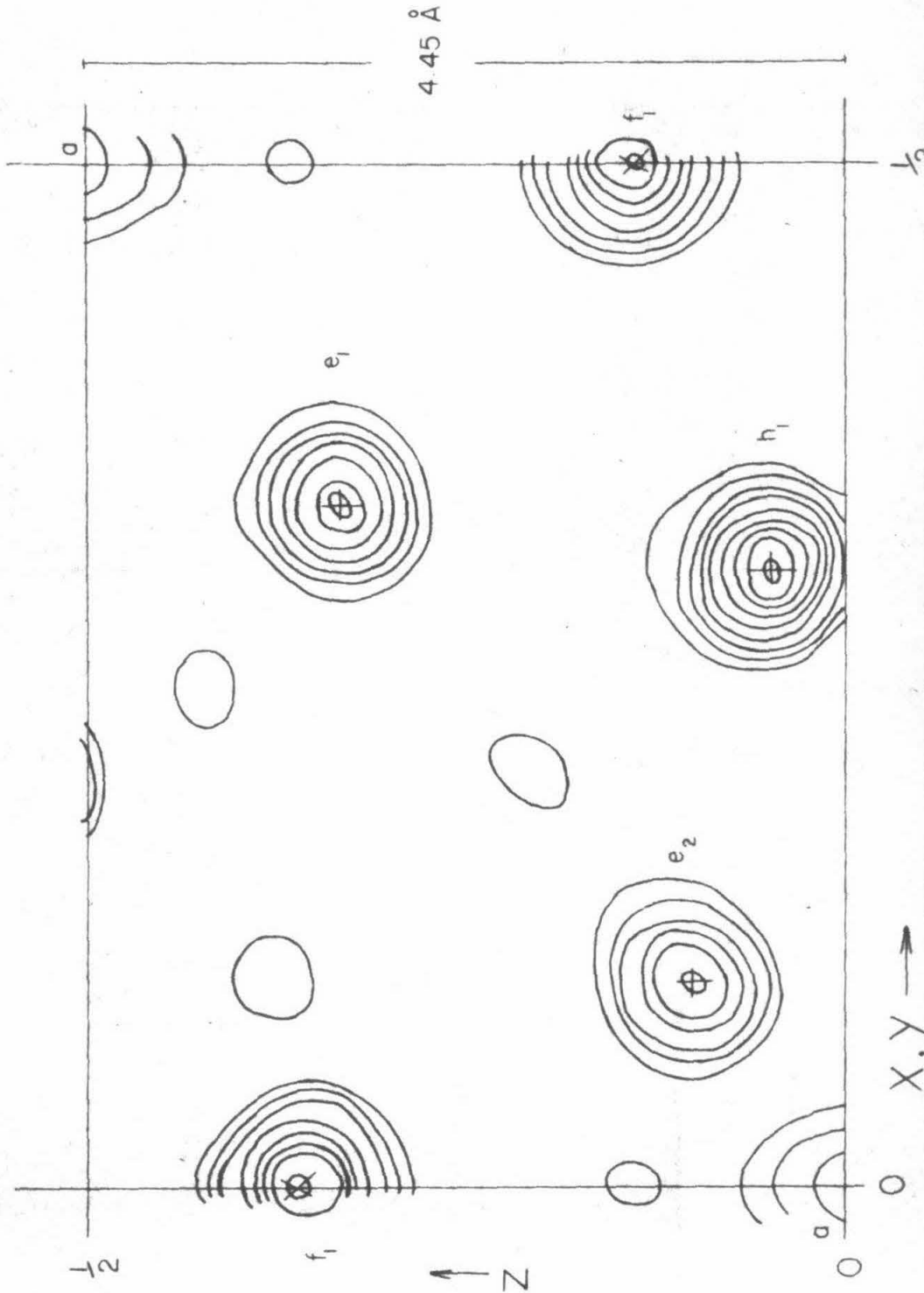


Figure 1. Electron-density map of the (110) plane of $\text{Ni}_5\text{Zn}_{21}$, calculated on the assumption that positions $e_1, e_2, f_1,$ and f_2 are completely occupied and that position a is unoccupied. The first contour is at 5 e. \AA^{-3} . The other contours are at intervals of 10 e. \AA^{-3} beginning at 10 e. \AA^{-3} .

Table 1

Refined atomic coordinates, temperature factors, and population factors

Kind of atom	Position	Occu-pancy	Coordinates	Temperature factor
Zn	2a, 000, $\frac{1}{2}\frac{1}{2}\frac{1}{2}$	43%	---	0.07 <u>+</u> 1.09
Ni	8e ₂ , XXX, etc.	57%	x _{e₂} = .1021 <u>+</u> .0035	0.57 <u>+</u> 0.44
Ni	8e ₁ , XXX, etc.	100%	x _{e₁} = .3332 <u>+</u> .0028	3.27 <u>+</u> 0.50
Zn	12f ₁ , X00, etc.	100%	x _{f₁} = .3462 <u>+</u> .0017	2.98 <u>+</u> 0.30
Zn	24h ₁ , XXZ, etc.	100%	x _{h₁} = .3035 <u>+</u> .0010 z _{h₁} = .0471 <u>+</u> .0010	2.40 <u>+</u> 0.17

Table 2

Observed and calculated structure factors. The column headings are k , l , F_o and F_c .

h=0				h=1			
0	0	-	1362	1	2	30	43
0	4	91	99	1	4	274	331
0	6	213	249	1	6	57	44
0	8	91	101	1	8	35	24
0	10	87	91	1	10	72	50
1	1	28	12	2	3	62	79
1	3	72	92	2	5	59	53
1	5	75	75	2	7	151	152
1	7	59	49	2	9	40	45
1	9	62	59	2	11	41	36
1	11	52	41	3	4	50	50
2	2	19	29	3	6	121	129
2	4	27	19	3	8	37	29
2	6	63	50	3	10	28	30
2	8	106	82	4	5	43	40
2	10	59	52	4	7	140	131
3	3	334	586	4	9	56	40
3	5	60	60	5	6	67	67
3	7	80	74	5	8	42	39
3	9	73	40	5	10	60	79
3	11	28	29	6	7	< 32	31
4	4	78	76	6	9	32	31
4	6	77	74	7	8	43	53
4	8	38	24				
4	10	19	9				
5	5	174	172				
5	7	32	20	2	2	149	186
5	9	35	35	2	4	102	113
6	6	157	150	2	6	61	65
6	8	< 32	0	2	8	69	73
7	7	16	5	2	10	97	93
7	9	< 10	16	3	3	121	151
8	8	79	98	3	5	61	51
				3	7	80	75
				3	9	59	52
				4	4	123	124
				4	6	63	64
				4	8	< 37	22

Table 2 (continued)

h=2 (continued)

4	10	50	31
5	5	71	78
5	9	38	30
6	6	114	118
6	8	33	21
7	7	37	12
8	8	< 9	5

h=5

5	6	< 27	15
5	8	17	17
6	7	40	33

h=6

6	6	108	102
---	---	-----	-----

h=3

3	4	87	85
3	6	194	193
3	8	69	54
3	10	< 44	28
4	5	65	50
4	7	48	40
4	9	31	31
5	6	58	46
5	8	106	88
6	7	< 32	7
6	9	69	77
7	8	< 19	17

h=4

4	4	323	291
4	6	65	56
4	8	51	43
4	10	< 9	29
5	5	55	41
5	7	56	45
5	9	45	50
6	6	41	40
6	8	26	21
7	7	103	97

Table 3

Bond distances and bond numbers in $\text{Ni}_5\text{Zn}_{21}$.

Position	Ligand	Bond distance(\AA)	Total bond numbers	
$\text{Zn}(a)$	$4\text{Ni}(e_1)$	2.57	1.87	
	<u>$6\text{Zn}(f_1)$</u>	3.08	<u>.50</u>	
	10		2.37	
$\text{Ni}(e_2)$	$3\text{Ni}(e_2)$	2.57	1.11	
	$3\text{Ni}(e_1)$	2.53	1.29	
	$3\text{Zn}(f_1)$	2.52	1.69	
	<u>$3\text{Zn}(h_1)$</u>	2.58	<u>1.34</u>	
	12		5.43	
$\text{Ni}(e_1)$	{ or	$1\text{Zn}(a)$	2.57	.46
		$3\text{Ni}(e_2)$	2.53	1.29
		$3\text{Zn}(f_1)$	2.57	1.38
		$3\text{Zn}(h_1)$	2.57	1.38
		<u>$3\text{Zn}(h_1)$</u>	2.57	<u>1.38</u>
	10 or 13		4.60 or 5.43	
$\text{Zn}(f_1)$	{ or	$1\text{Zn}(a)$	3.08	.08
		$2\text{Ni}(e_2)$	2.52	1.12
		$2\text{Ni}(e_1)$	2.57	.92
		$4\text{Zn}(h_1)$	2.76	1.13
		$2\text{Zn}(h_1)$	3.05	.18
		$2\text{Zn}(h_1)$	2.65	.86
		<u>$1\text{Zn}(f_1)$</u>	2.74	<u>.30</u>
	12 or 13		3.47 or 4.51	
$\text{Zn}(h_1)$	{ or	nothing		
		$1\text{Ni}(e_2)$	2.58	.45
		$1\text{Ni}(e_1)$	2.57	.46
		$1\text{Ni}(e_1)$	2.57	.46
		$2\text{Zn}(f_1)$	2.76	.56
		$1\text{Zn}(f_1)$	2.65	.43
		$1\text{Zn}(f_1)$	3.05	.09
		<u>$4\text{Zn}(h_1)$</u>	2.72	<u>1.05</u>
	11		3.05 or 3.50	

One may describe this disorder as if it were actually due to the presence of three kinds of unit cells in the crystal. One kind of cell may contain an atomic arrangement identical to that of γ brass. A second kind may be described as a modified γ brass structure in which the small tetrahedra around 000 and $\frac{1}{2}\frac{1}{2}\frac{1}{2}$ have been replaced by an atom at 000 and $\frac{1}{2}\frac{1}{2}\frac{1}{2}$. The third kind may also be described as a modified γ brass structure in which the small tetrahedron around $\frac{1}{2}\frac{1}{2}\frac{1}{2}$ has been replaced by an atom at $\frac{1}{2}\frac{1}{2}\frac{1}{2}$. The first two kinds of unit cells are body centered, and we call these γ, γ and $0, 0$. The third kind of unit cell is primitive and is called $0, \gamma$.

We cannot describe the actual distribution of these three kinds of unit cells within our crystal. However, the diffuse spots referred to earlier and corresponding to reflections from a primitive cell may be due to small domains of adjacent primitive cells just described. The diffuseness indicates that these domains are less than 100 unit-cube edges in length. A quantitative evaluation of this phenomenon may be made later.

The Diffuse Reflections

We calculated, but only very roughly, which reflections should be observed from the domains of primitive cells. We assumed that the primitive cell is body centered with the exception of 4 atoms at the vertices of the small tetrahedron around 000 and an atom at $\frac{1}{2}\frac{1}{2}\frac{1}{2}$.

Structure factors were calculated on this basis for reflections of the type $h + k + l = 2n + 1$. We only point out that the three observed diffuse reflections are among the nine reflections having the largest calculated structure factors (see table 4).

Structure-factor calculations for the disordered structure

For the sake of simplicity, let positions a and e_2 each have 50 percent occupancy. Furthermore, let the crystal be a twin of two crystals of equal size and shape having exactly the same orientation. Let one of the twins be a γ, γ type and the other an $0, 0$ type, which we have defined above.

The structure factor expression which we have used for our disordered, or composite, crystal is

$$F_c = \sqrt{(A_s + A_{e_2} + A_a)^2 + (B_s + B_{e_2})^2}$$

where A_s and B_s signify the contributions of positions e_1 , f_1 and h_1 .

Let A_s , B_s , and B_{e_2} be equal to zero. We consider two cases: 1) $A_a = A_{e_2}$ and 2) $A_a = -A_{e_2}$.

In the first case we would calculate for a composite crystal

$$F_c = \sqrt{(A_a + A_{e_2})^2} = \sqrt{(2A_a)^2} = 2A_a$$

and for the twin crystal, where position a is fully occupied in one half of the crystal and position e_2 in the other half,

Table 4

Diffuse reflections. The nine reflections most likely to be observed and their structure factors calculated on the basis of a greatly simplified model.

<u>hkl</u>	<u>F_c</u>	<u>F_o</u>
005	75	--
014	64	23
223	61	--
115	53	--
001	49	--
003	49	--
122	46	9
113	45	15
016	44	--
<hr/>	<hr/>	<hr/>
next largest		
227	37	

$$F_c = \sqrt{\frac{1}{2} F_{0,0}^2 + \frac{1}{2} F_{\gamma,\gamma}^2} = \sqrt{\frac{1}{2} (2A_a)^2 + \frac{1}{2} (2A_{e_2})^2} = 2A_a$$

The two results are the same. However, for the second case where $A_a = -A_{e_2}$, we would calculate for a composite crystal

$$F_c = \sqrt{(A_a + A_{e_2})^2} = \sqrt{(A_a - A_{e_2})^2} = 0$$

but for the twin crystal,

$$F_c = \sqrt{\frac{1}{2} (2A_a)^2 + \frac{1}{2} (-2A_a)^2} = 2A_a.$$

If our crystal contains small crystallites or domains of a significant size, it is obvious that our agreement is bound to be poor and that we cannot expect our electron-density maps to be correct.

References (Part I)

1. J. H. Richards and E. A. Hill, J. Am. Chem. Soc., 81, 3484 (1959).
2. E. A. Hill and J. H. Richards, J. Am. Chem. Soc., 83, 3840-3846 (1961).
3. E. A. Hill and J. H. Richards, J. Am. Chem. Soc., 83, 4216-4221 (1961).
4. R. E. Carter, Ph. D. Thesis, California Institute of Technology (1962).
5. D. Hall, Ph. D. Thesis, California Institute of Technology (1963).
6. J. A. Trotter, Acta Cryst., 11, 355-360 (1958).
7. J. B. Nelson and D. P. Riley, Proc. Phys. Soc., 57, 160-177 (1945).
8. J. Berghuis, I. J. Haanappel, M. Potters, B. O. Loopstra, C. H. MacGillavry and A. L. Veenendall, Acta Cryst., 8, 478-483 (1955).
9. J. A. Hoerni and J. A. Ibers, Acta Cryst., 7, 744-746 (1954).
10. L. H. Thomas and K. Umeda, J. Chem. Phys., 24, 293-305 (1957).
11. C. H. Dauben and D. H. Templeton, Acta Cryst., 8, 841 (1955).

12. R. McWeeny, Acta Cryst., 4, 513-519 (1951).
13. W. Cochran, Acta Cryst., 1, 138-142 (1948).
14. A. Hybl, Ph. D. Thesis, California Institute of Technology (1961).
15. E. W. Hughes, J. Am. Chem. Soc., 63, 1737-1752 (1941).
16. B. D. Sharma, private communication.
17. G. L. Hardgrove and D. H. Templeton, Acta Cryst., 12, 28-32 (1959).
18. J. D. Dunitz, L. E. Orgel, and A. Rich, Acta Cryst., 9, 373-375 (1956).
19. D. M. Blow, Acta Cryst., 13, 168 (1960).
20. L. Pauling, The Nature of the Chemical Bond, (1960), 3rd ed., Ithaca: Cornell University Press.
 - a) pp. 385-388
 - b) pp. 417-421
 - c) p. 403, table 11-1
21. D. Seus, Ph. D. Thesis, Inorganic Institute of the Technical University of Munich (1955).
22. J. A. Ibers and R. G. Snyder, Acta Cryst., 15, 923-930 (1962).

References (Part II)

1. G. Voss, Z. anorg. Chem., 57, 69-70 (1908).
2. W. Ekman, Z. physik. Chem., B12, 57-77 (1931).
3. C. E. Swartz and A. J. Phillips, Trans. AIME, 111, 333-336 (1934).
4. F. Lihl and E. Buhl, Z. Metallkunde, 35, 151-152 (1943).
5. L. Pauling, American Scientist, 43, 285 (1955).
6. S. Samson, private communication of work to be published.
7. International Tables for X-ray Crystallography, Vol. I (1952).
Birmingham: Kynoch Press.
8. S. Samson, Acta Chem. Scand., 3, 809-834 (1949).
9. L. H. Thomas and K. Umeda, J. Chem. Phys., 26, 293-305 (1957).
10. R. E. Marsh, Acta Cryst., 7, 379 (1954).
11. A. J. Bradley and C. H. Gregory, Phil. Mag., 12, 143-162 (1931).
12. E. W. Hughes, J. Am. Chem. Soc., 63, 1737-1752 (1941).
13. L. Pauling, The Nature of the Chemical Bond, (1960), 3rd ed.
Ithaca: Cornell University Press. p. 403, table 11-1.

References (Part III)

1. A. Osawa and Y. Ogawa, Z. Krist., 68, 177-188 (1928).
2. W. B. Pearson, A Handbook of Lattice Spacings and Structures of Metals and Alloys, (1958). New York: Pergamon Press.
3. W. Hume-Rothery and G. V. Raynor, The Structure of Metals and Alloys, (1956), London: The Institute of Metals.
4. W. Ekman, Z. physik. Chem., B12, 57-77 (1931).
5. R. E. Marsh, Acta Cryst., 7, 379 (1954).
6. L. Pauling, The Nature of the Chemical Bond, (1960), 3rd ed., Ithaca: Cornell University Press. pp. 400-403.

PROPOSITIONS

I. I propose that the inherent symmetry of the bond orbitals of the metal atom in a sandwich compound is a significant factor in determining the symmetry of the sandwich compound and that the metal-ring bonding itself is more important than van der Waals' forces between the rings in imposing stereospecificity on the rotational configuration.

Authors of review articles (1, 2) have not considered the symmetry of the metal orbitals as playing any role in determining the molecular symmetry of sandwich compounds. I quote P. L. Pauson (1a):

Ferrocene crystallizes in the monoclinic space-group $P2_1/c$ with two molecules in the unit cell. Hence the metal atom lies at a center of symmetry both within the unit cell and within the molecule. The chromium atom in the cubic crystals of bis-benzenechromium must also constitute a molecular center of symmetry. This leads to the opposed conformation of the rings in the latter and to the staggered conformation in ferrocene, but the analogous dicyclopentadienylruthenium and dicyclopentadienylosmium have the opposed conformation in their orthorhombic crystals. One reason for this difference from ferrocene may be the larger size of ruthenium and osmium which reduces the repulsion between hydrogen atoms attached to different rings.

And I quote Cotton and Wilkinson (2a):

It is interesting to note that in contrast to ferrocene, which has the staggered conformation in the crystal, ruthenocene is eclipsed. This difference is due to differences in the lattice forces and/or to

smaller van der Waals' forces when the rings are farther apart. It may be noted that in di(π -indenyl)iron, the benzene rings are in the gauche position, this form again being stabilized in the crystal by crystal forces or by weak van der Waals' forces between the atoms of the six-membered rings (3.43 Å apart). As with the other π -cyclopentadienyl compounds, in solution or in the vapor, the rings are probably freely rotating in the indenyl compounds, or nearly so.

And further on (2b):

It is therefore significant that ruthenocene has recently been found to exist in the eclipsed (D_{5h}) configuration; dibenzenechromium also exists in an eclipsed configuration in the crystal. This seems to indicate (1) that the configuration is determined mainly by lattice forces or (2) that the configuration in $(\pi-C_5H_5)_2Fe$ is determined by small van der Waals' forces which become insignificant when the rings are further apart as they are in $(\pi-C_5H_5)_2Ru$ or (3) a combination of these factors. What these results would appear to contradict clearly is the idea that the metal-ring bonding itself, presumably the same in essential features in both compounds, imposes any stereospecificity on the rotational configuration.

My proposal is in direct conflict with the last sentence quoted.

The data pertinent to the discussion that follows are presented in table 1. I shall use Pauson's nomenclature.

In both reviews the authors have implied that ferrocene is staggered because of repulsion between the atoms in different rings. I assert that this repulsion is secondary to some other phenomenon; my assertion rests on the observation that bis-benzenechromium exists in the eclipsed configuration. In both reviews, the eclipsed configuration of bis-benzenechromium is merely noted.

Table 1

Comparison of bond distances and ring-to-ring distances in some sandwich compounds

Eclipsed configuration	Mean distances in Angstroms		
	M-C	C-C	ring-to-ring
bis-benzenechromium (3)	2.135 \pm .010	1.439 \pm .014	3.226 \pm .014
	2.132 \pm .010	1.353 \pm .014	
ruthenocene (4)	2.21 \pm .02	1.43 \pm .02	3.68 \pm .02
bis-indenylruthenium (5)	2.19	1.43	3.67
osmocene (6)	2.22		3.71
<u>Staggered configuration</u>			
ferrocene (7)	2.05 \pm .03	1.41 \pm .03	3.32*
ferrocene (8)	2.064 \pm .013	1.440 \pm .029	3.32 \pm .06
bis-indenyliron (9)	2.10	1.43	3.43
nickelocene (10)	2.20 \pm .02	1.44 \pm .02	3.66*
nickelocene (11)	2.18	1.43	3.62*

*Calculated from mean M-C and C-C distances.

Even though the six-membered rings of bis-benzenechromium are closer to each other than the five-membered rings of ferrocene, bis-benzenechromium is eclipsed and ferrocene is staggered. The ring separation is 3.23 \AA in bis-benzenechromium (3) and 3.32 \AA in ferrocene (7,8). If repulsion between atoms of different rings were the cause of the staggered configuration of ferrocene, bis-benzenechromium would also be staggered. Note that dicyclopentadienylchromium is staggered (2).

Cotton and Wilkinson's argument that the configuration is determined mainly by lattice forces is harder to refute since "lattice forces" is not defined and its implications are rather vague. I will assume that lattice forces are sensitive to, or are a function of, the overall shape and size of a molecule and the way in which the molecules pack together. I believe there are two observations which indicate that lattice forces, whatever they may be, are not responsible for the molecular symmetry of ferrocene and ruthenocene in the crystalline state.

First, bis-indenyliron has the staggered configuration (9), just as ferrocene, and bis-indenylruthenium has the eclipsed configuration (5), just as ruthenocene. The differences in lattice forces that would make ferrocene and ruthenocene have different symmetries should be smaller between bis-indenyliron and bis-indenylruthenium.

The lattice forces making bis-indenylruthenium eclipsed (cis) will also tend to make bis-indenyliron eclipsed rather than staggered (gauche, in this case). The probability that the same symmetrical derivatives of ferrocene and ruthenocene will have the same configuration will increase as the size of the molecule increases. Obviously, the change from cyclopentadienyl groups to indenyl groups is not enough. Furthermore, both bis-indenyliron and bis-indenylruthenium crystallize in disordered modifications in which, seemingly at random, molecules throughout the crystal are rotated 180° about an axis which is perpendicular to the indenyl groups and which passes through the geometrical center of the molecule. This indicates that the lattice forces are not very selective.

Second, the molecules of nickelocene and ruthenocene are essentially the same size, yet nickelocene is staggered and ruthenocene is eclipsed. (Please refer to table 1.)

	<u>M-C</u>	<u>C-C</u>	<u>ring-ring</u>
Nickelocene	2.20 Å	1.44 Å	3.64 Å
Ruthenocene	2.21 Å	1.43 Å	3.68 Å

From this I infer that the different symmetries of nickelocene and ruthenocene are not due to lattice forces. Here are two sandwich compounds which differ only in the kind of metal atom inside the sandwich--and in their rotational configuration.

From these examples I deduce that ferrocene and ruthenocene have different rotational configurations because of different metal atoms and not because of van der Waals' forces between rings or because of lattice forces. I propose that the bond orbitals of the iron and ruthenium atoms have inherently different symmetries in these dicyclopentadienyl compounds and in their derivatives. The difference in symmetries may be linked to the availability of f-orbitals to the ruthenium atom for the formation of hybrid bond orbitals. I propose that molecules of ferrocene pack together in the crystalline state in such a way as to preserve the preferred symmetry of the iron-ring bonding. The symmetry determines the packing, not the packing the symmetry.

From ferrocene, bis-indenyliron, ruthenocene, and bis-indenylruthenium we can see that the iron atom occupies a center of symmetry (with respect to the Fe-C bonds) and that the ruthenium atom lies in a mirror plane. These two symmetries are also observed in the elemental structures where every iron atom is at a center of symmetry in its cubic closest packed form and where every ruthenium atom lies in a mirror plane, ruthenium being hexagonal closest packed. Likewise, osmocene is eclipsed (6) and osmium is hexagonal closest packed. The dicyclopentadienyl compounds of nickel, cobalt, chromium, and vanadium are staggered (2); nickel is cubic closest packed, cobalt has both hexagonal and cubic closest packed modifications, and chromium and vanadium are body centered cubic.

If lattice forces are in any case important in determining the rotational configuration in symmetrical metal-ring compounds, they should be most important when the attached groups are very large. For example, in a crystal of 1,1'-didodecylferrocene the five-membered rings might be eclipsed or staggered, depending on the way the long chains wanted to pack. And van der Waals' forces could come into play enough to alter symmetry. For example, bis-hexamethyl benzene chromium may well be staggered rather than eclipsed; if it is eclipsed it will illustrate that the symmetry of the metal-ring bonding is much more important than anyone has so far suspected.

However, in the fairly simple sandwich compounds that have been studied so far, it seems that the nature of the metal-ring bonding determines the symmetry.

References

1. H. Zeiss, Organometallic Chemistry, (1960), New York: Reinhold Publishing Corporation. Chapter 7, P. L. Pauson.
a) p. 346.
2. G. Wilkinson and F. A. Cotton, Progress in Inorganic Chemistry, (1959), New York: Interscience Publishers, Inc.
a) p. 19
b) p. 82
3. F. Jellinek, Nature, 187, 871-872 (1960).
4. G. L. Hardgrove and D. H. Templeton, Acta Cryst., 12, 28-32 (1959).
5. This thesis, Part I.
6. F. Jellinek, Z. Naturforsch., 14b, 737-738 (1959).
7. J. D. Dunitz, L. E. Orgel, and A. Rich, Acta Cryst., 9, 373-375 (1956).
8. A. Berndt, Ph. D. Thesis, California Institute of Technology, p. 36 (1957).
9. J. A. Trotter, Acta Cryst., 11, 355-360 (1958).
10. L. Pauling, The Nature of the Chemical Bond, (1960), 3rd ed., Ithaca: Cornell University Press. p. 388, unpublished work of K. Hedberg.
11. L. Hedberg and K. Hedberg, Yearly Report of the Division of Chemistry and Chemical Engineering at the California Institute of Technology, Report for 1954-1955, p. 49.

II. I propose that the arsenic atom in the arsenic(V)-catechol complex, $\text{AsO}(\text{OC}_6\text{H}_4\text{OH})_3$, is five-coordinated and that the five oxygen ligands are arranged at the vertices of a nearly regular trigonal bipyramid. It is commonly believed (1, 2) that an octahedral complex is formed by the reaction of aqueous solutions of catechol and arsenic acid.

The free acid of the arsenic(V)-catechol complex was first prepared by Weinland and Heinzler (3) by the addition of catechol to a boiling aqueous solution of arsenic acid. Upon cooling, colorless crystals separated which had a composition corresponding to $\text{HAs}(\text{C}_6\text{H}_4\text{O}_2)_3 \cdot 5\text{H}_2\text{O}$, to which they assigned the "structure" $\text{H}_3[\text{O}-\text{As}-(\text{OC}_6\text{H}_4\text{O})_3] \cdot 4\text{H}_2\text{O}$. Simple salts of this acid were prepared, and the compound behaved as a monobasic acid in all cases.

Subsequently, other investigators (4, 5, 6) have found:

- 1) The parent acid behaves as a monobasic acid with a value of 2.75 for the pKa (4).
- 2) The anion exists in optically active forms (4, 5).
- 3) Dehydration can remove only four molecules of water from the pentahydrate (4, 5, 6); this extra water of hydration is coordinated to the arsenic atom (4, 6).

Two different structures for the complex have been proposed; they are illustrated in figure 1. Structure II, which was proposed by

Rosenheim and Plato (5), is inadequate in that it cannot account for the observed acidity or for the water of hydration. Structure I, which was proposed by Craddock and Jones (4), can account for all of the properties listed above. However, I feel that the structure presented below can explain the properties of the complex in a more clear-cut fashion and that it is more consistent with the known chemistry of arsenic and of the group V A elements in general.

I propose that there are only five As-O bonds and that the oxygen atoms are arranged at the vertices of a nearly regular trigonal bipyramid; one isomer, one of an enantiomeric pair, based on such an arrangement is illustrated in figure 2(a). A five-fold coordination of the arsenic atom may also give rise to a number of enantiomeric pairs of molecules which owe their asymmetry to steric hindrance.

If we assume a nearly regular trigonal bipyramid, an As-O bond distance of 1.8 \AA (in arsenates the As-O bond distance is about 1.75 \AA (1)), and an As-O-C angle of 115° , we can get an idea of non-bonded distances with a few simple calculations. Figure 2(b) shows the short oxygen to hydrogen distance that would result from rotation of one of the equatorially bonded catechol groups about the As-O bond. Figure 2(c) shows the distances to be expected if the catechol groups lie in the equatorial plane; the drawing is in the equatorial plane, viewed down As-O bond. The short non-bonded

Figure 1. Structures that have been proposed for the arsenic(V)-catechol complex.

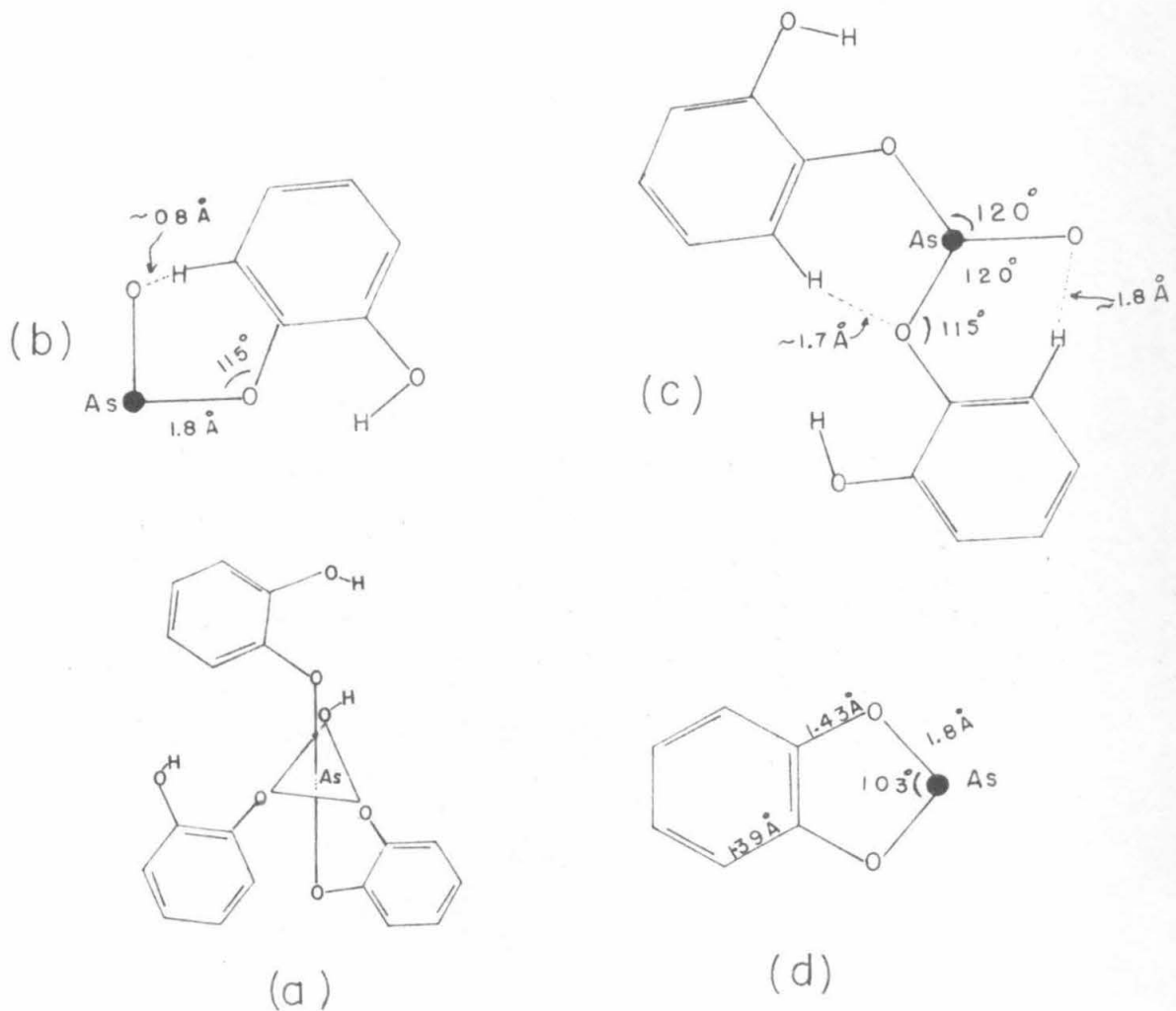
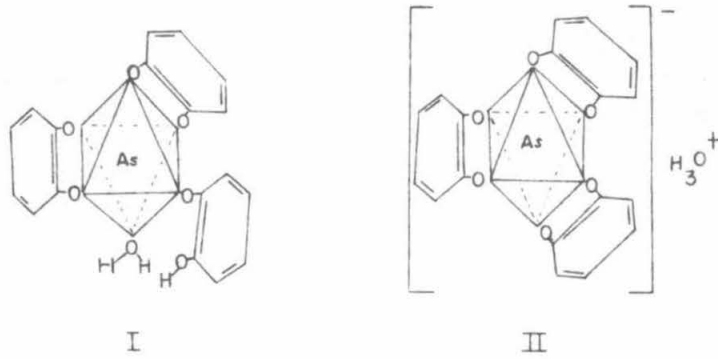


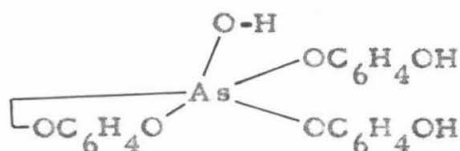
Figure 2. Information on structure in which the arsenic atom is five-coordinated (see text).

distances can be relieved by expanding the As-O-C angles or by twisting the catechol groups out of the plane. Figure 2(d) gives the expected geometry of the chelating catechol group. It seems that the O-As-O angle of 103° will result in a distorted trigonal bipyramid in which one of the oxygen atoms of the chelating group is at an apex and the other is at the equator. Expansion of the angle to 120° would demand As-O bond distances of 1.63 \AA .

At this point I must object to the statement by Wells (1a):

"An exceptional compound, in which As exhibits a covalency of 6, is the catechol derivative, the resolution of which into its optical antimers confirms the octahedral configuration of the six arsenic bonds." The resolution into optical antimers confirms that octahedral coordination is a possibility and no more proves an octahedral configuration than failure to resolve would disprove it. Furthermore, one can explain the optical activity on the basis of a tetrahedrally coordinated arsenic atom with the catechol groups arranged like a propeller; but such a structure cannot account for the acidity.

The observed acidity of this complex and the "coordinated water" are readily understood on the basis of the molecular structure as proposed here, which we can write as



First, the "coordinated water" is not; the extra oxygen atom belongs to a hydroxyl group and is covalently bonded to the arsenic atom. The measured value of the pKa for the free acid is 2.75 (4), which is very close to 2.22, the value of the pKa of arsenic acid (7); this is expected since the acid hydrogen comes from As-OH groups in both. To me, this is a better explanation for the acidity than the remark by Craddock and Jones (4), "...a value of 2.75 was found for the pKa. This is somewhat greater than would be expected for a species containing an already formed H_3O^+ ion but is not inconsistent with the ionization of a hydrogen from a molecule of water which is coordinated to the arsenic." Admittedly, one can explain any value of the pKa by invoking the requisite degree of coordination; very tightly coordinated water molecules would be expected to be very acidic, and so on.

A complex having a trigonal bipyramidal structure is consistent with known structures of PCl_5 and SbCl_5 (1); although the structure has not been determined, AsF_5 is known and probably is based on a trigonal bipyramidal arrangement. Moreover, Bertil (8) was able to make $\text{HOAs}(\text{C}_2\text{H}_4\text{O}_2)_2$ but could not isolate a pure compound with three glycol

groups. Presumably, in HOAs($C_2H_4O_2$)₂ the arsenic atom is five-coordinated.

I have grown crystals of the arsenic(V)-catechol complex and have collected enough X-ray data to state that the complex crystallizes in space group P_{bca} with 24 molecules per unit cell. All three axes are essentially the same length, $23.5 \text{ \AA} \pm 0.2 \text{ \AA}$.

References

1. A. F. Wells, Structural Inorganic Chemistry, (1962), 3rd ed. Oxford: The Clarendon Press.
a) p. 664.
2. F. Basolo and R. G. Pearson, Mechanisms of Inorganic Reactions, (1958). New York: John Wiley and Sons, Inc.
3. R. F. Weinland and J. Heinzler, Ber., 52, 1316-1329 (1919).
4. J. H. Craddock and M. M. Jones, J. Am. Chem. Soc., 83, 2839-2843 (1961).
5. A. Rosenheim and W. Plato, Ber., 58, 2000-2011 (1925).
6. H. Reihlen, A. Sapper and G. A. Kall, Z. anorg. Chem., 144, 218-226 (1925).
7. W. J. Blaedel and V. W. Meloche, Elementary Quantitative Analysis, (1957). Evanston: Row, Peterson and Company.
8. E. J. Bertil, J. prakt. Chem., 120, 179-184 (1928).

III. I propose that the following manuscripts entitled "Structure-factor and Least-Squares Calculation for Tetragonal, Trigonal, and Hexagonal Systems with Anisotropic Vibrations" and "Structure-factor and Least-Squares Calculation for Cubic Systems with Isotropic Vibrations" be submitted to Acta Crystallographica for publication.

Development of high-speed digital computers has relieved the crystallographer of laborious calculations by hand and has enabled him to tackle complex problems with hopes of solution in a reasonable time. However, this development has brought with it the problem of programming computers and of the crystallographer's desire to make use of the speed at his disposal to determine accurately the atomic parameters by including, among other factors, anisotropic thermal vibrations of the atoms in his analysis. These two problems together require a formulation of the structure-factor expressions that is readily adapted to computer coding; such a formulation exists for the monoclinic space groups (Rollett and Davis, 1955) and for the orthorhombic space groups (Hybl and Marsh, 1961). Moreover, the rapid changes in computers are forcing the crystallographer to spend much of his time learning and programming new computers. He can be relieved of this task if he can present his problem to a professional programmer in such a form that it is a coding problem rather than a crystallographic one. The formulations below and those of Rollett and Davis and of Hybl and Marsh are certainly a step toward the coding problem.

It is now practical, almost demanding, to program computers to carry out structure-factor least-squares calculations for any space groups designated by the program user. To program in this way requires a common form of the structure factor expressions, at least within a system. With the formulations presented below, which cover 156 space groups, the trigonometric part of any structure factor in 215 of the 230 space groups (all but triclinic and monoclinic) is now in the form of triple products of sines and cosines, e.g.

$$[\cos(2\pi hx) \sin(2\pi ky) \cos(2\pi lz)].$$

The International Tables (1952) gives all of the structure-factor expressions, but in several different forms, and, as far as I know, no one has attempted to explicitly formulate structure-factor expressions with anisotropic scattering factors for the tetragonal, trigonal, and hexagonal space groups.

(The formulations presented in the proposed paper on the cubic system are one result of writing a structure-factor least-squares program for the Burroughs 220.)

Structure-Factor and Least-Squares Calculation for
Tetragonal, Trigonal, and Hexagonal Systems with
Anisotropic Vibrations

Rollett and Davis (1955) and Hybl and Marsh (1961), hereafter HM, have derived sets of expressions that can be used to calculate structure factors and least-squares coefficients for any monoclinic space group and for any orthorhombic space group. In like manner, we present sets of analogous expressions for tetragonal, trigonal, and hexagonal symmetries. In developing these expressions we make use of the formulations of Trueblood (1956) and the International Tables (1952).

To simplify all discussion we present the case of one crystallographic atom in a general position. For a number of atoms, one must sum over all the atoms for the complete structure factor and take into account the lower multiplicity of atoms in special positions in the usual way.

Tetragonal system

We start with the expression for the scattering factor for a vibrating atom:

$$f_1 = f_0 \exp(-B_{11}h^2 + B_{22}k^2 + B_{33}l^2 + B_{12}hk + B_{13}hl + B_{23}kl)$$

where f_0 is the scattering factor for an atom at rest. The tetragonal symmetry gives rise, in general, to seven additional orientations of the vibrational ellipsoid; applying the transformations given by Trueblood, we write the corresponding scattering factors:

$$f_2 = f_0 \exp(-(B_{11}h^2 + B_{22}k^2 + B_{33}l^2 + B_{12}hk - B_{13}hl - B_{23}kl))$$

$$f_3 = f_0 \exp(-(B_{11}h^2 + B_{22}k^2 + B_{33}l^2 - B_{12}hk + B_{13}hl - B_{23}kl))$$

$$f_4 = f_0 \exp(-(B_{11}h^2 + B_{22}k^2 + B_{33}l^2 - B_{12}hk - B_{13}hl + B_{23}kl))$$

$$f_5 = f_0 \exp(-(B_{11}k^2 + B_{22}h^2 + B_{33}l^2 - B_{12}hk + B_{13}kl - B_{23}hl))$$

$$f_6 = f_0 \exp(-(B_{11}k^2 + B_{22}h^2 + B_{33}l^2 - B_{12}hk - B_{13}kl + B_{23}hl))$$

$$f_7 = f_0 \exp(-(B_{11}k^2 + B_{22}h^2 + B_{33}l^2 + B_{12}hk - B_{13}kl - B_{23}hl))$$

$$f_8 = f_0 \exp(-(B_{11}k^2 + B_{22}h^2 + B_{33}l^2 + B_{12}hk + B_{13}kl + B_{23}hl))$$

In table 1 (all tables are given at the end of the discussion), we define the 16 triple products of sines and cosines which are sufficient for expressing the trigonometric part of any structure factor in the tetragonal system; the 8 products in terms of hx , ky , and lz are the T_i 's defined by HM. We have chosen to express the structure factors and their derivatives in a minimum number of simple, common terms in order to facilitate bookkeeping and to reduce computational time. The 16 expressions which we have chosen are presented in table 2; only the first 8 are needed for the space groups of Laue

symmetry 4/m. The derivatives of these basic expressions are given in table 3.

The real and imaginary parts of the structure factor, A and B ($F_c^2 = \rho_c^2 (A^2 + B^2)$), for any class of reflection in the tetragonal system are listed in table 4 in terms which are defined in table 2; the space-group multiplicity is reflected in ρ_c . For acentric primitive space groups, ρ_c is one; a center of symmetry contributes a factor of two, as does a body-centered lattice.

An example is presented to illustrate the use of the tables.

We assume space group $I4_{1/a}$ and a reflection characterized by $h + k + l = 4n + 2$, $h = 2n$ and $k = 2n$.

$$F_c/4 = A_c/4 = (1-5), \quad (B = 0)$$

where the factor of 4 is from ρ_c and 1 and 5 are expressions defined in table 2. We refer to table 2 and write

$$F_c = 4[(f_1 + f_2)(c_1 - e_1) - (f_1 - f_2)(i_1 + g_1) - (f_5 - f_6)(d_1 + f_1') - (f_5 - f_6)(j_1 - h_1)]$$

where f_1 , f_2 , f_5 and f_6 are scattering factors defined in the text and c_1 , e_1 , i_1 , g_1 , d_1 , f_1' , j_1 , and h_1 are triple products defined in table 1. From table 3, we see that some derivatives of F_c are:

$$\frac{\partial F_c}{\partial x} = 4 \left\{ \begin{aligned} &-2\pi h [(f_1 + f_2)(m_1 + o_1) + (f_1 - f_2)(q_1 - k_1)] \\ &-2\pi k [(f_5 + f_6)(n_1 - p_1) - (f_5 - f_6)(r_1 + l_1)] \end{aligned} \right\}$$

$$\frac{\partial Fc}{\partial z} = 4 [2\pi l (-3) + 2\pi l (7)]$$

$$\frac{\partial Fc}{\partial B_{11}} = 4 [-h^2 (1) + k^2 (5)]$$

$$\frac{\partial Fc}{\partial B_{13}} = 4 [hl (2) + kl (6)] .$$

In our formulation there is no single term which gives the structure factor expression for an isotropic atom as does expression $E_1 = f_1 + f_2 + f_3 + f_4$ formulated by HM. Such a formulation for the tetragonal system is impractical as it would require splitting the system into the two Laue groups $4/m$ and $4/m\bar{m}$, and even then, a larger number of more cumbersome expressions would have to be defined.

To illustrate this, consider space group $P4_2$ where the combinations (1-5) and (1+5) are given for A for the two parity conditions. Expressed in the form of HM, (1-5) becomes

$$\begin{aligned} & \frac{1}{2} [(f_1 + f_2 + f_5 + f_6)(c_1 - e_1 - d_1 - f_1') + (f_1 + f_2 - f_5 - f_6)(c_1 - e_1 + d_1 + f_1') \\ & - (f_1 - f_2 + f_5 - f_6)(i_1 + g_1 + j_1 - h_1) - (f_1 - f_2 - f_5 + f_6)(i_1 + g_1 - j_1 + h_1)] \\ & = \frac{1}{2} [E_1 T_1 + E_2 T_2 - E_3 T_3 - E_4 T_4] \end{aligned}$$

(the E's and T's not related to those defined by HM) and (1+5) becomes

$$\frac{1}{2} [E_1 T_2 + E_2 T_1 - E_3 T_4 - E_4 T_3] .$$

To formulate in these terms requires 8 products between 8 terms; in our formulation, 4 products between 8 simpler terms are required. Furthermore, the derivatives become quite complicated; take $E_1 T_1$ in the case just discussed,

$$\frac{\partial E_1 T_1}{\partial B_{11}} = \frac{\delta(f_1 + f_2 + f_5 + f_6) T_1}{\partial B_{11}} = [-h^2(f_1 + f_2) - k^2(f_5 + f_6)] T_1$$

If we did formulate our expressions in this way, we would be forced to handle the derivatives by the simpler expressions presented in table 2. Thus we would add to our computational time and our book-keeping headaches by formulating the structure factors in terms like $(f_1 + f_j + f_k + f_l)$ as HM did for the orthorhombic system, where such a formulation is convenient and efficient.

The isotropic case will have to be handled in a special way. As the terms are written in table 2, the right hand side of each expression, which contains $(f_i - f_j)$, is zero for an isotropic atom. It should be simple to program in such a way that within the computer the 16 expressions are split into 32 expressions; the $(f_i - f_j)$ terms could then be disregarded for an isotropic atom. (Expressions 9 through 16 should be disregarded for space groups of Laue symmetry 4/m.)

For the general case, for an isotropic atom i all the f 's are equal to $f_0 \exp(-B' \frac{\sin^2 \theta}{\lambda^2})$ and

$$\frac{\partial F_c^2}{\partial B'_i} = 2A \frac{\partial A_i}{\partial B'_i} + 2B \frac{\partial B_i}{\partial B'_i} = -\frac{\sin^2 \theta}{\lambda^2} [2A A_i + 2B B_i]$$

Table 1. Definition of triple products. $C = \cos 2\pi$, $S = \sin 2\pi$.

hx	ky	lz	hy	kx	lz
$c_1 \equiv Chx \cdot Cky \cdot Clz$			$d_1 \equiv Chy \cdot Ckx \cdot Clz$		
$e_1 \equiv Shx \cdot Sky \cdot Clz$			$f_1' \equiv Shy \cdot Skx \cdot Clz$		
$g_1 \equiv Chx \cdot Sky \cdot Slz$			$h_1 \equiv Chy \cdot Skx \cdot Slz$		
$i_1 \equiv Shx \cdot Cky \cdot Slz$			$j_1 \equiv Shy \cdot Ckx \cdot Slz$		
$k_1 \equiv Shx \cdot Sky \cdot Slz$			$l_1 \equiv Shy \cdot Skx \cdot Slz$		
$m_1 \equiv Shx \cdot Cky \cdot Clz$			$n_1 \equiv Shy \cdot Ckx \cdot Clz$		
$o_1 \equiv Chx \cdot Sky \cdot Clz$			$p_1 \equiv Chy \cdot Skx \cdot Clz$		
$q_1 \equiv Chx \cdot Cky \cdot Slz$			$r_1 \equiv Chy \cdot Ckx \cdot Slz$		

Table 2. Definitions of combinations of triple products and scattering factors for the tetragonal system.

$$(f_1 + f_2)(c_1 - e_1) - (f_1 - f_2)(i_1 + g_1) \equiv 1$$

$$(f_1 + f_2)(i_1 + g_1) - (f_1 - f_2)(c_1 - e_1) \equiv 2$$

$$(f_1 + f_2)(q_1 - k_1) + (f_1 - f_2)(m_1 + o_1) \equiv 3$$

$$(f_1 + f_2)(m_1 + o_1) + (f_1 - f_2)(q_1 - k_1) \equiv 4$$

$$(f_5 + f_6)(d_1 + f_1') + (f_5 - f_6)(j_1 - h_1) \equiv 5$$

$$(f_5 + f_6)(j_1 - h_1) + (f_5 - f_6)(d_1 + f_1') \equiv 6$$

$$(f_5 + f_6)(r_1 + l_1) - (f_5 - f_6)(n_1 - p_1) \equiv 7$$

$$(f_5 + f_6)(n_1 - p_1) - (f_5 - f_6)(r_1 + l_1) \equiv 8$$

$$(f_3 + f_4)(c_1 + e_1) - (f_3 - f_4)(i_1 - g_1) \equiv 9$$

$$(f_3 + f_4)(i_1 - g_1) - (f_3 - f_4)(c_1 + e_1) \equiv 10$$

$$(f_3 + f_4)(q_1 + k_1) + (f_3 - f_4)(m_1 - o_1) \equiv 11$$

$$(f_3 + f_4)(m_1 - o_1) + (f_3 - f_4)(q_1 + k_1) \equiv 12$$

$$(f_7 + f_8)(d_1 - f_1') + (f_7 - f_8)(j_1 + h_1) \equiv 13$$

$$(f_7 + f_8)(j_1 + h_1) + (f_7 - f_8)(d_1 - f_1') \equiv 14$$

$$(f_7 + f_8)(r_1 - l_1) - (f_7 - f_8)(n_1 + p_1) \equiv 15$$

$$(f_7 + f_8)(n_1 + p_1) - (f_7 - f_8)(r_1 - l_1) \equiv 16$$

Table 3. Derivatives of the expressions defined in Table 2 for the tetragonal system.

Expression	$\frac{\partial}{2\pi\partial x}$ and $\frac{\partial}{2\pi\partial y}$		Exp.	$\frac{\partial}{2\pi l\partial z}$	$\frac{-\partial}{\partial B_{11}}, \frac{-\partial}{\partial B_{22}}, \frac{-\partial}{\partial B_{33}}, \frac{-\partial}{\partial B_{12}}$				$\frac{-\partial}{\partial B_{13}}$ and $\frac{-\partial}{\partial B_{23}}$			
	Mult. const. x	y			Mult. constant $B_{11} B_{22} B_{33} B_{12}$	Exp.	Mult. Constant $B_{13} B_{23}$	Exp.				
1	-h	-k	4	-3	h^2	k^2	l^2	+hk	1	-hl	-kl	2
2	h	k	3	4	h^2	k^2	l^2	+hk	2	-hl	-kl	1
3	-h	-k	2	1	h^2	k^2	l^2	+hk	3	+hl	+kl	4
4	h	k	1	-2	h^2	k^2	l^2	+hk	4	+hl	+kl	3
5	k	-h	8	-7	k^2	h^2	l^2	-hk	5	+kl	-hl	6
6	-k	h	7	8	k^2	h^2	l^2	-hk	6	+kl	-hl	5
7	k	-h	6	5	k^2	h^2	l^2	-hk	7	-kl	+hl	8
8	-k	h	5	-6	k^2	h^2	l^2	-hk	8	-kl	+hl	7
9	-h	k	12	-11	h^2	k^2	l^2	-hk	9	-hl	+kl	10
10	h	-k	11	12	h^2	k^2	l^2	-hk	10	-hl	+kl	9
11	-h	k	10	9	h^2	k^2	l^2	-hk	11	+hl	-kl	12
12	h	-k	9	-10	h^2	k^2	l^2	-hk	12	+hl	-kl	11
13	-k	-h	16	-15	k^2	h^2	l^2	+hk	13	-kl	-hl	14
14	k	h	15	16	k^2	h^2	l^2	+hk	14	-kl	-hl	13
15	-k	-h	14	13	k^2	h^2	l^2	+hk	15	+kl	+hl	16
16	k	h	13	-14	k^2	h^2	l^2	+hk	16	+kl	+hl	15

Table 4. A tabulation of the tetragonal space groups according to index parities.

Space Group	ρ_c	Planes	A	B
75-P4	1	All planes	1 + 5	3 + 7
76-P4 ₁	1	$l = 4n$	1 + 5	3 + 7
		$l = 4n + 1$	-2 + 8	4 + 6
		$l = 4n + 2$	1 - 5	3 - 7
		$l = 4n + 3$	-2 - 8	4 - 6
77-P4 ₂	1	$l = 2n$	1 + 5	3 + 7
		$l = 2n + 1$	1 - 5	3 - 7
78-P4 ₃	1	$l = 4n$	1 + 5	3 + 7
		$l = 4n + 1$	-2 - 8	4 - 6
		$l = 4n + 2$	1 - 5	3 - 7
		$l = 4n + 3$	-2 + 8	4 + 6
79-I4	2	$h + k + l = 2n$	1 + 5	3 + 7
80-I4 ₁	2	$h + k + l = 2n$ $2k + l = 4n$	1 + 5	3 + 7
		$2k + l = 4n + 1$	1 - 7	3 + 5
		$2k + l = 4n + 2$	1 - 5	3 - 7
		$2k + l = 4n + 2$	1 + 7	3 - 5
81-P4̄	1	All planes	1 + 5	3 - 7
82-I4̄	2	$h + k + l = 2n$	1 + 5	3 - 7
83-P4/m	2	All planes	1 + 5	
84-P4 2/m	2	$l = 2n$	1 + 5	
		$l = 2n + 1$	1 - 5	
85-P4/n	2	$\frac{h}{2n}$ $\frac{k}{2n}$	1 + 5	
		$2n$ $2n + 1$	-2 + 6	
		$2n + 1$ $2n$	-2 - 6	
		$2n + 1$ $2n + 1$	1 - 5	

Table 4. (continued) (2)

Space Group	ρ_c	Planes		A	B	
86-P42/n	2	$\frac{h+k}{2n}$	$\frac{k+l}{2n}$	1+5		
		$2n$	$2n$	1+5		
		$2n$	$2n+1$	1-5		
		$2n+1$	$2n$	-2+6		
		$2n+1$	$2n+1$	-2+6		
87-I 4/m	4	$h+k+l = 2n$		1+5		
88-I 41/a	4	$\frac{h+k+l}{4n}$	$\frac{h}{2n}$	$\frac{k}{2n}$	1+5	
		$4n$	$2n$	$2n+1$	-2+5	
		$4n$	$2n+1$	$2n$	1-6	
		$4n$	$2n+1$	$2n+1$	-2-6	
		$4n+2$	$2n$	$2n$	1-5	
		$4n+2$	$2n$	$2n+1$	-2-5	
		$4n+2$	$2n+1$	$2n$	1+6	
		$4n+2$	$2n+1$	$2n+1$	-2+6	
89-P422	1	All planes		1+5+9+13	3+7-11-15	
90-P4 ₁ 2 ₁ 2	1	$h+k = 2n$		1+5+9+13	3+7-11-15	
		$h+k = 2n+1$		1-5-9+13	3-7+11-15	
91-P4 ₁ 22	1	$l = 4n$		1+5+9+13	3+7-11-15	
		$l = 4n+1$		-2+8-10+16	4+6-12-14	
		$l = 4n+2$		1-5+9-13	3-7-11+15	
		$l = 4n+3$		-2-8-10-16	4-6-12+14	
92-P4 ₁ 2 ₁ 2	1	$2h+2k+l = 4n$		1+5+9+13	3+7-11-15	
		" $= 4n+1$		-2+8+12+14	4+6-10+16	
		" $= 4n+2$		1-5-9+13	3-7+11-15	
		" $= 4n+3$		-2-8-12+14	4-6+10+16	
93-P4 ₂ 22	1	$l = 2n$		1+5+9+13	3+7-11-15	
		$l = 2n+1$		1-5+9-13	3-7-11+15	
94-P4 ₂ 2 ₁ 2	1	$h+k+l = 2n$		1+5+9+13	3+7-11-15	
		$h+k+l = 2n+1$		1-5-9+13	3-7+11-15	

Table 4. (continued) (3)

Space Group	σ_c	Planes	A	B
95-P4 ₃ 22	1	$l = 4n$	1+5+9+13	3+7-11-15
		$l = 4n + 1$	-2-8-10-16	4-6-12-14
		$l = 4n + 2$	1-5+9-13	3-7-11+15
		$l = 4n + 3$	-2+8-10+16	4+6-12-14
96-P4 ₃ 2 ₁ 2	1	$2h + 2k + l = 4n$	1+5+9+13	3+7-11-15
		$= 4n + 1$	-2-8-12+14	4-6+10+16
		$= 4n + 2$	1-5-9+13	3-7+11-15
		$= 4n + 3$	-2+8+12+14	4+6-10+16
97-I422	2	$h + k + l = 2n$	1+5+9+13	3+7-11-15
98-I4 ₁ 22	2	$2k + l = 4n$	1+5+9+13	3+7-11-15
		$2k + l = 4n + 1$	1-7+11+13	3+5+9-15
		$2k + l = 4n + 2$	1-5-9+13	3-7+11-15
		$2k + l = 4n + 3$	1+7-11+13	3-5-9-15
99-P4mm	1	All planes	1+5+9+13	3+7+11+15
100-P4bm	1	$h + k = 2n$	1+5+9+13	3+7+11+15
		$h + k = 2n + 1$	1+5-9-13	3+7-11-15
101-P4 ₂ cm	1	$l = 2n$	1+5+9+13	3+7+11+15
		$l = 2n + 1$	1-5-9+13	3-7-11+15
102-P4 ₂ nm	1	$h + k + l = 2n$	1+5+9+13	3+7+11+15
		$h + k + l = 2n + 1$	1-5-9+13	3-7-11+15
103-P4cc	1	$l = 2n$	1+5+9+13	3+7+11+15
		$l = 2n + 1$	1+5-9-13	3+7-11-15
104-P4nc	1	$h + k + l = 2n$	1+5+9+13	3+7+11+15
		$h + k + l = 2n + 1$	1+5-9-13	3+7-11-15
105-P4 ₂ mc	1	$l = 2n$	1+5+9+13	3+7+11+15
		$l = 2n + 1$	1-5+9-13	3-7+11-15

Table 4. (continued) (4)

Space Group	σ_c	Planes	A	B	
106-P4 ₂ bc	1	$h + k$			
		$2n$	$2n$	1+5+9+13	3+7+11+15
		$2n$	$2n + 1$	1-5+9-13	3-7+11-15
		$2n + 1$	$2n$	1+5-9-13	3+7-11-15
		$2n + 1$	$2n + 1$	1-5-9+13	3-7-11+15
107-I4 ₁ mm	2	$h + k + l = 2n$	1+5+9+13	3+7+11+15	
108-I4cm	2	$l = 2n$	1+5+9+13	3+7+11+15	
		$l = 2n + 1$	1+5-9-13	3+7-11-15	
109-I4 ₁ md	2	$2k + l = 4n$	1+5+9+13	3+7+11+15	
		$2k + l = 4n + 1$	1-7+9-15	3+5+11+13	
		$2k + l = 4n + 2$	1-5+9-13	3-7+11-15	
		$2k + l = 4n + 3$	1+7+9+15	3-5+11-13	
110-I4 ₁ cd	2	$2k + l = 4n$	1+5+9+13	3+7+11+15	
		$2k + l = 4n + 1$	1-7-9+15	3+5-11-13	
		$2k + l = 4n + 2$	1-5+9-13	3-7+11-15	
		$2k + l = 4n + 3$	1+7-9-15	3-5-11+13	
111-P4 ₂ m	1	All planes	1+5+9+13	3-7-11+15	
112-P4 ₂ c	1	$l = 2n$	1+5+9+13	3-7-11+15	
		$l = 2n + 1$	1+5-9-13	3-7+11-15	
113-P4 ₂ ₁ m	1	$h + k = 2n$	1+5+9+13	3-7-11+15	
		$h + k = 2n + 1$	1+5-9-13	3-7+11-15	
114-P4 ₂ ₁ c	1	$h + k + l = 2n$	1+5+9+13	3-7-11+15	
		$h + k + l = 2n + 1$	1+5-9-13	3-7+11-15	
115-P4 ₂ m2	1	All planes	1+5+9+13	3-7+11-15	
116-P4 ₂ c2	1	$l = 2n$	1+5+9+13	3-7+11-15	
		$l = 2n + 1$	1+5-9-13	3-7-11+15	
117-P4 ₂ b2	1	$h + k = 2n$	1+5+9+13	3-7+11-15	
		$h + k = 2n + 1$	1+5-9-13	3-7-11+15	

Table 4. (continued) (5)

Space Group	ρ_c	Planes	A	B
118- $P\bar{4}n_2$	1	$h + k + l = 2n$ $h + k + l = 2n + 1$	1+5+9+13 1+5-9-13	3-7+11-15 3-7-11+15
119- $I\bar{4}m2$	2	$h + k + l = 2n$	1+5+9+13	3-7+11-15
120- $I\bar{4}c2$	2	$h + k + l = 2n$ $l = 2n$ " $l = 2n + 1$	1+5+9+13 1+5-9-13	3-7+11-15 3-7-11+15
121- $I\bar{4}2m$	2	$h + k + l = 2n$	1+5+9+13	3-7-11+15
122- $I\bar{4}2d$	2	$2k + l = 4n$ $2k + l = 4n + 1$ $2k + l = 4n + 2$ $2k + l = 4n + 3$	1+5+9+13 1+5+11-15 1+5-9-13 1+5-11+15	3-7-11+15 3-7+9+13 3-7+11-15 3-7-9-13
123- $P4/m\ mm$	2	All planes	1+5+9+13	
124- $P4/m\ cc$	2	$l = 2n$ $l = 2n + 1$	1+5+9+13 1+5-9-13	
125- $P4/n\ bm$	2	$\frac{h}{2n}$ $\frac{k}{2n}$ $2n$ $2n + 1$ $2n + 1$ $2n$ $2n + 1$ $2n + 1$	1+5+9+13 -2+6-10+14 -2-6+10+14 1-5-9+13	
126- $P4/n\ nc$	2	$\frac{h+k}{2n}$ $\frac{k+l}{2n}$ $\frac{l}{2n}$ $2n$ $2n + 1$ $2n$ $2n + 1$ $2n$ $2n$ $2n + 1$ $2n + 1$ $2n$ $2n$ $2n$ $2n + 1$ $2n$ $2n + 1$ $2n + 1$ $2n + 1$ $2n$ $2n + 1$ $2n + 1$ $2n + 1$ $2n + 1$	1+5+9+13 1-5-9+13 -2-6+10+14 -2+6-10+14 1-5+9-13 1+5-9-13 -2+6+10-14 -2-6-10-14	
127- $P4/m\ bm$	2	$h + k = 2n$ $h + k = 2n + 1$	1+5+9+13 1+5-9-13	

Table 4. (continued) (6)

Space Group	ρ_c	Planes		A	
128-P4/mnc	2	$h + k + l = 2n$		1+5+9+13	
		$h + k + l = 2n + 1$		1+5-9-13	
129-P4/nmm	2	$\frac{h}{2n}$	$\frac{k}{2n}$	1+5+9+13	
		$2n$	$2n + 1$	-2+6+10-14	
		$2n + 1$	$2n$	-2-6-10-14	
		$2n + 1$	$2n + 1$	1-5-9+13	
130-P4/ncc	2	$\frac{h+k}{2n}$	$\frac{k+l}{2n}$	$\frac{l}{2n}$	1+5+9+13
		$2n$	$2n + 1$	$2n$	1-5-9+13
		$2n + 1$	$2n$	$2n$	-2-6-10-14
		$2n + 1$	$2n + 1$	$2n$	-2+6+10-14
		$2n$	$2n$	$2n + 1$	1-5+9-13
		$2n$	$2n + 1$	$2n + 1$	1+5-9-13
		$2n + 1$	$2n$	$2n + 1$	-2+6-10+14
		$2n + 1$	$2n + 1$	$2n + 1$	-2-6+10+14
131-P4 ₂ /mmc	2		$l = 2n$	1+5+9+13	
			$l = 2n + 1$	1-5+9-13	
132-P4 ₂ /mcm	2		$l = 2n$	1+5+9+13	
			$l = 2n + 1$	1-5-9+13	
133-P4 ₂ /nbc	2	$\frac{h}{2n}$	$\frac{k}{2n}$	$\frac{l}{2n}$	1+5+9+13
		$2n$	$2n + 1$	$2n$	-2+6-10+14
		$2n + 1$	$2n$	$2n$	-2-6+10+14
		$2n + 1$	$2n + 1$	$2n$	1-5-9+13
		$2n$	$2n$	$2n + 1$	1-5+9-13
		$2n$	$2n + 1$	$2n + 1$	-2-6-10-14
		$2n + 1$	$2n$	$2n + 1$	-2+6+10-14
		$2n + 1$	$2n + 1$	$2n + 1$	1+5-9-13
134-P4 ₂ /n ₂ nm	2	$\frac{h+k}{2n}$	$\frac{k+l}{2n}$		1+5+9+13
		$2n$	$2n + 1$		1-5-9+13
		$2n + 1$	$2n$		-2-6+10+14
		$2n + 1$	$2n + 1$		-2+6-10+14

Table 4. (continued) (7)

Space Group	ρ_c	Planes		A	
135-P42/m bc	2	$\frac{h+k}{2n}$	$\frac{l}{2n}$	1+5+9+13	
		2n	2n+1	1-5+9-13	
		2n+1	2n	1+5-9-13	
		2n+1	2n+1	1-5-9+13	
136-P42/m nm	2	$h+k+l = 2n$		1+5+9+13	
		$h+k+l = 2n+1$		1-5-9+13	
137-P42/n mc	2	$\frac{h}{2n}$	$\frac{k}{2n}$	$\frac{l}{2n}$	1+5+9+13
		2n	2n+1	2n	-2+6+10-14
		2n+1	2n	2n	-2-6-10-14
		2n+1	2n+1	2n	1-5-9+13
		2n	2n	2n+1	1-5+9-13
		2n	2n+1	2n+1	-2-6+10+14
		2n+1	2n	2n+1	-2+6-10+14
		2n+1	2n+1	2n+1	1+5-9-13
138-P42/n cm	2	$\frac{h+l}{2n}$	$\frac{k+l}{2n}$		
		2n	2n+1	1+5+9+13	
		2n	2n+1	-2+6+10-14	
		2n+1	2n	-2-6-10-14	
		2n+1	2n+1	1-5-9+13	
139-I4/m mm	4	$h+k+l = 2n$		1+5+9+13	
140-I4/m cm	4	$h+k+l = 2n, l=2n$		1+5+9+13	
		"	$l=2n+1$	1+5-9-13	

Table 4. (continued) (8)

Space Group	ρ_c	Planes		A	
141-141/a md	4	<u>$h + k + l$</u>	<u>h</u>	<u>k</u>	
		$4n$	$2n$	$2n$	1+5+9+13
		$4n$	$2n$	$2n + 1$	-2-5+10-13
		$4n$	$2n + 1$	$2n$	1+6+9+14
		$4n$	$2n + 1$	$2n + 1$	-2-6+10-14
		$4n + 2$	$2n$	$2n$	1-5+9-13
		$4n + 2$	$2n$	$2n + 1$	-2+5+10+13
		$4n + 2$	$2n + 1$	$2n$	1-6+9-14
		$4n + 2$	$2n + 1$	-2+6+10+14	
142-141/a cd	4	<u>$h + k + l$</u>	<u>h</u>	<u>k</u>	
		$4n$	$2n$	$2n$	1+5+9+13
		$4n$	$2n$	$2n + 1$	-2-5-10+13
		$4n$	$2n + 1$	$2n$	1+6-9-14
		$4n$	$2n + 1$	$2n + 1$	-2-6+10-14
		$4n + 2$	$2n$	$2n$	1-5+9-13
		$4n + 2$	$2n$	$2n + 1$	-2+5-10-13
		$4n + 2$	$2n + 1$	$2n$	1-6-9+14
		$4n + 2$	$2n + 1$	-2+6+10+14	

Trigonal and hexagonal systems

We choose to tabulate our formulations for the two systems separately, but we will discuss them at the same time since they are directly related, yet sufficiently different to warrant a separation of tables. For both systems the formulations are based on the hexagonal coordinates and we have substituted $i = -(h + k)$ throughout.

We will again write the trigonometric part of the structure factor in the form of triple products of sines and cosines. In addition to the triple products defined in table 1 for the tetragonal system, we will need those defined in table 5.

Twelve orientations of the vibrational ellipsoid are found in the hexagonal system; the corresponding scattering factors are listed in table 6. Only nine of these scattering factors are needed in the trigonal system; the three that appear in the hexagonal system but not in the trigonal are f_2 , f_6 and f_4 , and correspond to rotations of the reference vibrational ellipsoid of 60° , 180° , and 300° about the 6-fold axis. The first six of the f 's are related to each other by the 6-fold rotation axis; the second six are related to the first six by a 2-fold axis parallel to \underline{a} in the (001) plane.

Just as in the tetragonal system, consideration of bookkeeping and computational time has led us to use simple terms for expressing the structure factors. The 18 expressions chosen for the trigonal system are defined in table 7 and their derivatives are given in table 8.

The 24 expressions for the hexagonal system are defined in table 10; these hexagonal expressions are directly related to identically numbered trigonal expressions in table 7. The derivatives of the hexagonal expressions are listed in table 11.

Tables 9 and 12, in conjunction with the tables of definition, allow us to write the appropriate structure factor expression for any class of reflections in any trigonal or hexagonal space group.

We give three examples to illustrate the use of these tables. Consider the reflections with $l = 3n + 1$ in space groups $P3_212$. In table 9, where the trigonal space groups are tabulated, we find

$$A = (1 + 13) - \frac{1}{2}(5 + 9 + 17 + 21) + \sqrt{3}/2 (7 - 11 - 19 + 23)$$

$$\text{and } B = (3 - 15) - \frac{1}{2}(7 + 11 - 19 - 23) - \sqrt{3}/2 (5 - 9 + 17 - 21)$$

where $\frac{1}{2}$ and $\sqrt{3}/2$ have their usual meanings and the numbers in parentheses represent expressions defined in table 7. Consider any reflection in space group $R\bar{3}$. From table 9 and table 7, we write

$$F_c = A = 6 \left\{ f_1 [(c_1 - e_1) - (i_1 + g_1)] + f_3 [(d_3 - f_3') - (j_3 + h_3)] \right. \\ \left. + f_5 [(d_2 - f_2') - (j_2 - h_2)] \right\}$$

where f_1 , f_3 and f_5 are scattering factors defined in table 6, c_1 , e_1 , i_1 and g_1 are triple products defined in table 1, and d_3 , f_3' , j_3 , h_3 , d_2 , f_2' , j_2 and h_2 are triple products defined in table 5. To avoid confusion with the numbers that define expressions, we transfer the

factor of 6 to the left side of the equation and write some of the derivatives of $Fc/6$ by consulting table 8.

$$\begin{aligned} \frac{1}{6} \frac{\partial Fc}{\partial x} &= 2\pi [-h(3) - k(7) - i(11)] \\ &= -2\pi h f_1 [q_1 - k_1 + (m_1 + o_1)] - 2\pi k f_3 [(r_3 - \ell_3) + (n_3 + p_3)] \\ &\quad + 2\pi(h+k) f_5 [(r_2 - \ell_2) + (n_2 + p_2)] \\ \frac{1}{6} \frac{\partial Fc}{\partial B_{11}} &= -h^2(1) - k^2(5) - (h^2 + k^2 + 2hk)(9) \end{aligned}$$

Consider the reflections $\ell = 2n + 1$ in space group $P 6_3/m$.

Consulting table 12 and table 10, we write

$$\begin{aligned} \frac{Fc}{2} = \frac{A}{2} &= (2 + 6 + 10) = -(f_1 + f_2)(i_1 + g_1) + (f_1 - f_2)(c_1 - e_1) \\ &\quad - (f_3 + f_4)(j_3 + h_3) + (f_3 - f_4)(d_3 - f_3') \\ &\quad - (f_5 + f_6)(j_2 + h_2) + (f_5 - f_6)(d_2 - f_2') \end{aligned}$$

Referring to table 11, we write some of the derivatives

$$\begin{aligned} \frac{1}{2} \frac{\partial Fc}{\partial y} &= [-k(3) + (h+k)(7) - h(11)] 2\pi \\ \frac{1}{2} \frac{\partial Fc}{\partial z} &= -2\pi \ell (4 + 8 + 12) \\ \frac{1}{2} \frac{\partial Fc}{\partial B_{13}} &= -h\ell(1) - k\ell(5) + (h\ell + k\ell)(9) \end{aligned}$$

For an isotropic atom in the trigonal system, the calculation is straightforward. All the scattering factors become equal to

to $\exp(-B' \frac{\sin^2 \theta}{\lambda^2})$, and the necessary products of table 7 are formed without special considerations. For the hexagonal system, the isotropic case is worth special consideration when setting up a computer program; the right hand side of each expression in table 10 is zero, $(f_i - f_j) = 0$ for an isotropic atom.

I thank Dr. Richard E. Marsh for helpful discussions and acknowledge the tenure of a United States Rubber Company fellowship.

Table 5. Definition of additional triple products needed for trigonal and hexagonal systems. $C = \cos 2\pi$, $S = \sin 2\pi$, $i = -h-k$.

	hx	iy	lz		hy	ix	lz
c_2	\equiv	$Chx \cdot Ciy \cdot Clz$		d_2	\equiv	$Chy \cdot Cix \cdot Clz$	
e_2	\equiv	$Shx \cdot Siy \cdot Clz$		f_2'	\equiv	$Shy \cdot Six \cdot Clz$	
g_2	\equiv	$Chx \cdot Siy \cdot Slz$		h_2	\equiv	$Chy \cdot Six \cdot Slz$	
i_2	\equiv	$Shx \cdot Ciy \cdot Slz$		j_2	\equiv	$Shy \cdot Cix \cdot Slz$	
k_2	\equiv	$Shx \cdot Siy \cdot Slz$		l_2	\equiv	$Shy \cdot Six \cdot Slz$	
m_2	\equiv	$Shx \cdot Ciy \cdot Clz$		n_2	\equiv	$Shy \cdot Cix \cdot Clz$	
o_2	\equiv	$Chx \cdot Siy \cdot Clz$		p_2	\equiv	$Chy \cdot Six \cdot Clz$	
q_2	\equiv	$Chx \cdot Ciy \cdot Slz$		r_2	\equiv	$Chy \cdot Cix \cdot Slz$	
	ix	ky	lz		iy	kx	lz
c_3	\equiv	$Cix \cdot Cky \cdot Clz$		d_3	\equiv	$Ciy \cdot Ckx \cdot Clz$	
e_3	\equiv	$Six \cdot Sky \cdot Clz$		f_3'	\equiv	$Siy \cdot Skx \cdot Clz$	
g_3	\equiv	$Cix \cdot Sky \cdot Slz$		h_3	\equiv	$Ciy \cdot Skx \cdot Slz$	
i_3	\equiv	$Six \cdot Cky \cdot Slz$		j_3	\equiv	$Siy \cdot Ckx \cdot Slz$	
k_3	\equiv	$Six \cdot Sky \cdot Slz$		l_3	\equiv	$Siy \cdot Skx \cdot Slz$	
m_3	\equiv	$Six \cdot Cky \cdot Clz$		n_3	\equiv	$Siy \cdot Ckx \cdot Clz$	
o_3	\equiv	$Cix \cdot Sky \cdot Clz$		p_3	\equiv	$Ciy \cdot Skx \cdot Clz$	
q_3	\equiv	$Cix \cdot Cky \cdot Slz$		r_3	\equiv	$Ciy \cdot Ckx \cdot Slz$	

Table 6. Definition of scattering factors for trigonal and hexagonal systems (f_2 , f_4 and f_6 do not occur in trigonal)

$$\begin{aligned}
 f_1 &= f_0 \exp - [B_{11}h^2 + B_{22}k^2 + B_{33}l^2 + B_{12}hk + B_{13}hl + B_{23}kl] \\
 f_2 &= f_0 \exp - [B_{11}h^2 + B_{22}k^2 + B_{33}l^2 + B_{12}hk - B_{13}hl - B_{23}kl] \\
 f_3 &= f_0 \exp - [B_{11}k^2 + B_{22}(h^2 + k^2 + 2hk) + B_{33}l^2 - B_{12}(k^2 + hk) \\
 &\quad + B_{13}kl - B_{23}(hl + kl)] \\
 f_4 &= f_0 \exp - [B_{11}k^2 + B_{22}(h^2 + k^2 + 2hk) + B_{33}l^2 - B_{12}(k^2 + hk) \\
 &\quad - B_{13}kl + B_{23}(hl + kl)] \\
 f_5 &= f_0 \exp - [B_{11}(h^2 + k^2 + 2hk) + B_{22}h^2 + B_{33}l^2 - B_{12}(h^2 + hk) \\
 &\quad - B_{13}(hl + kl) + B_{23}hl] \\
 f_6 &= f_0 \exp - [B_{11}(h^2 + k^2 + 2hk) + B_{22}h^2 + B_{33}l^2 - B_{12}(h^2 + hk) \\
 &\quad + B_{13}(hl + kl) - B_{23}hl] \\
 f_7 &= f_0 \exp - [B_{11}k^2 + B_{22}h^2 + B_{33}l^2 + B_{12}hk + B_{13}kl + B_{23}hl] \\
 f_8 &= f_0 \exp - [B_{11}k^2 + B_{22}h^2 + B_{33}l^2 + B_{12}hk - B_{13}kl - B_{23}hl] \\
 f_9 &= f_0 \exp - [B_{11}(h^2 + k^2 + 2hk) + B_{22}k^2 + B_{33}l^2 - B_{12}(k^2 + hk) \\
 &\quad - B_{13}(hl + kl) + B_{23}kl] \\
 f_{10} &= f_0 \exp - [B_{11}(h^2 + k^2 + 2hk) + B_{22}k^2 + B_{33}l^2 - B_{12}(k^2 + hk) \\
 &\quad + B_{13}(hl + kl) - B_{23}kl] \\
 f_{11} &= f_0 \exp - [B_{11}h^2 + B_{22}(h^2 + k^2 + 2hk) + B_{33}l^2 - B_{12}(h^2 + hk) \\
 &\quad + B_{13}hl - B_{23}(hl + kl)] \\
 f_{12} &= f_0 \exp - [B_{11}h^2 + B_{22}(h^2 + k^2 + 2hk) + B_{33}l^2 - B_{12}(h^2 + hk) \\
 &\quad - B_{13}hl + B_{23}(hl + kl)]
 \end{aligned}$$

Table 7. Definition of combinations of triple-products and scattering factors for the trigonal system (see Tables 1, 5 and 6.).

$$\begin{aligned}
 f_1[(c_1 - e_1) - (i_1 + g_1)] &\equiv 1 \\
 f_1[(q_1 - k_1) + (m_1 + o_1)] &\equiv 3 \\
 f_3[(d_3 - f_3') - (j_3 + h_3)] &\equiv 5 \\
 f_3[(r_3 - l_3) + (n_3 + p_3)] &\equiv 7 \\
 f_5[(d_2 - f_2') - (j_2 + h_2)] &\equiv 9 \\
 f_5[(r_2 - l_2) + (n_2 + p_2)] &\equiv 11 \\
 f_7[(d_1 - f_1') - (j_1 + h_1)] &\equiv 13 \\
 -f_8[j_1 + h_1) + (d_1 - f_1')] &\equiv 14 \\
 f_7[(r_1 - l_1) + (n_1 - p_1)] &\equiv 15 \\
 f_8[(n_1 + p_1) - (r_1 - l_1)] &\equiv 16 \\
 f_9[(c_3 - e_3) - (i_3 + g_3)] &\equiv 17 \\
 -f_{10}[(i_3 + g_3) + (c_3 - e_3)] &\equiv 18 \\
 f_9[(q_3 - k_3) + (m_3 + o_3)] &\equiv 19 \\
 f_{10}[m_3 + o_3) - (q_3 - k_3)] &\equiv 20 \\
 f_{11}[(c_2 - e_2) - (i_2 + g_2)] &\equiv 21 \\
 -f_{12}[(i_2 + g_2) + (c_2 - e_2)] &\equiv 22 \\
 f_{11}[(q_2 - k_2) + (m_2 + o_2)] &\equiv 23 \\
 f_{12}[(m_2 + o_2) - (q_2 - k_2)] &\equiv 24
 \end{aligned}$$

Table 8. Derivatives of the expressions defined in Table 7 for the trigonal system.

				$\frac{\partial}{2\pi\partial x}$	$\frac{\partial}{2\pi\partial y}$	$\frac{\partial}{2\pi\partial z}$	$\frac{-\partial}{\partial B_{11}}$	$\frac{-\partial}{\partial B_{22}}$	$\frac{-\partial}{\partial B_{33}}$	$\frac{-\partial}{\partial B_{12}}$	$\frac{-\partial}{\partial B_{13}}$	$\frac{-\partial}{\partial B_{23}}$
Multiplicative constant				Exp.	Multiplicative constant x 1 st column							
x	y	z			B ₁₁	B ₂₂	B ₃₃	B ₁₂	B ₁₃	B ₂₃		
1	-h	-k	-l	3	h^2	k^2	l^2	hk	hl	kl		
3	h	k	l	1	h^2	k^2	l^2	hk	hl	kl		
5	-k	-i	-l	7	k^2	S	l^2	-t	kl	-v		
7	k	i	l	5	k^2	S	l^2	-t	kl	-v		
9	-i	-h	-l	11	S	h^2	l^2	-t	-v	hl		
11	i	h	l	9	S	h^2	l^2	-t	-v	hl		
13	-k	-h	-l	15	k^2	h^2	l^2	hk	kl	hl		
14	k	h	-l	16	k^2	h^2	l^2	hk	-kl	-hl		
15	k	h	l	13	k^2	h^2	l^2	hk	kl	hl		
16	-k	-h	l	14	k^2	h^2	l^2	hk	-kl	-hl		
17	-i	-k	-l	19	S	k^2	l^2	-t	-v	kl		
18	i	k	-l	20	S	k^2	l^2	-t	v	-kl		
19	i	k	l	17	S	k^2	l^2	-t	-v	kl		
20	-i	-k	l	18	S	k^2	l^2	-t	v	-kl		
21	-h	-i	-l	23	h^2	S	l^2	-t	hl	-v		
22	h	i	-l	24	h^2	S	l^2	-t	-hl	v		
23	h	i	l	21	h^2	S	l^2	-t	hl	-v		
24	-h	-i	l	22	h^2	S	l^2	-t	-hl	v		

$$i = -h-k$$

$$h^2 + k^2 + 2hk = S, \quad k^2 + hk = t,$$

$$h^2 + hk = u, \quad hl + kl = v$$

Table 9. A tabulation of the trigonal space groups according to index parities.

Space Group	ρ_c	Planes	A	B
143-P3	1	All planes	1+5+9	3+7+11
144-P3 ₁	1	$l = 3n$ $l = 3n + \underline{1}$	1+5+9 $1 - \frac{1}{2}(5+9) \mp \sqrt{3/2}(7-11)$	3+7+11 $3 - \frac{1}{2}(7+11) \pm \sqrt{3/2}(5-9)$
145-P3 ₂	1	$l = 3n$ $l = 3n + \underline{1}$	1+5+9 $1 - \frac{1}{2}(5+9) + \sqrt{3/2}(7-11)$	3+7+11 $3 - \frac{1}{2}(7+11) \mp \sqrt{3/2}(5-9)$
146-R3	3	$-h + k + l = 3n$	1+5+9	3+7+11
147-P $\bar{3}$	2	All planes	1+5+9	---
148-R $\bar{3}$	6	All planes	1+5+9	---
149-P312	1	All planes	1+5+9+13+17+21	3+7+11-15-19-23
150-P321	1	All planes	1+5+9-14-18-22	3+7+11+16+20+24
151-P3 ₁ 12	1	$l = 3n$ $l = 3n + \underline{1}$	1+5+9+13+17+21 $1+13-\frac{1}{2}(5+9+17+21) \mp \sqrt{3/2}(7-11-19+23)$	3+7+11-15-19-23 $3-15-\frac{1}{2}(7+11-19-23) \pm \sqrt{3/2}(5-9+17-21)$
152-P3 ₁ 21	1	$l = 3n$ $l = 3n + \underline{1}$	1+5+9-14-18-22 $1-14-\frac{1}{2}(5+9-18-22) \mp \sqrt{3/2}(7-11+20-24)$	3+7+11+16+20+24 $3+16-\frac{1}{2}(7+11+20+24) \pm \sqrt{3/2}(5-9-18+22)$
153-P3 ₂ 12	1	$l = 3n$ $l = 3n + \underline{1}$	same as $l = 3n$, P3 ₁ 12 same as $l = 3n \mp 1$, P3 ₁ 12	
154-P3 ₂ 21	1	$l = 3n$ $l = 3n + \underline{1}$	same as $l = 3n$, P3 ₁ 21 same as $l = 3n \mp 1$, P3 ₁ 21	
155-R32	3	$-h + k + l = 3n$	1+5+9-14-18-22	3+7+11+16+20+24

Table 9. (continued) (2)

Space Group	ρ_c	Planes	A	B
156-P3m1	1	All planes	1+5+9-14-18-22	3+7+11-16-20-24
157-P31m	1	All planes	1+5+9+13+17+21	3+7+11+15+19+23
158-P3c1	1	$l = 2n$	1+5+9-14-18-22	3+7+11-16-20-24
		$l = 2n + 1$	1+5+9+14+18+22	3+7+11+16+20+24
159-P31c	1	$l = 2n$	1+5+9+13+17+21	3+7+11+15+19+23
		$l = 2n + 1$	1+5+9-13-17-21	3+7+11-15-19-23
160-R3m	3	$-h + k + l = 3n$	1+5+9-14-18-22	3+7+11-16-20-24
161-R3c	3	$-h + k + l = 3n;$	1+5+9-14-18-22	3+7+11-16-20-24
		$l = 2n$		
		$l = 2n + 1$	1+5+9+14+18+22	3+7+11+16+20+24
162-P $\bar{3}$ 1m	2	All planes	1+5+9+13+17+21	---
163-P $\bar{3}$ 1c	2	$l = 2n$	1+5+9+13+17+21	---
		$l = 2n + 1$	1+5+9-13-17-21	---
164-P $\bar{3}$ m1	2	All planes	1+5+9-14-18-22	---
165-P $\bar{3}$ c1	2	$l = 2n$	1+5+9-14-18-22	---
		$l = 2n + 1$	1+5+9+14+18+22	---
166-R $\bar{3}$ m	6	All planes	1+5+9-14-18-22	---
167-R $\bar{3}$ c	6	$-h + k + l = 3n,$	1+5+9-14-18-22	---
		$l = 2n$		
		$l = 2n + 1$	1+5+9+14+18+22	---

Table 10. Definition of combinations of triple products and scattering factors for the hexagonal system (see Tables 1, 5 and 6).

$$\begin{aligned}
 (f_1 + f_2)(c_1 - e_1) - (f_1 - f_2)(i_1 + g_1) &\equiv 1 \\
 -(f_1 + f_2)(i_1 + g_1) + (f_1 - f_2)(c_1 - e_1) &\equiv 2 \\
 (f_1 + f_2)(q_1 - k_1) + (f_1 - f_2)(m_1 + o_1) &\equiv 3 \\
 (f_1 + f_2)(m_1 + o_1) + (f_1 - f_2)(q_1 - k_1) &\equiv 4 \\
 (f_3 + f_4)(d_3 - f'_3) - (f_3 - f_4)(j_3 + h_3) &\equiv 5 \\
 -(f_3 + f_4)(j_3 + h_3) + (f_3 - f_4)(d_3 - f'_3) &\equiv 6 \\
 (f_3 + f_4)(r_3 - l_3) + (f_3 - f_4)(n_3 + p_3) &\equiv 7 \\
 (f_3 + f_4)(n_3 + p_3) + (f_3 - f_4)(r_3 - l_3) &\equiv 8 \\
 (f_5 + f_6)(d_2 - f'_2) - (f_5 - f_6)(j_2 + h_2) &\equiv 9 \\
 -(f_5 + f_6)(j_2 + h_2) + (f_5 - f_6)(d_2 - f'_2) &\equiv 10 \\
 (f_5 + f_6)(r_2 - l_2) + (f_5 - f_6)(n_2 + p_2) &\equiv 11 \\
 (f_5 + f_6)(n_2 + p_2) + (f_5 - f_6)(r_2 - l_2) &\equiv 12 \\
 (f_7 + f_8)(d_1 - f'_1) - (f_7 - f_8)(j_1 + h_1) &\equiv 13 \\
 -(f_7 + f_8)(j_1 + h_1) + (f_7 - f_8)(d_1 - f'_1) &\equiv 14 \\
 (f_7 + f_8)(r_1 - l_1) + (f_7 - f_8)(n_1 + p_1) &\equiv 15 \\
 (f_7 + f_8)(n_1 + p_1) + (f_7 - f_8)(r_1 - l_1) &\equiv 16 \\
 (f_9 + f_{10})(c_3 - e_3) - (f_9 - f_{10})(i_3 + g_3) &\equiv 17 \\
 -(f_9 + f_{10})(i_3 + g_3) + (f_9 - f_{10})(c_3 - e_3) &\equiv 18 \\
 (f_9 + f_{10})(q_3 - k_3) + (f_9 - f_{10})(m_3 + o_3) &\equiv 19 \\
 (f_9 + f_{10})(m_3 + o_3) + (f_9 - f_{10})(q_3 - k_3) &\equiv 20 \\
 (f_{11} + f_{12})(c_2 - e_2) - (f_{11} - f_{12})(i_2 + g_2) &\equiv 21 \\
 -(f_{11} + f_{12})(i_2 + g_2) + (f_{11} - f_{12})(c_2 - e_2) &\equiv 22 \\
 (f_{11} + f_{12})(q_2 - k_2) + (f_{11} - f_{12})(m_2 + o_2) &\equiv 23 \\
 (f_{11} + f_{12})(m_2 + o_2) + (f_{11} - f_{12})(q_2 - k_2) &\equiv 24
 \end{aligned}$$

Table 11. Derivatives of the expressions defined in Table 9 for the hexagonal system.

$\frac{\partial}{2\pi\partial x}$ and $\frac{\partial}{2\pi\partial y}$				$\frac{\partial}{2\pi l\partial z}$	$-\frac{\partial}{\partial B_{11}}$, $-\frac{\partial}{\partial B_{22}}$, $-\frac{\partial}{\partial B_{33}}$, $-\frac{\partial}{\partial B_{12}}$	$-\frac{\partial}{\partial B_{13}}$ and $-\frac{\partial}{\partial B_{23}}$						
Mult. const.		Term		Mult. constant				Term	Mult. Constant		Term	
x	y			B_{11}	B_{22}	B_{33}	B_{12}		B_{13}	B_{23}		
1	-h	-k	4	-3	h^2	k^2	l^2	hk	1	hl	kl	2
2	-h	-k	3	-4	h^2	k^2	l^2	hk	2	hl	kl	1
3	h	k	2	1	h^2	k^2	l^2	hk	3	hl	kl	4
4	h	k	1	2	h^2	k^2	l^2	hk	4	hl	kl	3
5	-k	-i	8	-7	k^2	S	l^2	-t	5	kl	-v	6
6	-k	-i	7	-8	k^2	S	l^2	-t	6	kl	-v	5
7	k	i	6	5	k^2	S	l^2	-t	7	kl	-v	8
8	k	i	5	6	k^2	S	l^2	-t	8	kl	-v	7
9	-i	-h	12	-11	S	h^2	l^2	-u	9	-v	hl	10
10	-i	-h	11	-12	S	h^2	l^2	-u	10	-v	hl	9
11	i	h	10	9	S	h^2	l^2	-u	11	-v	hl	12
12	i	h	9	10	S	h^2	l^2	-u	12	-v	hl	11
13	-k	-h	16	-15	k^2	h^2	l^2	hk	13	kl	hl	14
14	-k	-h	15	-16	k^2	h^2	l^2	hk	14	kl	hl	13
15	k	h	14	13	k^2	h^2	l^2	hk	15	kl	hl	16
16	k	h	13	14	k^2	h^2	l^2	hk	16	kl	hl	15
17	-i	-k	20	-19	S	k^2	l^2	-t	17	-v	kl	18
18	-i	-k	19	-20	S	k^2	l^2	-t	18	-v	kl	17
19	i	k	18	17	S	k^2	l^2	-t	19	-v	kl	20
20	i	k	17	18	S	k^2	l^2	-t	20	-v	kl	19
21	-h	-i	24	-23	h^2	S	l^2	-u	21	hl	-v	22
22	-h	-i	23	-24	h^2	S	l^2	-u	22	hl	-v	21
23	h	i	22	21	h^2	S	l^2	-u	23	hl	-v	24
24	h	i	21	22	h^2	S	l^2	-u	24	hl	-v	23

$i = -h-k$ $h^2 + k^2 + 2hk = S$, $k^2 + hk = t$, $h^2 + hk = u$, $hl + kl = v$

Table 12. A tabulation of the hexagonal space groups according to index parities.

Space Group	ρ_c	Planes	A	B
168-P6	1	All planes	1+5+9	3+7+11
169-P6 ₁	1	$l = 6n$	1+5+9	3+7+11
		$l = 6n + 1$	$2 - \frac{1}{2}(+6+10)$ $-\sqrt{3}/2(8-12)$	$4 - \frac{1}{2}(8+12)$ $+\sqrt{3}/2(6-10)$
		$l = 6n + 2$	$1 - \frac{1}{2}(5+9)$ $+\sqrt{3}/2(7-11)$	$3 - \frac{1}{2}(7+11)$ $-\sqrt{3}/2(5-9)$
		$l = 6n + 3$	2+6+10	4+8+12
		$l = 6n + 4$	$1 - \frac{1}{2}(5+9)$ $-\sqrt{3}/2(7-11)$	$3 - \frac{1}{2}(7-11)$ $+\sqrt{3}/2(5-9)$
		$l = 6n + 5$	$2 - \frac{1}{2}(6+10)$ $+\sqrt{3}/2(8-12)$	$4 - \frac{1}{2}(8+12)$ $-\sqrt{3}/2(6-10)$
170-P6 ₅	1	$l = 6n$	as for $l = 6n$ in P6 ₁	
		$l = 6n + 1$	as for $l = 6n + 5$ in P6 ₁	
		$l = 6n + 2$	as for $l = 6n + 4$ in P6 ₁	
		$l = 6n + 3$	as for $l = 6n + 3$ in P6 ₁	
		$l = 6n + 4$	as for $l = 6n + 2$ in P6 ₁	
		$l = 6n + 5$	as for $l = 6n + 1$ in P6 ₁	
171-P6 ₂	1	$l = 3n$	1+5+9	3+7+11
		$l = 3n + 1$	$1 - \frac{1}{2}(5+9)$ $+\sqrt{3}/2(7-11)$	$3 - \frac{1}{2}(7+11)$ $\mp \sqrt{3}/2(5-9)$
172-P6 ₄	1	$l = 3n$	as for $l = 3n$ in P6 ₂	
		$l = 3n + 1$	as for $l = 3n \mp 1$ in P6 ₂	
173-P6 ₃	1	$l = 2n$	1+5+9	3+7+11
		$l = 2n + 1$	2+6+10	4+8+12
174-P6̄	1	All planes	1+5+9	4+8+12
175-P6/m	2	All planes	1+5+9	

Table 12. (continued) (2)

Space Group	ρ_c	Planes	A	B
176-P63/m	2	$l = 2n$ $l = 2n + 1$	1+5+9 2+6+10	--- ---
177-P622	1	All planes	1+5+9+13+17+21	3+7+11-15-19-23
178-P6 ₁ 22	1	$l = 6n$ $l = 6n + 1$ $l = 6n + 2$ $l = 6n + 3$ $l = 6n + 4$ $l = 6n + 5$	1+5+9+13+17+21 2-22- $\frac{1}{2}$ (6+10-14-18) - $\sqrt{3}/2$ (8-12+16-20) 1+21- $\frac{1}{2}$ (5+9+13+17) + $\sqrt{3}/2$ (7-11-15-19) 2+6+10-14-18-22 1+21- $\frac{1}{2}$ (5+9+13+17) - $\sqrt{3}/2$ (7-11-15+19) 2-22- $\frac{1}{2}$ (6+10-14-18) + $\sqrt{3}/2$ (8-12+16-20)	3+7+11-15-19-23 4+24- $\frac{1}{2}$ (8+12+16+20) + $\sqrt{3}/2$ (6-10-14+18) 3-23- $\frac{1}{2}$ (7+11-15-19) - $\sqrt{3}/2$ (5-9+13-17) 4+8+12+16+20+24 3-23- $\frac{1}{2}$ (7+11-15-19) + $\sqrt{3}/2$ (5-9+13-17) 4+24- $\frac{1}{2}$ (8+12+16+20) - $\sqrt{3}/2$ (6-10-14+18)
179-P6 ₅ 22	1	$l = 6n$ $l = 6n + 1$ $l = 6n + 2$ $l = 6n + 3$ $l = 6n + 4$ $l = 6n + 5$	as for $l = 6n$, P6 ₁ 22 as for $l = 6n + 5$, P6 ₁ 22 as for $l = 6n + 4$, P6 ₁ 22 as for $l = 6n + 3$, P6 ₁ 22 as for $l = 6n + 2$, P6 ₁ 22 as for $l = 6n + 1$, P6 ₁ 22	
180-P6 ₂ 22	1	$l = 3n$ $l = 3n + 1$	1+5+9+13+17+21 1+21- $\frac{1}{2}$ (5+9+13+17) + $\sqrt{3}/2$ (7-11-15+19)	3+7+11-15-19-23 3-23- $\frac{1}{2}$ (7+11-15-19) - $\sqrt{3}/2$ (5-9+13-17)
181-P6 ₄ 22	1	$l = 3n$ $l = 3n + 1$	as for $l = 3n$, P6 ₁ 22 as for $l = 3n + 1$, P6 ₂ 22	
182-P6 ₃ 22	1	$l = 2n$ $l = 2n + 1$	1+5+9+13+17+21 2+6+10-14-18-22	3+7+11-15-19-23 4+8+12+16+20+24
183-P6mm	1	All planes	1+5+9+13+17+21	3+7+11+15+19+23
184-P6cc	1	$l = 2n$ $l = 2n + 1$	1+5+9+13+17+21 1+5+9-13-17-21	3+7+11+15+19+23 3+7+11-15-19-23

Table 12. (continued) (3)

Space Group	ρ_c	Planes	A	B
185-P $\bar{6}_3$ cm	1	$l = 2n$ $l = 2n + 1$	1+5+9+13+17+21 2+6+10+14+18+22	3+7+11+15+19+23 4+8+12+16+20+24
186-P $\bar{6}_3$ mc	1	$l = 2n$ $l = 2n + 1$	1+5+9+13+17+21 2+6+10-14-18-22	3+7+11+15+19+23 4+8+12-16-20-24
187-P $\bar{6}$ m2	1	All planes	1+5+9+13+17+21	4+8+12-16-20-24
188-P $\bar{6}$ c2	1	$l = 2n$ $l = 2n + 1$	1+5+9+13+17+21 2+6+10+14+18+22	4+8+12-16-20-24 3+7+11-15-19-23
189-P $\bar{6}$ 2m	1	All planes	1+5+9+13+17+21	4+8+12+16+20+24
190-P $\bar{6}$ 2c	1	$l = 2n$ $l = 2n + 1$	1+5+9+13+17+21 2+6+10-14-18-22	4+8+12+16+20+24 3+7+11-15-19-23
191-P6/m mm	2	All planes	1+5+9+13+17+21	---
192-P6/m cc	2	$l = 2n$ $l = 2n + 1$	1+5+9+13+17+22 1+5+9-13-17-21	--- ---
193-P63/m cm	2	$l = 2n$ $l = 2n + 1$	1+5+9+13+17+21 2+6+10+14+18+22	--- ---
194-P63/m mc	2	$l = 2n$ $l = 2n + 1$	1+5+9+13+17+21 2+6+10-14-18-22	--- ---

References

International Tables for X-Ray Crystallography (1952), Vol. I.

Birmingham: Kynoch Press.

Hybl, A. and Marsh, R. E. (1961). Acta Cryst., 14, 1046 .

Rollett, J. S. and Davies, D. R. (1955). Acta Cryst., 8, 125.

Trueblood, K. N. (1956). Acta Cryst., 9, 359.

**Structure-Factor and Least-Squares Calculation
for Cubic Systems with Isotropic Vibrations**

A set of expressions is presented for calculating structure factors and least-squares coefficients for cubic structures with isotropic temperature factors. The expressions will complement those presented by Hybl and Marsh (1961) for the orthorhombic system; however, we will not now carry their treatment of anisotropic temperature factors into the cubic system. Based on these expressions, the Burroughs 220 computer has been programmed to perform structure-factor least-squares calculations for any cubic space group; to direct the course of calculations for a particular space group, the computer must know only the space group number.

All of the geometrical structure factors for the cubic system have been reduced to sums of triple products of sines and cosines. A total of 48 different triple products are utilized; these triple products and the 16 sums of 3 triple products are defined in table 1. The triple products are divided into two groups, I and II. Space groups of symmetry T or T_h require expressions in group I only; furthermore, the derivatives with respect to the parameters x , y , and z (and, of course, B) of any triple product in group I (or II) are other triple products in group I (or II) multiplied by $\pm 2\pi \begin{pmatrix} h \\ k \\ l \end{pmatrix}$.

The sums in group I are directly related to sums in group II: C transforms to D, E to F, G to H, I to J, ...etc., simply by interchanging h and k (see table 1). The derivatives of a sum can be written down immediately by inspection of table 2 when the derivatives of each triple product are listed. For example, the derivative of C ($C = c_1 + c_2 + c_3$) with respect to x is equal to $2\pi(-hm_1 - lq_2 - ko_3)$.

The geometrical structure factors for each set of conditions on the indices for every cubic space group are presented in table 3 in terms of the sums of triple products defined in table 1. The presentation follows that of the International Tables (1952); in cases where the International Tables give a choice of origins, the origin is taken at a center. Corrections in O^7 and O_h^7 have been made as directed by the errata sheet.

For our program we have utilized the similarities in the structure factor expressions for different space groups. For example, the structure factor expressions for T^1 , T^2 and T^3 are the same except for a different multiplicity factor; the same applies for space groups T_h^1 , T_h^3 and T_h^5 , O^1 , O^3 and O^5 , T_d^1 , T_d^2 and T_d^3 , and O_h^1 , O_h^5 , and O_h^9 . Some pairs of space groups whose similarities have been utilized are T^4 and T^5 , T_h^2 and T_h^4 , T_h^4 and O_h^7 , O^6 and O^7 , O^8 and T_d^6 , T_d^6 and O_h^{10} , O_h^2 and O_h^4 , and O_h^7 and O_h^8 . There are other similarities which we have utilized, and we are sure there are some which were not exploited. We give one example to illustrate

the use of the tables. Consider reflections $h + k = 2n + 1$, $k + l = 2n + 1$ in space group T_h^2 (for one atom in a general position):

$$F_c = -8I = -8(i_1 + i_2 + i_3)$$

$$\begin{aligned} \frac{\partial F_c}{\partial x} &= -8(2\pi) (hq_1 + lm_2 - kk_3) \\ &= -8(2\pi) [h \cos(2\pi hx) \cos(2\pi ky) \sin(2\pi lz) \\ &\quad + l \sin(2\pi hy) \cos(2\pi kz) \cos(2\pi lx) \\ &\quad - k \sin(2\pi hz) \sin(2\pi kx) \sin(2\pi ly)] \end{aligned}$$

We get F_c from table 3, I from table 1, and the derivatives from table 2.

I thank Drs. Richard E. Marsh and Sten Samson for helpful discussions and encouragement.

References

International Tables for X-Ray Crystallography (1952), Vol. I.

Birmingham: Kynoch Press.

Hybl, A. and Marsh, R. E. (1961). Acta Cryst., 14, 1046.

Table 1. Definition of triple products and sums of triple products.

$$C = \cos 2\pi \quad S = \sin 2\pi$$

Group I	hx	ky	lz	hy	kz	lx	hz	kx	ly	
C	Chx	Cky	Clz	+ Chy	Ckz	Clx	+ Chz	Ckx	Cly	$\equiv c_1 + c_2 + c_3$
E	Shx	Sky	Clz	+ Shy	Skz	Clx	+ Shz	Skx	Cly	$\equiv e_1 + e_2 + e_3$
G	Chx	Sky	Slz	+ Chy	Skz	Slx	+ Chz	Skx	Sly	$\equiv g_1 + g_2 + g_3$
I	Shx	Cky	Slz	+ Shy	Ckz	Slx	+ Shz	Ckx	Sly	$\equiv i_1 + i_2 + i_3$
K	Shx	Sky	Slz	+ Shy	Skz	Slx	+ Shz	Skx	Sly	$\equiv k_1 + k_2 + k_3$
M	Shx	Cky	Clz	+ Shy	Ckz	Clx	+ Shz	Ckx	Cly	$\equiv m_1 + m_2 + m_3$
O	Chx	Sky	Clz	+ Chy	Skz	Clx	+ Chz	Skx	Cly	$\equiv o_1 + o_2 + o_3$
Q	Chx	Cky	Slz	+ Chy	Ckz	Slx	+ Chz	Ckx	Sly	$\equiv q_1 + q_2 + q_3$
Group II	hy	kx	lz	hz	ky	lx	hx	kz	ly	
D	Chy	Ckx	Clz	+ Chz	Cky	Clx	+ Chx	Ckz	Cly	$\equiv d_1 + d_2 + d_3$
F	Shy	Skx	Clz	+ Shz	Sky	Clx	+ Shx	Skz	Cly	$\equiv f_1 + f_2 + f_3$
H	Chy	Skx	Slz	+ Chz	Sky	Slx	+ Chx	Skz	Sly	$\equiv h_1 + h_2 + h_3$
J	Shy	Ckx	Slz	+ Shz	Cky	Slx	+ Shx	Ckz	Sly	$\equiv j_1 + j_2 + j_3$
L	Shy	Skx	Slz	+ Shz	Sky	Slx	+ Shx	Skz	Sly	$\equiv l_1 + l_2 + l_3$
N	Shy	Ckx	Clz	+ Shz	Cky	Clx	+ Shx	Ckz	Cly	$\equiv n_1 + n_2 + n_3$
P	Chy	Skx	Clz	+ Chz	Sky	Clx	+ Chx	Skz	Cly	$\equiv p_1 + p_2 + p_3$
R	Chy	Ckx	Slz	+ Chz	Cky	Slx	+ Chx	Ckz	Sly	$\equiv r_1 + r_2 + r_3$

Table 2. Derivatives of triple products. All derivatives to be multiplied by 2π . For example, read $hm1 \equiv 2\pi hm1$.

<u>Group I</u>	x	y	z	<u>Group II</u>	x	y	z
c 1	-hm1	-ko1	-lq1	d1	-kp1	-hn1	-lr1
c 2	-lq2	-hm2	-ko2	d2	-lr2	-kp2	-hr2
c 3	-ko3	-lq3	-hm3	d3	-hn3	-lr3	-kp3
e1	ho1	km1	-lk1	f1	+kn1	hp1	-ll1
e2	-lk2	ho2	km2	f2	-ll2	kn2	hp2
e3	+km3	-lk3	ho3	f3	hp3	-ll3	kn3
g1	-hk1	kq1	lo1	h1	kr1	-hl1	lp1
g2	lo2	-hk2	-kq2	h2	lp2	kr2	-hl2
g3	kq3	lo3	-hk3	h3	-hl3	lp3	kr3
i1	hq1	-kk1	lm1	j1	-kl1	hr1	ln1
i2	lm2	hq2	-kk2	j2	ln2	-kl2	hr2
i3	-kk3	lm3	hq3	j3	hr3	ln3	-kl3
k1	hg1	ki1	le1	l1	kj1	hh1	lf1
k2	le2	hg2	ki2	l2	lf2	kj2	hh2
k3	ki3	le3	hg3	l3	hh3	lf3	kj3
m1	hc1	-ke1	-li1	n1	-kf1	hd1	-lj1
m2	-li2	hc2	-ke2	n2	-lj2	-kf2	hd2
m3	-ke3	-li3	hc3	n3	hd3	-lj3	-kf3
o1	-he1	kc1	-lg1	p1	kd1	-hf1	-lh1
o2	-lg2	-he2	kc2	p2	-lh2	kd2	-hf2
o3	kc3	-lg3	-he3	p3	-hf3	-lh3	kd3
q1	-hi1	-kg1	lc1	r1	-kh1	-hj1	+ld1
q2	lc2	-hi2	-kg2	r2	ld2	-kh2	-hj2
q3	-kg3	lc3	-hi3	r3	-hj3	ld3	-kh3

Note the cyclic relationship.

Table 3. A tabulation of the cubic space groups according to index parities.

Space Group	ρ_c^\dagger	Planes	A	B	
T^1 -P23	4	All planes	C	-K	
T^2 -F23	16	h, k, l all even or all odd	C	-K	
T^3 -I23	8	$h + k + l = 2n$	C	-K	
T^4 -P2 ₁ 3	4	$\frac{h+k}{2n}$	$\frac{k+l}{2n}$	C	-K
		$2n$	$2n+1$	-G	M
		$2n+1$	$2n$	-I	O
		$2n+1$	$2n+1$	-E	Q
T^5 -I2 ₁ 3	8	$h+k+l = \frac{h}{2n}$	$\frac{k}{2n}$	C	-K
		$2n$	$2n+1$	-I	O
		$2n+1$	$2n$	-E	Q
		$2n+1$	$2n+1$	-G	M
				$\frac{A}{-}$	
T_h^1 -Pm3	8'	All planes		C	
T_h^2 -Pn3	8	$\frac{h+k}{2n}$	$\frac{k+l}{2n}$		C
		$2n$	$2n+1$		-E
		$2n+1$	$2n$		-G
		$2n+1$	$2n+1$		-I
T_h^3 -Fm3	32	h, k, l all even or all odd		C	

Table 3. (continued) (2)

Space Group	ρ_c	Planes	A			
T_h^4 -Fd3	16	$\frac{h+k}{4n}$	$\frac{k+l}{4n}$	$\frac{l+h}{4n}$	2C	
		4n	4n + 2	4n + 2	-2E	
		4n + 2	4n	4n + 2	-2G	
		4n + 2	4n + 2	4n	-2I	
		4n	4n	4n + 2	C-E-G+I	
		4n	4n + 2	4n	C-E+G-I	
		4n + 2	4n	4n	C+E-G-I	
		4n + 2	4n + 2	4n + 2	-C-E-G-I	
T_h^5 -Im3	16	$h+k+l = 2n$			C	
T_h^6 -Pa3	8	$\frac{h+k}{2n}$	$\frac{k+l}{2n}$		C	
		2n	2n + 1		-G	
		2n + 1	2n		-I	
		2n + 1	2n + 1		-E	
T_h^7 -Ia3	16	$h+k+l = 2n$	$\frac{h}{2n}$	$\frac{k}{2n}$	C	
			2n	2n + 1	-I	
			2n + 1	2n	-E	
			2n + 1	2n + 1	-G	
O^1 -P432	4	All planes			C+D	-K+L
		O^2 -P4 ₂ 32	4	$h+k+l = 2n$		
$h+k+l = 2n+1$				C-D	-K-L	
O^3 -F432	16	h, k, l all even or all odd			C+D	-K+L
O^4 -F4 ₁ 32	16	$\frac{h, k, l}{\text{all even}}$	$\frac{h+k+l}{4n}$		C+D	-K+L
		all odd	4n + 1		C-L	-K+D
		all even	4n + 2		C-D	-K-L
		all odd	4n + 3		C+L	-K-D

Table 3. (continued) (3)

Space Group	ρ_c	Planes	A	B																																																																																																																							
O^5-I432	8	$h + k + l = 2n$	C+D	-K+L																																																																																																																							
O^6-P4_332	4	<table border="1"> <thead> <tr> <th></th> <th>$\frac{h}{2n}$</th> <th>$\frac{k}{2n}$</th> <th>$\frac{l}{2n}$</th> <th>$\frac{h+k+l}{4n}$</th> <th></th> <th></th> </tr> </thead> <tbody> <tr><td>(1)</td><td>$2n$</td><td>$2n$</td><td>$2n$</td><td>$4n$</td><td>C+D</td><td>-K+L</td></tr> <tr><td>(2)</td><td>$2n+1$</td><td>$2n+1$</td><td>$2n+1$</td><td>$4n+1$</td><td>C-L</td><td>-K+D</td></tr> <tr><td>(3)</td><td>$2n$</td><td>$2n$</td><td>$2n$</td><td>$4n+2$</td><td>C-D</td><td>-K-L</td></tr> <tr><td>(4)</td><td>$2n+1$</td><td>$2n+1$</td><td>$2n+1$</td><td>$4n+3$</td><td>C+L</td><td>-K-D</td></tr> <tr><td>(5)</td><td>$2n+1$</td><td>$2n+1$</td><td>$2n$</td><td>$4n$</td><td>-G-J</td><td>M-P</td></tr> <tr><td>(6)</td><td>$2n$</td><td>$2n$</td><td>$2n+1$</td><td>$4n+1$</td><td>-G+P</td><td>M-J</td></tr> <tr><td>(7)</td><td>$2n+1$</td><td>$2n+1$</td><td>$2n$</td><td>$4n+2$</td><td>-G+J</td><td>M+P</td></tr> <tr><td>(8)</td><td>$2n$</td><td>$2n$</td><td>$2n+1$</td><td>$4n+3$</td><td>-G-P</td><td>M+J</td></tr> <tr><td>(9)</td><td>$2n$</td><td>$2n+1$</td><td>$2n+1$</td><td>$4n$</td><td>-I-F</td><td>O-R</td></tr> <tr><td>(10)</td><td>$2n+1$</td><td>$2n$</td><td>$2n$</td><td>$4n+1$</td><td>-I+R</td><td>O-F</td></tr> <tr><td>(11)</td><td>$2n$</td><td>$2n+1$</td><td>$2n+1$</td><td>$4n+2$</td><td>-I+F</td><td>O+R</td></tr> <tr><td>(12)</td><td>$2n+1$</td><td>$2n$</td><td>$2n$</td><td>$4n+3$</td><td>-I-R</td><td>O+F</td></tr> <tr><td>(13)</td><td>$2n+1$</td><td>$2n$</td><td>$2n+1$</td><td>$4n$</td><td>-E-H</td><td>Q-N</td></tr> <tr><td>(14)</td><td>$2n$</td><td>$2n+1$</td><td>$2n$</td><td>$4n+1$</td><td>-E+N</td><td>Q-H</td></tr> <tr><td>(15)</td><td>$2n+1$</td><td>$2n$</td><td>$2n+1$</td><td>$4n+2$</td><td>-E+H</td><td>Q+N</td></tr> <tr><td>(16)</td><td>$2n$</td><td>$2n+1$</td><td>$2n$</td><td>$4n+3$</td><td>-E-N</td><td>Q+H</td></tr> </tbody> </table>		$\frac{h}{2n}$	$\frac{k}{2n}$	$\frac{l}{2n}$	$\frac{h+k+l}{4n}$			(1)	$2n$	$2n$	$2n$	$4n$	C+D	-K+L	(2)	$2n+1$	$2n+1$	$2n+1$	$4n+1$	C-L	-K+D	(3)	$2n$	$2n$	$2n$	$4n+2$	C-D	-K-L	(4)	$2n+1$	$2n+1$	$2n+1$	$4n+3$	C+L	-K-D	(5)	$2n+1$	$2n+1$	$2n$	$4n$	-G-J	M-P	(6)	$2n$	$2n$	$2n+1$	$4n+1$	-G+P	M-J	(7)	$2n+1$	$2n+1$	$2n$	$4n+2$	-G+J	M+P	(8)	$2n$	$2n$	$2n+1$	$4n+3$	-G-P	M+J	(9)	$2n$	$2n+1$	$2n+1$	$4n$	-I-F	O-R	(10)	$2n+1$	$2n$	$2n$	$4n+1$	-I+R	O-F	(11)	$2n$	$2n+1$	$2n+1$	$4n+2$	-I+F	O+R	(12)	$2n+1$	$2n$	$2n$	$4n+3$	-I-R	O+F	(13)	$2n+1$	$2n$	$2n+1$	$4n$	-E-H	Q-N	(14)	$2n$	$2n+1$	$2n$	$4n+1$	-E+N	Q-H	(15)	$2n+1$	$2n$	$2n+1$	$4n+2$	-E+H	Q+N	(16)	$2n$	$2n+1$	$2n$	$4n+3$	-E-N	Q+H		
	$\frac{h}{2n}$	$\frac{k}{2n}$	$\frac{l}{2n}$	$\frac{h+k+l}{4n}$																																																																																																																							
(1)	$2n$	$2n$	$2n$	$4n$	C+D	-K+L																																																																																																																					
(2)	$2n+1$	$2n+1$	$2n+1$	$4n+1$	C-L	-K+D																																																																																																																					
(3)	$2n$	$2n$	$2n$	$4n+2$	C-D	-K-L																																																																																																																					
(4)	$2n+1$	$2n+1$	$2n+1$	$4n+3$	C+L	-K-D																																																																																																																					
(5)	$2n+1$	$2n+1$	$2n$	$4n$	-G-J	M-P																																																																																																																					
(6)	$2n$	$2n$	$2n+1$	$4n+1$	-G+P	M-J																																																																																																																					
(7)	$2n+1$	$2n+1$	$2n$	$4n+2$	-G+J	M+P																																																																																																																					
(8)	$2n$	$2n$	$2n+1$	$4n+3$	-G-P	M+J																																																																																																																					
(9)	$2n$	$2n+1$	$2n+1$	$4n$	-I-F	O-R																																																																																																																					
(10)	$2n+1$	$2n$	$2n$	$4n+1$	-I+R	O-F																																																																																																																					
(11)	$2n$	$2n+1$	$2n+1$	$4n+2$	-I+F	O+R																																																																																																																					
(12)	$2n+1$	$2n$	$2n$	$4n+3$	-I-R	O+F																																																																																																																					
(13)	$2n+1$	$2n$	$2n+1$	$4n$	-E-H	Q-N																																																																																																																					
(14)	$2n$	$2n+1$	$2n$	$4n+1$	-E+N	Q-H																																																																																																																					
(15)	$2n+1$	$2n$	$2n+1$	$4n+2$	-E+H	Q+N																																																																																																																					
(16)	$2n$	$2n+1$	$2n$	$4n+3$	-E-N	Q+H																																																																																																																					
O^7-P4_132	4	See O^6 , parity condition	<table border="1"> <tbody> <tr><td>(1)</td><td>C+D</td><td>-K+L</td></tr> <tr><td>(2)</td><td>C+L</td><td>-K-D</td></tr> <tr><td>(3)</td><td>C-D</td><td>-K-L</td></tr> <tr><td>(4)</td><td>C-L</td><td>-K+D</td></tr> <tr><td>(5)</td><td>-G-J</td><td>M-P</td></tr> <tr><td>(6)</td><td>-G-P</td><td>M+J</td></tr> <tr><td>(7)</td><td>-G+J</td><td>M+P</td></tr> <tr><td>(8)</td><td>-G+P</td><td>M-J</td></tr> <tr><td>(9)</td><td>-I-F</td><td>O-R</td></tr> <tr><td>(10)</td><td>-I-R</td><td>O+F</td></tr> <tr><td>(11)</td><td>-I+F</td><td>O+R</td></tr> <tr><td>(12)</td><td>-I+R</td><td>O-F</td></tr> <tr><td>(13)</td><td>-E-H</td><td>Q-N</td></tr> <tr><td>(14)</td><td>-E-N</td><td>Q+H</td></tr> <tr><td>(15)</td><td>-E+H</td><td>Q+N</td></tr> <tr><td>(16)</td><td>-E+N</td><td>Q-H</td></tr> </tbody> </table>	(1)	C+D	-K+L	(2)	C+L	-K-D	(3)	C-D	-K-L	(4)	C-L	-K+D	(5)	-G-J	M-P	(6)	-G-P	M+J	(7)	-G+J	M+P	(8)	-G+P	M-J	(9)	-I-F	O-R	(10)	-I-R	O+F	(11)	-I+F	O+R	(12)	-I+R	O-F	(13)	-E-H	Q-N	(14)	-E-N	Q+H	(15)	-E+H	Q+N	(16)	-E+N	Q-H																																																																								
(1)	C+D	-K+L																																																																																																																									
(2)	C+L	-K-D																																																																																																																									
(3)	C-D	-K-L																																																																																																																									
(4)	C-L	-K+D																																																																																																																									
(5)	-G-J	M-P																																																																																																																									
(6)	-G-P	M+J																																																																																																																									
(7)	-G+J	M+P																																																																																																																									
(8)	-G+P	M-J																																																																																																																									
(9)	-I-F	O-R																																																																																																																									
(10)	-I-R	O+F																																																																																																																									
(11)	-I+F	O+R																																																																																																																									
(12)	-I+R	O-F																																																																																																																									
(13)	-E-H	Q-N																																																																																																																									
(14)	-E-N	Q+H																																																																																																																									
(15)	-E+H	Q+N																																																																																																																									
(16)	-E+N	Q-H																																																																																																																									

Table 3. (continued) (4)

Space Group	ρ_c	Planes	A	B
$O^8 - I4_132$	8	$\frac{h}{2n}$ $\frac{k}{2n}$ $\frac{l}{2n}$ $\frac{h+k+l}{4n}$	C+D	-K+L
		2n 2n+1 2n+1 4n	-I-F	O-R
		2n+1 2n 2n+1 4n	-E-H	Q-N
		2n+1 2n+1 2n 4n	-G-J	M-P
		2n 2n 2n 4n+2	C-D	-K-L
		2n 2n+1 2n+1 4n+2	-I+F	O+R
		2n+1 2n 2n+1 4n+2	-E+H	Q+N
		2n+1 2n+1 2n 4n+2	-G+J	M+P
$T_d^1 - P\bar{4}3m$	4	All planes	C+D	-K-L
$T_d^2 - F\bar{4}3m$	16	h, k, l all even or all odd	C+O	-K-L
$T_d^3 - I\bar{4}3m$	8	$h + k + l = 2n$	C+D	-K-L
$T_d^4 - P\bar{4}3n$	4	$h + k + l = 2n$	C+D	-K-L
		$h + k + l = 2n + 1$	C-D	-K+L
$T_d^5 - F\bar{4}3c$	16	h, k, l all even	C+D	-K-L
		h, k, l all odd	C-D	-K+L
$T_d^6 - I\bar{4}3d$	8	$\frac{h}{2n}$ $\frac{k}{2n}$ $\frac{l}{2n}$ $\frac{h+k+l}{4n}$	C+D	-K-L
		2n 2n+1 2n+1 4n	-I-F	O+R
		2n+1 2n 2n+1 4n	-E-H	Q+N
		2n+1 2n+1 2n 4n	-G-J	M+P
		2n 2n 2n 4n+2	C-D	-K+L
		2n 2n+1 2n+1 4n+2	-I+F	O-R
		2n+1 2n 2n+1 4n+2	-E+H	Q-N
		2n+1 2n+1 2n 4n+2	-G+J	M-P
			A	
$O_h^1 - Pm\bar{3}m$	8	All planes		C+D

Table 3. (continued) (5)

Space Group	ρ_c	Planes	A		
O_h^2 -Pn3n	8	$\frac{h}{2n}$	$\frac{k}{2n}$	$\frac{l}{2n}$	C+D
		2n	2n+1	2n+1	-G-H
		2n+1	2n+1	2n	-E-F
		2n+1	2n	2n+1	-I-J
		2n+1	2n+1	2n+1	C-D
		2n+1	2n	2n	-G+H
		2n	2n	2n+1	-E+F
		2n	2n+1	2n	-I+J
O_h^3 -Pm3n	8	$h + k + l = 2n$			C+D
		$h + k + l = 2n + 1$			C-D
O_h^4 -Pn3m	8	$\frac{h+k}{2n}$	$\frac{k+l}{2n}$		C+D
		2n	2n+1		-E-F
		2n+1	2n		-G-H
		2n+1	2n+1		-I-J
O_h^5 -Fm3m	32	h, k, l all even or all odd			C+D
O_h^6 -Fm3c	32	h, k, l all even			C+D
		h, k, l all odd			C-D
O_h^7 -Fd3m	16	$\frac{h+k}{4n}$	$\frac{k+l}{4n}$	$\frac{l+h}{4n}$	2(C+D)
		4n	4n+2	4n+2	-2(E+F)
		4n+2	4n	4n+2	-2(G+H)
		4n+2	4n+2	4n	-2(I+J)
		4n	4n	4n+2	(C-E-G+I +D-F-H+J)
		4n	4n+2	4n	(C-E+G-I +D-F+H-J)
		4n+2	4n	4n	(C+E-G-I +D+F-H-J)
		4n+2	4n+2	4n+2	-(C+E+G+I +D+F+H+J)

Table 3. (continued) (6)

Space Group	ρ_c	Planes	A					
O_h^8 -Fd3c	16	$\frac{h+k}{4n}$	$\frac{k+l}{4n}$	$\frac{l+h}{4n}$		2(C+D)		
		$\frac{4n}{4n}$	$\frac{4n+2}{4n}$	$\frac{4n+2}{4n}$		-2(E+F)		
		$\frac{4n+2}{4n}$	$\frac{4n}{4n}$	$\frac{4n+2}{4n}$		-2(G+H)		
		$\frac{4n+2}{4n}$	$\frac{4n+2}{4n}$	$\frac{4n}{4n}$		-2(I+J)		
		$\frac{4n}{4n}$	$\frac{4n}{4n}$	$\frac{4n+2}{4n}$		-(C-E+G-I -D+F-H+J)		
		$\frac{4n}{4n}$	$\frac{4n+2}{4n}$	$\frac{4n}{4n}$		-(C+E-G-I -D-F+H+J)		
		$\frac{4n+2}{4n}$	$\frac{4n}{4n}$	$\frac{4n}{4n}$		-(C-E-G+I -D+F+H-J)		
		$\frac{4n+2}{4n}$	$\frac{4n+2}{4n}$	$\frac{4n+2}{4n}$		-(C+E+G+I -D-F-H-J)		
		O_h^9 -Im3m	16	$h+k+l = 2n$				C+D
O_h^{10} -Ia3d	16	$\frac{h}{2n}$	$\frac{k}{2n}$	$\frac{l}{2n}$	$\frac{h+k+l}{4n}$	C+D		
		$\frac{2n}{2n}$	$\frac{2n+1}{2n}$	$\frac{2n+1}{2n}$	$\frac{4n}{4n}$	-I-F		
		$\frac{2n+1}{2n}$	$\frac{2n}{2n}$	$\frac{2n+1}{2n}$	$\frac{4n}{4n}$	-E-H		
		$\frac{2n+1}{2n}$	$\frac{2n+1}{2n}$	$\frac{2n}{2n}$	$\frac{4n}{4n}$	-G-J		
		$\frac{2n}{2n}$	$\frac{2n}{2n}$	$\frac{2n}{2n}$	$\frac{4n+2}{4n}$	C-D		
		$\frac{2n}{2n}$	$\frac{2n+1}{2n}$	$\frac{2n+1}{2n}$	$\frac{4n+2}{4n}$	-I+F		
		$\frac{2n+1}{2n}$	$\frac{2n}{2n}$	$\frac{2n+1}{2n}$	$\frac{4n+2}{4n}$	-E+H		
		$\frac{2n+1}{2n}$	$\frac{2n+1}{2n}$	$\frac{2n}{2n}$	$\frac{4n+2}{4n}$	-G+J		

† ρ_c is the factor by which A and B must be multiplied to give contribution of entire unit cell.

IV. I propose that the trial structure defined below be used as a starting point in a refinement of the crystal structure of the γ_1 -phase compound of the nickel-cadmium system.

Space group	$T_d^1 - P\bar{4}3m$
Atomic parameters	
4 Ni in 4(e)	a, a, a; with a = 0.126
4 Cd in 4(e)	b, b, b; with b = -0.169
6 Cd in 6(f)	c, o, o; with c = 0.342
12 Cd in 12(h)	d, d, e; with d = 0.312
	e = 0.047
1 Cd in 1(b)	$\frac{1}{2} \frac{1}{2} \frac{1}{2}$
4 Ni in 4(e)	f, f, f; with f = 0.314
6 Ni in 6(f)	g, $\frac{1}{2} \frac{1}{2}$; with g = 0.799
12 Cd in 12(h)	h, h, i; with h = 0.796
	i = 0.547

14 Ni and 35 Cd (28.6 at. % Ni)

Lihl and Buhl (1) reported the γ_1 phase of the nickel-cadmium system to be homogeneous between about 29 and 29.5 at. % Ni with a γ -brass type structure. I propose that the structure is essentially defined by the trial structure given above; the trial structure is not a γ -brass type.

In an ingot whose overall composition was approximately 55 at. % Ni, I found a cubic crystal with a cell edge of $a_0 \cong 9.7 \text{ \AA}$, which corresponds very closely to the value for a_0 of 9.675 \AA reported by Lihl and Buhl for the γ_1 phase. I have obtained an almost complete three-dimensional set of intensity data from equi-inclination Weissenberg photographs. The intensities were estimated with great haste, corrected for Lorentz and polarization effects, and correlated to obtain a list of structure factors on the same scale.

The first structure-factor least-squares refinement cycle on the basis of the proposed trial structure gave an agreement index of $R = 0.29$; and a second cycle reduced this to $R = 0.26$. An electron-density map of the (110) plane was then calculated, and the map indicated no serious error in the trial structure. At a corresponding stage ($R = 0.28$) in the refinement of " $\text{Ni}_5\text{Zn}_{21}$ " (2), an electron-density map was calculated which immediately indicated the error in the trial structure.

I must admit that the observed structure factors used in these calculations are probably of poor quality because of the haste in which they were obtained. Furthermore, the trial structure that I have proposed may be based on an incorrect composition. The occupancy of possible positions was assigned to give an overall composition of approximately 29% as reported by Lihl and Buhl. An experimental

composition has not been obtained by me; however, these preliminary calculations indicate no change in the assigned occupancies.

In spite of this, I assert that the geometrical structure is essentially correct. As indicated above, the electron-density map contained no spurious peaks; furthermore, there was a negative peak at the position where one would expect a peak if the structure were a γ -brass structure as reported by Lihl and Buhl. A γ -brass type trial structure was constructed after the above calculations were carried out; a few least squares cycles have brought the agreement index only to $R = 0.40$.

References

1. F. Lihl and E. Buhl, Z. Metallkunde, 46, 787-791 (1955).
2. This thesis, Part III.

V. I propose that the crystal structure of " Cu_9Al_4 " be carefully investigated to determine its structure and to determine its ideal composition.

The crystal structure and composition of " Cu_9Al_4 " are very important since " Cu_9Al_4 " and Cu_5Zn_8 , γ brass, seem to have given rise to the class of electron compounds known as the γ -brass type compounds. Ekman (1), using the powder method, found several alloys to be isotypic with γ brass. He assigned them ideal compositions which give the ratio of valence electrons to atoms a value of 21/13. He felt that this ratio of electrons to atoms was instrumental in determining a γ -brass type structure, since the only two γ -brass structures known at that time were " Cu_9Al_4 " and Cu_5Zn_8 , which both exhibit an electron:atom ratio of 21:13 if copper is assumed to be univalent, zinc divalent, and aluminum trivalent. Since that time, many alloys have been reported as γ -brass types, and all have ideal compositions which give electron:atom ratios of 21:13. Hume-Rothery and Raynor (2) state: "Thus, the so-called ' γ -brass' structure occurs at an electron:atom ratio of 21:13." This sort of statement is commonly called a Hume-Rothery rule. They list 26 alloys with a γ -brass type structure. Because of the work reported in parts II and III of this thesis, " $\text{Ni}_5\text{Cd}_{21}$ " and " Ni_5Zn_4 " can be removed from that list. I have examined the literature, drawing analogies to " $\text{Ni}_5\text{Cd}_{21}$ " and " $\text{Ni}_5\text{Zn}_{21}$ " where it

seemed appropriate, and I have concluded that there is sufficient evidence to remove 14 other alloys from that list, reducing the number from 26 to 10. I am willing to admit that five of these can occur with γ -brass type structures at electron:atom ratios of 21:13. It seems that the classification of γ -brass compounds will break down under careful scrutiny.

I assert that " Cu_9Al_4 " became such and has persisted as such on the basis of fallacious reasoning and in contradiction to known experimental facts. In doing so, I necessarily assert that the γ -brass classification was based on unsound logic from the very beginning. My reasons are pointed out in the following analysis of Bradley's determination (3) of the crystal structure of " Cu_9Al_4 ". All of the quotes are from his paper. At the time Bradley wrote this, the copper-aluminum phase with which he worked was called the δ -phase.

Bradley derived the crystal structure of " Cu_9Al_4 " in the following manner. Powder photographs of the δ -Cu-Al phase were similar to those of $\text{Cu}_5\text{-Zn}_8$. However, the differences in the photographs were sufficiently marked to indicate that "the structures are not quite the same in every respect." The relative intensities of the Cu_5Zn_8 photographs were not in every sense the same as those of corresponding lines of the δ -Cu-Al photographs. There were, moreover, additional lines on the δ -Cu-Al photographs corresponding to reflections with $h + k + l = 2n + 1$, indicating that the unit cube is

primitive and not body centered. He states, with his emphases, "intensity changes cannot be accounted for by supposing that the positions of the atoms have suffered a slight displacement, the effect of which would be to produce a slight change in the least deviated reflections and a much larger change in the most deviated reflections. This is just the reverse of what one observes. It is therefore safe to conclude that the atoms, as a whole, occupy almost identical positions in the two alloys." I don't follow his reasoning in the first sentence, but I want to emphasize "slight" instead of "displacement." Here he makes his first fallacious assumption, that any displacement is a slight one; he does not consider that there may be major changes in a few of the positions.

He reasons further that the primitive cell can be based on 8 independent sets of atoms, constituting 52 atoms in the unit cube as in Cu_5Zn_8 .

The 8 sets and their coordinates are:

$4e_1$ at a, a, a ; etc., and $4e_1'$ at $\frac{1}{2} + a, \frac{1}{2} + a, \frac{1}{2} + a$; etc., $a = 0.10_3$

$4e_2$ at b, b, b ; etc., and $4e_2'$ at $\frac{1}{2} + b, \frac{1}{2} + b, \frac{1}{2} + b$; etc., $b = 0.16_7$

$6f$ at $c, 0, 0$; etc., and $6f'$ at $\frac{1}{2} + c, \frac{1}{2}, \frac{1}{2}$; etc., $c = 0.35_8$

$12h$ at d, d, e ; etc., and $12h'$ at $\frac{1}{2} + d, \frac{1}{2} + d, \frac{1}{2} + e$; etc., $d = 0.30_5$

As one can see, he has preserved the body-centering translation, as far as the geometry is concerned; we will soon see that he makes this

a primitive structure by assigning the aluminum atoms to two sets which are not related by the body-centering translation of $\frac{1}{2}\frac{1}{2}\frac{1}{2}$. However, this is where he makes a second fallacious assumption, and a serious one. Any change in occupancy from a perfect body-centered cell will destroy the geometrical translation of $\frac{1}{2}\frac{1}{2}\frac{1}{2}$. Yet this highly idealized model is recorded as structure type $D8_3$ and several alloys have been assigned the same structure (4). He is justified in making crude calculations on such a proposal, but he is not justified in distinguishing between small differences, which he does immediately.

Bradley next turns to the problem of fitting the aluminum atoms into the eight possible sets of atoms. This is the crucial part, for this is where the ideal composition is fixed and where, hence, the electron:atom ratio of 21:13 may have been conceived, though another investigator had to deliver it.

Because the composition of the alloys with which he worked varied from approximately 31-35.3 at. % Al (he later fixed the homogeneity range as 31.3-35.3 at. % Al (5)), he assumed the ideal composition to correspond either to Cu_9Al_4 (30.8 at. % Al) or to $Cu_{17}Al_9$ (34.6 at. % Al). He lists the possible ways of building up the structure, using the 8 sets of atoms given above:

a) for Cu_9Al_4 , $\text{Cu}_{36}\text{Al}_{16}$

(1) $4e_1$, $4e_1'$, $4e_2$, $4e_2'$

(2) $12h$, $4e_1$

(3) $12h$, $4e_1'$

(4) $12h$, $4e_2$

(5) $12h$, $4e_2'$

(6) $6f$, $6f'$, $4e_1$

(7) $6f$, $6f'$, $4e_2$

b) for $\text{Cu}_{17}\text{Al}_9$, $\text{Cu}_{34}\text{Al}_{18}$

(8) $12h$, $6f$

(9) $12h$, $6f'$

For $\text{Cu}_{34}\text{Al}_{18}$, he has not considered the possibilities,

(10) $6f$, $4e_1$, $4e_1'$, $4e_2$

(11) $6f$, $4e_1$, $4e_1'$, $4e_2'$

(12) $6f$, $4e_1$, $4e_2$, $4e_2'$

(13) $6f$, $4e_1'$, $4e_2$, $4e_2'$.

This oversight marks his third fallacious assumption; he considers only 9 of the 13 possible arrangements.

He then eliminates all but (3) and (4) as possible solutions. He does this by calculating quantities proportional to the intensities for the

powder lines representing reflections from planes with $h + k + l = 2n + 1$; he does this so that he has to consider only the differences in scattering between copper and aluminum. The basis for his rejection of (8) as a possible atomic arrangement is worth considering. I list the observed intensities for the 13 powder lines which he considered and the quantities proportional to the intensities, calculated on the basis of structures (3) and (8).

Σh^2	Observed Intensity	Cu_9Al_4 (3)	$\text{Cu}_{17}\text{Al}_9$ (8)
3	-	2	8
5	m.	10	5
9	m.	23	39
11	-	-	3
13	-	0	1
17	-	1	-
19	-	4	4
21	-	1	8
25	-	-	1
27	w.	7	8
29	v.w.	4	1
33	v.w.	10	12
35	-	2	2

(I assume that m. is for medium, w. is for weak, v. w. is for very weak, and the dash (-) is for unobserved.)

I cannot see how one could reject (8) as a possibility, considering all the assumptions that were involved. Yet, on this very

calculation rests the determination of the second γ -brass type compound, " Cu_9Al_4 ." Furthermore, the homogeneity range was very carefully determined as extending from 31.3 to 35.3 at. % Al (5). The composition corresponding to Cu_9Al_4 is 30.8 at. % Al and lies outside the homogeneity range, and the composition corresponding to $\text{Cu}_{17}\text{Al}_9$ is 34.6 at. % Al and lies within the range. Yet as late as 1951, Bradley persisted in referring to the γ -brass type compound " Cu_9Al_4 " (6).

On the basis of the method that was used to derive the ideal formula Cu_9Al_4 and on the basis of the experimentally determined composition, I demand that " Cu_9Al_4 " be stricken from the lists of 21:13 compounds and propose that a very careful determination of its structure and composition be undertaken.

Bradley assumes that the differences in the atomic arrangements between Cu_5Zn_8 and " Cu_9Al_4 " are very small and proposes a highly idealized structure for " Cu_9Al_4 ." He calculates intensities for a few powder lines for most of the possible atomic arrangements for this idealized structure and on the basis of the resulting small differences decides in favor of a composition which is not in the range of homogeneity. To coin a phrase from Hybl and Marsh (7), "this cascade of errors culminates" in another Hume-Rothery rule.

References

1. W. Ekman, Z. physik. Chem., B12, 57-77 (1931).
2. W. Hume-Rothery and G. V. Raynor, The Structure of Metals and Alloys, (1956), London: The Institute of Metals. pp. 196-197.
3. A. J. Bradley, Phil. Mag., 6, 878-888 (1928).
4. W. B. Pearson, A Handbook of Lattice Spacings and Structures of Metals and Alloys, (1958), New York: Pergamon Press.
5. A. J. Bradley, H. J. Goldschmidt, and H. Lipson, J. Inst. Metals, 63, 149-161 (1938).
6. A. J. Bradley, Nature, 168, 166 (1951).
7. A. Hybl and R. E. Marsh, Acta Cryst., 14, 1046-1051 (1961).